UNIVERSITY OF WESTMINSTER

WestminsterResearch
http://www.westminster.ac.uk/westminsterresearch

Space-partitioning with cascade-connected ANN structures for positioning in mobile communication systems.

Milos Borenović

School of Electronics and Computer Science

This is an electronic version of a PhD thesis awarded by the University of Westminster. © The Author, 2010.

This is an exact reproduction of the paper copy held by the University of Westminster library.

The WestminsterResearch online digital archive at the University of Westminster aims to make the research output of the University available to a wider audience. Copyright and Moral Rights remain with the authors and/or copyright owners.
Users are permitted to download and/or print one copy for non-commercial private study or research. Further distribution and any use of material from within this archive for profit-making enterprises or for commercial gain is strictly forbidden.

Whilst further distribution of specific materials from within this archive is forbidden, you may freely distribute the URL of WestminsterResearch: (http://westminsterresearch.wmin.ac.uk/).

In case of abuse or copyright appearing without permission e-mail repository@westminster.ac.uk

Space-partitioning with Cascade-connected ANN Structures for Positioning in Mobile Communication Systems

Milos Borenovic

A thesis submitted in partial fulfilment of the requirements for the degree of Doctor of Philosophy

School of Electronics and Computer Science
University of Westminster

September 2010

Abstract

The world around us is getting more connected with each day passing by – new portable devices employing wireless connections to various networks wherever one might be. Location-aware computing has become an important bit of telecommunication services and industry. For this reason, the research efforts on new and improved localisation algorithms are constantly being performed. Thus far, the satellite positioning systems have achieved highest popularity and penetration regarding the global position estimation. In spite the numerous investigations aimed at enabling these systems to equally procure the position in both indoor and outdoor environments, this is still a task to be completed.

This research work presented herein aimed at improving the state-of-the-art positioning techniques through the use of two highly popular mobile communication systems: WLAN and public land mobile networks. These systems already have widely deployed network structures (coverage) and a vast number of (inexpensive) mobile clients, so using them for additional, positioning purposes is rational and logical.

First, the positioning in WLAN systems was analysed and elaborated. The indoor test-bed, used for verifying the models' performances, covered almost 10,000m^2 area. It has been chosen carefully so that the positioning could be thoroughly explored. The measurement campaigns performed therein covered the whole of test-bed environment and gave insight into location dependent parameters available in WLAN networks. Further analysis of the data lead to developing of positioning models based on ANNs.

The best single ANN model obtained 9.26m average distance error and 7.75m median distance error. The novel positioning model structure, consisting of cascade-connected ANNs, improved those results to 8.14m and 4.57m, respectively. To adequately compare the proposed techniques with other, well-known research techniques, the *environment positioning error* parameter was introduced. This parameter enables to take the size of the test environment into account when comparing the accuracy of the indoor positioning techniques.

Concerning the PLMN positioning, in-depth analysis of available system parameters and signalling protocols produced a positioning algorithm, capable of fusing the system received signal strength parameters received from multiple systems and multiple operators. Knowing that most of the areas are covered by signals from more than one network operator and even more than one system from one operator, it becomes easy to note the great practical value of this novel algorithm. On the other hand, an extensive drive-test measurement campaign, covering more than 600km in the central areas of Belgrade, was performed. Using this

algorithm and applying the single ANN models to the recorded measurements, a 59m average distance error and 50m median distance error were obtained. Moreover, the positioning in indoor environment was verified and the degradation of performances, due to the cross-environment model use, was reported: 105m average distance error and 101m median distance error.

When applying the new, cascade-connected ANN structure model, distance errors were reduced to 26m and 2m, for the average and median distance errors, respectively.

The obtained positioning accuracy was shown to be good enough for the implementation of a broad scope of location based services by using the existing and deployed, commonly available, infrastructure.

Contents

Acronyms and Abbreviations

2G	Second Generation
3G	Third Generation
3GPP	Third Generation Partnership Project
A-GPS	Assisted Global Positioning System
ANN	Artificial Neural Networks
AOA	Angle of Arrival
AP	Access Point
ARM	Automatic Radio Management
BA List	Broadcast Control Channel Allocation List
BER	Bit Error Rate
BS	Base Station
BTS	Base Transceiver Station
C-C	Cascade-Connected
CDF	Cumulative Distribution Function
Cell-ID	Cell Identification
COO	Cell of Origin
DCM	Database Correlation Method
DCS	Digital Communication System
DE	Distance Error
DGPS	Differential Global Positioning System
DOA	Direction of Arrival
DSSS	Direct-Sequence Spread Spectrum
E-CIDTA	Enhanced Cell-ID + TA
E-OTD	Enhanced Observed Time Difference
ESA	European Space Agency
ESS	Extended Service Set
ETSI	European Telecommunications Standards Institute
FCC	Federal Communications Commission
FMC	First Measurement Campaign

GNSS	Global Navigation Satellite System
GPS	Global Positioning System
GSM	Global System for Mobile Communications
IMT-2000	International Mobile Telecommunications-2000
IPS	Indoor Positioning System
IR	Infrared
IrDA	Infrared Data Association
ITU	International Telecommunication Union
LBS	Location Based Services
LCS	Location Services
LMU	Location Measurement Unit
LoS	Line of Sight
LTG	Linear Threshold Gate
MEO	Medium Earth Orbit
MI	Model Input
MLC	Mobile Location Centre
MS	Mobile Station
MSE	Mean Square Error
N	Noise
NN	Nearest Neighbour
OTDOA	Observed Time Difference of Arrival
PDA	Personal Digital Assistant
PDF	Probability Distribution Function
PLMN	Public Land Mobile Network
PMF	Probability Mass Function
RBF	Radial Basis Function
RF	Radio Frequency
RFID	Radio-Frequency Identification
RI	Reference Input
RMS	Root Mean Square
RN	Room Number
RP	Reference Point
RSCP	Received Signal Code Power

RSS	Received Signal Strength
RSSI	Received Signal Strength Indication
RT	Room Type
RTT	Round Trip Time
SA	Selective Availability
SIG	Special Interest Group
SLMC	Serving Location Mobile Centre
SMC	Second Measurement Campaign
SNR	Signal to Noise Ratio
SQL	Structured Query Language
SRNC	Serving Radio Network Controller
TA	Timing Advance
TDMA	Time Division Multiple Access
TDOA	Time Difference of Arrival
TOA	Time of Arrival
TTFF	Time to First Fix
UMTS	Universal Mobile Telecommunications System
UWB	Ultra-WideBand
W-CDMA	Wideband Code Division Multiple Access
WLAN	Wireless Local Area Network

List of Figures

List of Tables

1 Introduction

1.1 Basic Idea and Motivation

Nowadays people travel far greater distances in a single day than our not so distant ancestors had travelled in their lifetimes. Technological revolution had brought human race in an excited state and steered it towards globalization. Nevertheless, the process of globalization is not all about new and faster means of transportation nor about people covering superior distances. Immense amount of information, ubiquitous and easily accessible, formulate the essence of this process. Consequently, ways through which the information flows are getting too saturated for free usage. So, for example, frequency spectrum had become a vital natural resource with a price tagged on its lease. However, the price of not having the information is usually much higher. By employing various wireless technologies we are trying to make the most efficient use of the frequency spectrum. These new technologies have brought along the inherent habit of users to be able to exchange information regardless of their whereabouts. Higher uncertainty of the users' position has produced an increase in the amount of information contained within. As a result, services built on the location awareness of the mobile devices and/or networks, usually referred to as Location Based Services (LBS, also referred to as LoCation Services – LCS), have been created. Example of services using the mobile location can be: location of emergency calls, mobile yellow pages, tracking and monitoring, location sensitive billing /commercials, etc. With the development of these services, more efforts are being pushed into getting the maximum of location-dependent information from a wireless technology. Simply, greater the amount of information available – more accurate the location[1] estimate is.

[1] Sometimes, in literature, the words *position* and *location* have different meaning. Most often, *position* translates to the set of numerical values (such as geographical coordinates) which describe the user's placement, whereas the *location* usually refers to the descriptive information depicting the user's whereabouts (such as Piccadilly Circus, London, UK). Nevertheless, this work treats both words interchangeably.

Current research community aims to develop a positioning algorithm that will extract as much location dependent information as possible from modern, widely used, radio interfaces. This algorithm would have to produce better performing positioning technique. The goal of this research was not much different. However, the additional limitation for the research presented herein was that it had to be achieved for the already deployed, highly popular and widespread mobile radio communication systems without the use of any additional hardware. So, the obtained solutions would have to be applicable to any of the many already existing communication networks. This had to be achieved by analysing the existing widely used air-layers and location dependent information therein available. Then the appropriate methods of harvesting and employing that extra available information had to be studied, developed and verified.

The main tasks completed during this research were:

- Overview of the fundamental parameters and properties of the physical layer of WLAN and PLMN (Public Land Mobile Network) systems,
- Planning and execution of the measurement campaigns used to test and verify the proposed positioning models,
- Implementation of the ANN (Artificial Neural Network) based models to positioning in WLAN systems,
- Improvement of the positioning capabilities of the basic ANN based positioning models by introducing the novel ANN based positioning model,
- Comprehensive comparison of the proposed WLAN ANN models with the other, well-known, WLAN positioning techniques, including the formulation of the new positioning performance parameters used to justly compare the aforementioned positioning techniques,
- Devising the positioning algorithm for PLMN positioning that can benefit, in terms of positioning performances, from increasing the number of input values from multiple systems and multiple network operators,
- Implementation of the ANN based models to positioning in PLMN systems employing the above stated algorithm, and
- Comprehensive comparison of the proposed PLMN ANN models with the other, well-known, PLMN positioning techniques.

1.2 Thesis Outline

The work presented in this document, can be fundamentally categorized on the grounds of mobile communication system in which the positioning was investigated. Positioning in the two popular communication environments were scrutinized: WLAN and modern public land mobile networks (GSM/UMTS).

In order to explore and generate the positioning models, numerous tasks divided into several task groups ought to be completed. The methodology of obtaining the models was fairly similar for the both communication environments. First of all, the investigation of the fundamental properties and parameters of radio interface had to be carried out. Then, the measurement campaigns for each environment had to be designed and implemented to include the identified location dependent system parameters. After the study and statistical analysis of the results obtained by measurement campaign (analysis of the correlation between measured parameters, location, etc.) the optimal set of parameters to be used for positioning was identified. Next, the optimal positioning algorithms had to be devised, verified and compared to the other available positioning solutions.

The aforementioned steps are the milestones of a several years long work. This document gives its summation.

Chapter two gives an overview of positioning in mobile communication systems. Major performance parameters, classifications of positioning systems and approaches to determining the position of a user or entity are given therein. In addition, the existing positioning techniques in indoor and outdoor environment have been analysed with the emphasis on WLAN and cellular positioning systems, respectively.

An introduction to artificial neural networks and their use for positioning is given in chapter three. The neuron model, neural network structures and learning rules are presented to a goal of selecting the most appropriate neural network structure from positioning point of view.

Chapter four illustrates the research on positioning in WLAN environment including the chosen test-bed, measurement campaigns and derived models. Mutual model comparison as well as comparison to other relevant WLAN positioning techniques concludes this chapter.

Similar chapter structure is repeated in chapter five, this time with positioning in PLMN. Additionally, the performances and benefits of using the introduced positioning models were compared in-between WLAN and PLMN positioning.

Finally, chapter six gathers the essential results of the work and gives guidelines the future research might follow upon.

1.3 Outputs of the Thesis

The thesis produced a set of models applicable to the already deployed mobile communication networks in both indoor and outdoor environments. It ought to be pointed out that most of the other, well-known, research efforts usually strive for uncompromised accuracy, neglecting the other equally important parameters (e.g. practical feasibility) along the way.

The proposed multilayer feedforward ANNs have shown good positioning performances in both WLAN and PLMN environments, even with low RPs (Reference Points) density. Single ANN models were thoroughly explored in terms of optimal training lengths, variable input number and type. The performances of all the models were validated through the use of extensive measurement campaigns.

- Several new performance evaluation parameters that ought to enable the indoor positioning techniques to be compared and classified in a more comprehensive and inclusive manner were proposed. These parameters take into account the accuracy, size of the environment, and the density of the infrastructure. Most importantly, the *environmental positioning error* parameter ought to enable positioning techniques to be compared inclusive of the size of their test bed, which was seldom the case before. The proposed performance parameters contribute to more broad scrutiny of the indoor positioning techniques.
- The extensive experimental analysis of RSSI (Received Signal Strength Indication), SNR (Signal to Noise Ratio) and Noise level parameters usefulness for WLAN positioning purposes had shown that, contrary to the common knowledge, SNR parameter is equally suitable for WLAN positioning purposes as RSSI parameter.
- Regarding the PLMN positioning, the devised positioning algorithm, suitable to use with the ANNs, benefits from using the RSSI values from multiple systems, belonging to multiple operators. Moreover, the PLMN models were tested indoors and the degradation of accuracy performances, due to cross-environment model use, was reported.
- Foremost, this work brought the space-partitioning into positioning. The principle enables to dismantle the positioning process into two stages and solve each stage independently with the most suitable model. Moreover, the cascade-connected ANN based models suitable for use with space-partitioning were proposed. This positioning solution enhances the accuracy performance parameters: the average and median error are reduced whereas the high percentile DEs (Distance Errors) are more or less unchanged. It ought to be pointed out that the transformation of the DE distribution

function is favourable for the use of overlaid tracking algorithms that would filter-out high distance errors and additionally improve the positioning performances. If the space-partitioning principle is implemented through the use of cascade-connected ANNs, the latency of these models is very good, the scalability is fair, whereas the complexity when partitioning to a large number of subspaces might present a slight negative side.

2 On the Topic of Positioning

2.1 Performance Parameters

At the first glance, the determination of user's location can be seen as a simple mechanism consisting in calculating the geographic coordinates of the user. However, it is extremely difficult to obtain the exact location of a user, in 100% of the cases, wherever the user is and whatever his/her environment is.

Many different factors may have an effect on location determination and the fact is that only an estimate of the user's location can be obtained. It is therefore important to know how close to reality this location estimate is. To achieve that, it is necessary to characterise this location estimate. Other than that, it is also significant to describe the positioning technique itself in terms of its practicality and viability. All this is generally done through a set of performance parameters [2.1].

The first group of performance parameters is used to characterise the quality of a location estimate.

2.1.1 Accuracy

Accuracy is undoubtedly the most important performance parameter as it illustrates the essential characteristic of a positioning technique. This parameter enables to determine whether the calculated position is geographically close to the exact position. To achieve that, three different values must be taken into consideration:

- Distance Error,
- Uncertainty, and
- Confidence.

The Distance Error (DE) corresponds to the difference between the exact location of the user (i.e. of his/her terminal) and the calculated position, obtained through a position determination method. It is also referred to as Location Error or Quadratic Error in terms of two-dimensional positioning. Distance Error is generally expressed in units of length, such as meters.

Determining the Distance Error can be very useful in depicting the particular position determination cases. However, in order to express the positioning capabilities of a technique it is usually much more suitable to exploit the Distance Error statistics via Uncertainty and Confidence parameters.

Bearing in mind that the calculated user's location is not the exact location but is biased by the Distance Error, it can be seen that the calculated position does not enable resolving the single point at which the user is located, rather an area. Depending on the positioning techniques used, this area may have different shapes (e.g. a circle, an ellipse, an annuli, etc). For that reason, the Uncertainty value represents the distance from the "centre" of this area to the edge of the furthest boundary of this area. In other words, the Uncertainty value can be seen as the maximum potential Distance Error. The value of uncertainty is expressed with the same unit as for the Distance Error.

However, the Uncertainty value it is not sufficient to describe the Accuracy of a positioning technique. The determination of the Uncertainty value goes through a statistical process and does not enable to guarantee that 100% of the calculated positions have a Distance Error lower than the uncertainty value. That is the reason why the Uncertainty value is usually associated with a Confidence value, which expresses the degree of confidence that one can have into the position estimate. This degree of confidence is generally expressed in percentage or as a value of probability.

As a consequence, it is the combination of Uncertainty and Confidence that validly describe the accuracy of a positioning technique. The Confidence values commonly used to describe the accuracy of a positioning technique comprise 10%, 33%, 50%, 67%, 90%, and 95%. Sometimes, the Confidence values are also referred to as percentile DE (e.g. 95-th percentile DE). The 50-th percentile DE is the median positioning error.

If the finite set of DEs is available, the average DE is also used to illustrate the accuracy performance:

$$\bar{x} = \frac{\sum_{i=1}^{n} x_i}{n}, \tag{2.1}$$

where $\mathbf{x} = [x_1, x_2, \ldots, x_i, \ldots, x_n]$ is the vector of available DEs.

The other way of expressing the Accuracy, i.e. the performance or requirement associated to location determination, is through the distance error's Probability Distribution Function (PDF) and Cumulative Distribution Function (CDF). If the DE is observed as a continuous random

process, and a random DE variable is denoted as X, the PDF of X is a function $f(x)$ such that for two numbers, a and b with $a \le b$ [2.2]:

$$P(a \le x \le b) = \int_{x=a}^{b} f(x)\,dx. \tag{2.2}$$

Fig. 2-1 illustrates the DE's PDFs of two positioning systems where the second one, f_2, has superior accuracy.

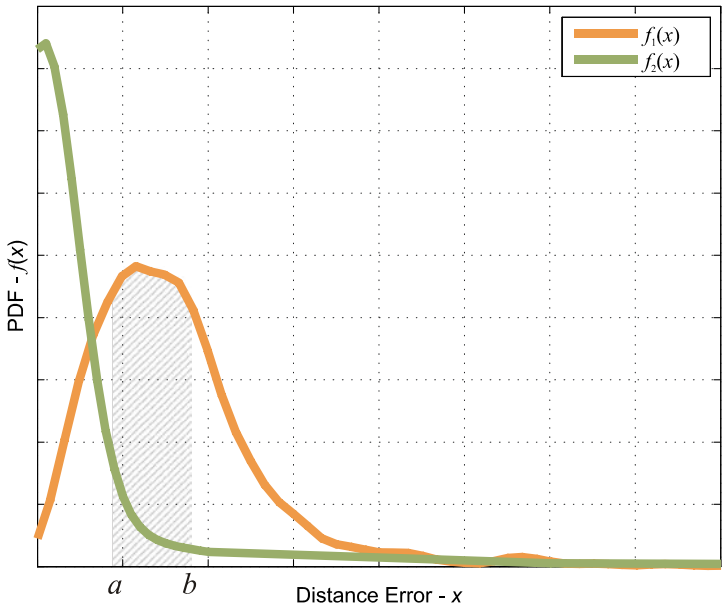

Fig. 2-1 DE's Probability Distribution Function of two positioning systems with different accuracy

Considering an optimally implemented positioning technique, ideally, the PDF of error for each coordinate (x and y) ought to have standard normal distribution. This conclusion can be drawn from the following:

- First, if the distribution function is not centred on zero, simple translation (adding or subtracting a constant value) would improve the technique's accuracy. Ergo, in order for the technique to be optimal, its coordinate errors distributions must be zero centred.
- Second, the positioning model ought to "learn" all signal properties and underlying relations except for the noise. Therefore, the positioning error for each coordinate, ideally, should be solely the product of the noise process. As most actual noise processes are considered to be with Gaussian distribution, the optimally implemented positioning technique should have the same distribution for the coordinate positioning error.

What about the distribution of quadratic or distance error which consists of more than one coordinate? In general, multi-dimensional case, the specific answer might not be easy to find. However, if the two-dimensional surrounding is assumed (as will be the case throughout this

work) where the coordinate's errors are uncorrelated and of equal variance, the resulting DE will have a Rayleigh distribution. This distribution function depicts a random process where the components are uncorrelated and normally distributed with equal variances [2.3]:

$$f(x,\sigma)=\frac{x}{\sigma^2}e^{-x^2/2\sigma^2}, \tag{2.3}$$

where σ^2 is the variance. The assumptions made will be fulfilled for general small area surface positioning which presents the most common form of positioning problem.

CDF is the probability that the observed value of *X* will be at most *x*, or:

$$F(x)=P(X\le x)=\int_{z=0}^{x} f(z)\,dz, \tag{2.4}$$

where *z* is a dummy integration variable, and f is the distribution function.

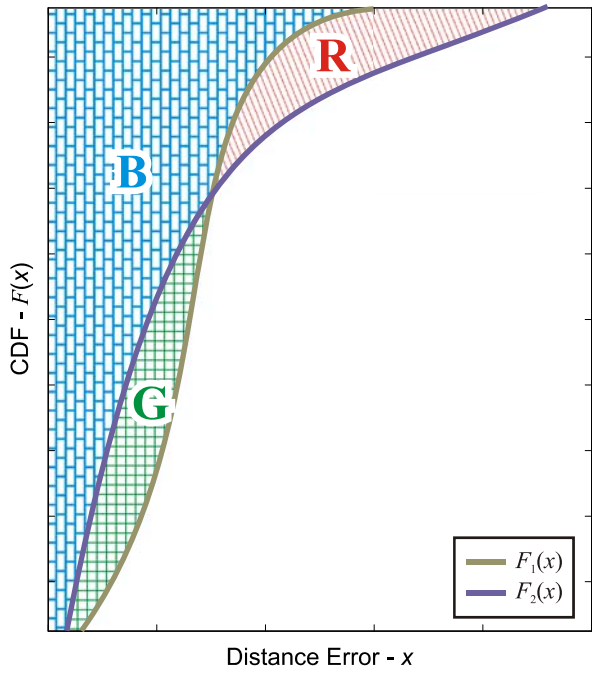

Fig. 2-2 Cumulative Distribution Function of two positioning systems

Fig. 2-2 illustrates CDFs of two positioning systems with different accuracy performances.

If we assume there are *n* position estimations and *m* possible DE values, starting from eq. (2.1) the following can be written:

$$\begin{aligned}\bar{x}&=\frac{k_1x_1+k_2x_2+\ldots+k_ix_i+\ldots+k_mx_m}{n}\\&=\frac{k_1}{n}x_1+\frac{k_2}{n}x_2+\ldots+\frac{k_i}{n}x_i+\ldots+\frac{k_m}{n}x_m\end{aligned} \tag{2.5}$$

where $\sum_{i=1}^{m} k_i = n$ and k_i is the number of times the DE was equal to x_i. Now, it can be clearly seen that the $\frac{k_i}{n}$ terms represent the probability of DE equals x_i, or:

$$\bar{x} = p(x_1)x_1 + p(x_2)x_2 + \ldots + p(x_i)x_i + \ldots + p(x_m)x_m . \tag{2.6}$$

For $m \to \infty, n \to \infty$ eq. (2.6) becomes:

$$\bar{x} = \int_0^1 x(p)\,dp , \tag{2.7}$$

or, in terms of CDF function, *F*:

$$\bar{x} = \int_{y=0}^{1} F^{-1}(y)\,dy \tag{2.8}$$

From Fig. 2-2, it can be seen that in the region of lower percentiles, the second system has superior accuracy – $F_2(x) > F_1(x)$, whereas in higher percentiles the first system is more precise – $F_2(x) < F_1(x)$. If the green areas are denoted as positioning gain, and red areas as positioning loss in terms of system two performances over system one, from eq. (2.8) the following can be concluded regarding the average DEs:

$$\begin{aligned} \overline{x_1} &= \int_{y=0}^{1} F_1^{-1}(y)\,dy = A(B) + A(G) \\ \overline{x_2} &= \int_{y=0}^{1} F_2^{-1}(y)\,dy = A(B) + A(R) \end{aligned} , \tag{2.9}$$

where the operator $A(\cdot)$ denotes the area size. From eq. (2.9) directly follows:

$$\begin{aligned} A(G) > A(R) &\Rightarrow \overline{x_2} < \overline{x_1} \\ A(G) = A(R) &\Rightarrow \overline{x_2} = \overline{x_1} . \\ A(G) < A(R) &\Rightarrow \overline{x_2} > \overline{x_1} \end{aligned} \tag{2.10}$$

In other words, eq. (2.10) stipulates that if the gain and loss areas have the same area size, the systems' average positioning error will be equal. Moreover, if the gain area is greater than the loss area the system will have smaller average DE, and the other way around. The actual difference of average DEs can be easily expressed as:

$$\begin{aligned} \overline{x_1} - \overline{x_2} &= \int_{y=0}^{1} \left[F_1^{-1}(y) - F_2^{-1}(y) \right] dy \\ &= A(B) + A(G) - A(B) - A(R) . \\ &= A(G) - A(R) \end{aligned} \tag{2.11}$$

The PDF can be extracted from CDF and *vice versa* using the following set of equations:

$$\begin{aligned} F(x) &= \int_{z=0}^{x} f(z)\,dz \\ f(x) &= -\frac{d\left(F(x)\right)}{dx} \end{aligned}, \tag{2.12}$$

In literature, the CDF is more commonly used (than PDF) to depict the accuracy performances. Moreover, using the CDF is more inclusive than using Uncertainty/Confidence pair due to the fact that a particular Uncertainty/Confidence pair can always be read of the CDF plot for every confidence or uncertainty value.

2.1.2 Other Performance Parameters

Coverage and Availability – Accuracy is not the only parameter to be considered in order to characterise a location estimate. Coverage and Availability must be considered too. These two parameters are linked together:

- The Coverage area for a positioning method corresponds to the area in which the location service is potentially available, and
- The Availability expresses the percentage of time during which the location service is available in the coverage area and provides the required level of performance.

Latency – Location information makes sense only if it is obtained within a timeframe which remains acceptable for the provision of the LBSs based on this information. Latency represents the period of time between the position request and the provision of the location estimate and it is generally expressed in seconds.

Direction and Velocity – Although the herein presented work is restrained to the initial position determination algorithms, there are additional tracking algorithms that rely on multiple sequential position determinations in order to estimate the speed vector of the user. In such cases, two additional parameters have to be calculated: the Direction followed by the user and his/her Velocity. These parameters are generally expressed in degrees and meters per second respectively.

Scalability – The scalability is a desired and welcomed characteristic of a positioning system. It represents the positioning system's ability to readily respond to any augmentation. The augmentation can be in terms of Coverage area, Availability, frequency and total number of positioning requests, etc.

Complexity – There are many definitions for complexity depending on the domain of application. Nevertheless, in terms of positioning systems, complexity is most often referred to as the property that describes the difficulty of setting up the positioning system.

Cost effectiveness – This abstract characteristic of a positioning system is not entirely independent of its other performance parameters (e.g. Complexity and Scalability). For example, the greater the Complexity of the system, the lower the Cost effectiveness. One of the ways of describing it is as a ratio between the benefits it provides (how broad range of LBSs it enables) and the costs it induces for the user.

As it can be seen from the aforementioned, the latter three parameters do not have standardized units and are usually of descriptive nature.

2.2 Classifications of Positioning Systems

There are more than a few classifications of positioning systems. Some are very strict and others are very arbitrary and overlapping. Without the need to judge or justify any of them, the most common ones are given herein.

Regarding the type of provided information, positioning techniques can be split into two main categories.

- Absolute positioning methods consist in determining user location from scratch, generally by using a receiver and a terrestrial or satellite infrastructure. A well-known example of systems based on "absolute positioning" is the American GPS.
- Relative positioning methods consist in determining user location by calculating the movements made from an initial position which is known. These methods do not rely on an external infrastructure but require additional sensors (e.g. accelerometers, gyroscopes, odometers, etc). Inertial Navigation Systems used in commercial and military aircraft are a good example of systems based on relative positioning.

LBSs currently offered by wireless telecommunication operators or by service providers are all based on absolute positioning methods and not on relative positioning methods, since these services are offered to users whose initial position is generally not known.

Within the "absolute positioning" family, the measurements and processing required for determining user's location can be performed in many different ways and rely on different means. Thus, many different absolute positioning methods can be used for determining user's location. These methods can be clustered into different groups, depending on the infrastructure used. Hence, the positioning techniques can be divided into:

- Satellite-based,

- Cellular-based, and
- Other.

The first group, which is known by the largest audience, is the "Satellite positioning" group. This group relates to the positioning methods which are based on the use of orbiting satellites, such as the GPS, GLONASS or Galileo. Many applications and services based on satellite positioning have been developed during the past years (e.g. in-vehicle navigation, fleet management, tracking and tracing applications, etc), but they generally required the use of dedicated receivers. Today, more and more devices such as PDAs or mobile phones include a satellite positioning capability, and this trend should persist in the future.

The second group, the "Cellular positioning" group, corresponds to the location technologies which have been developed for Public Land Mobile Networks (PLMN). Initially deployed in the US under the pressure of the FCC mandate which forces US carriers to locate users placing calls to the E911 emergency number [2.4] and boosted by European E112 [2.5], location technologies are now being implemented in most of European wireless telecommunication networks for commercial purposes. Most of cellular positioning methods are incorporated in mobile telecommunication standards, but some solutions remain based on proprietary techniques.

The third and last group, the "Other positioning" group, corresponds to those technologies which have not been developed specifically for positioning purposes, but that can be used, in addition to their primary function, for determining user's location. These technologies encompass WLAN and Bluetooth for instance.

Another distinction can be made, depending on the "place" where the position calculation is made. In some cases, the main processing is performed at the terminal level. In other cases, the main processing is performed in the network. Therefore, the positioning techniques can be classified into:

- Network-based (also referred to as the mobile-assisted), and
- Terminal- or Mobile-based (also referred to as the network-assisted).

Satellite technologies, as a rule, fit in the Terminal-based positioning techniques. As for the positioning techniques from the cellular and other groups, they cannot be *a priori* associated to either of the Terminal- or Network-based groups.

Finally, due to the fact that different physical phenomena dominantly influence the radio propagation in indoor and outdoor environments, different propagation models are being used to depict the propagation in these environments. Moreover, the main sources of interference in these systems are usually distinct. For instance, the intersystem interference is dominant for WLAN systems, whereas the intrasystem interference prevails within PLMN systems. Owing

to all that, the positioning techniques can also be classified according to the environment of their primary coverage into:

- Outdoor, and
- Indoor.

Bearing in mind the ongoing convergence process of telecommunication systems and numerous, newly developed, hybrid positioning techniques, the indoor/outdoor categorization as well as other aforementioned classifications ought to be regarded more as guidelines than as strict lines that divide techniques into disjoint sets. Nevertheless, the last classification was used to group the positioning techniques in this document.

2.3 Approaches to Localization

The approaches and metrics used in order to obtain the user's position are also worth discussing. There are a few fundamental methods of acquiring the user's location:

1) Based on the identification of "base station" to which the user is associated (Cell-ID or Cell of Origin – COO) – This simple approach assumes that the estimated location of a user is equal to the location of a "base station" to which the user is associated. In other words, the user is estimated to be in a location of the "nearest" node of the network.

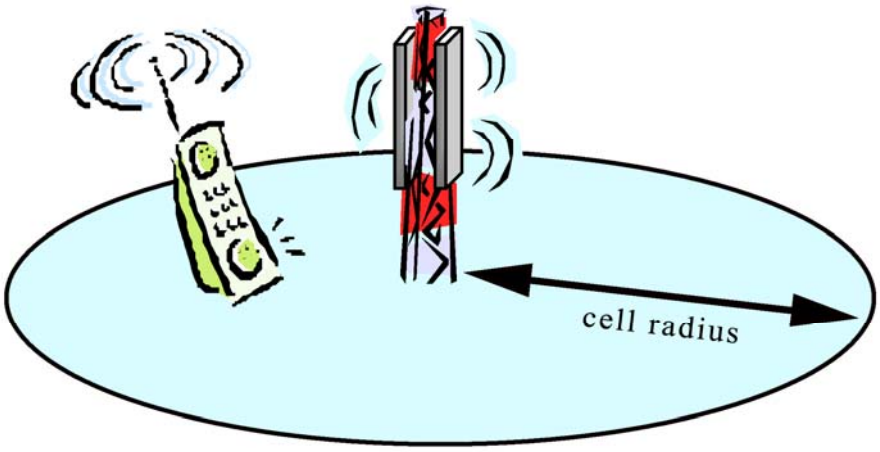

Fig. 2-3 Cell-ID Positioning Approach [2.1]

This method is used both in indoor and outdoor environments (GSM, UMTS). Its popularity, despite usually inferior performances, is due to the simplicity of implementation. Obviously, the accuracy is proportional to the density of the network nods. This approach is illustrated in Fig. 2-3.

2) Based on the time of signal arrival (Time of Arrival – TOA) – Being that the waves (electromagnetic, light and sound) are propagating through the free space at constant speed – v_{prop}, it is possible to assess the distance between the transmitter and a receiver based on the time that the wave propagates in-between those two points. This approach assumes that the receiver is informed of the exact time of signal's departure. Being that this is not always easily accomplished, the alternative approach takes into account the time needed for signal to propagate in both directions (Round Trip Time – RTT). This way, one station is transmitting the predefined sequence. The other station, upon receiving the sequence, after a strictly defined time interval, t^{proc}, (used for allowing the stations of different processing power to process the received information), resends the sequence. The station that initially sent the sequence can now, by subtracting the known interval of time that the signal was delayed at second station from the measured time interval, asses the time that signal propagated to the other station and back and, consequently, the distance between the stations:

$$t^{total} = t^{A-B} + t^{proc} + t^{B-A}$$
$$t^{A-B} \approx t^{B-A} \rightarrow d \approx v_{prop} \cdot \left(\frac{t^{total} - t^{proc}}{2} \right) \tag{2.13}$$

This approach is a popular one, since it does not require the stations to be synchronised. The RTT positioning approach is illustrated in Fig. 2-4.

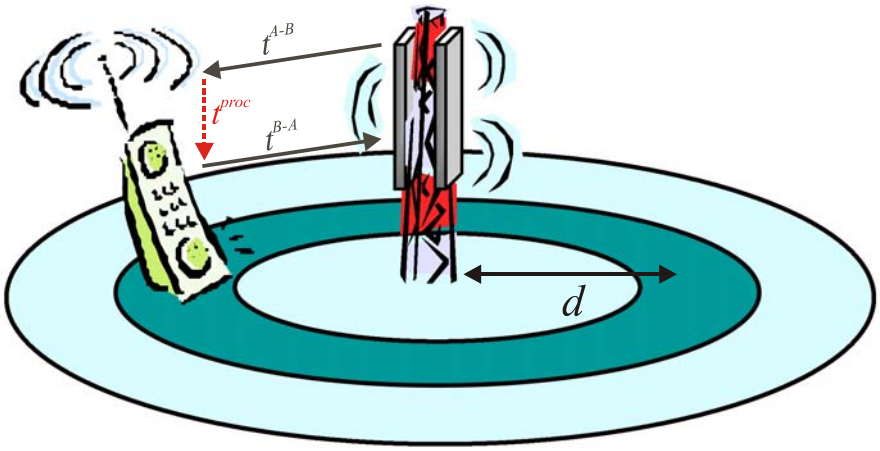

Fig. 2-4 Round-Trip-Time Positioning Approach

3) The distance between the stations can be measured based on the differences in times of signal arrival (Time Difference of Arrival – TDOA) – With this approach, the problem

of precisely synchronised time in transmitter and receiver is resolved by using several receivers that are synchronised whereas the transceiver, whose location is being determined, does not have to be synchronised with the receivers. Upon receipt of the transmitted signal, a network node computes the differences in times of the signal's arrival at different receivers. For each couple of receivers *i* and *j*, and the two-dimensional setting, the following set of equations can be written:

$$\begin{aligned} \Delta t_{ij} &= t_{tx-i} - t_{tx-j} \\ \Delta t_{ij} &= \frac{d_{tx-i} - d_{tx-j}}{v_{prop}} \\ \Delta t_{ij} v_{prop} &= \sqrt{\left(x_i - x_{tx}\right)^2 + \left(y_i - y_{tx}\right)^2} - \sqrt{\left(x_j - x_{tx}\right)^2 + \left(y_j - y_{tx}\right)^2} \end{aligned} \tag{2.14}$$

where Δt_{ij} is the measured time difference of arrival, v_{prop} is the wave propagation speed, t_{tx-i} and t_{tx-j} is the time signal travels from transmitter to receiver *i* and *j*, respectively. Likewise, d_{tx-i} and d_{tx-j} are the distances between the transmitter and receivers *i* and *j*, respectively, whereas $\left(x_i, y_i\right)$, $\left(x_j, y_j\right)$ and $\left(x_{tx}, y_{tx}\right)$ are the coordinates of *i*-th and *j*-th receiver and the estimated coordinates of the transmitter, respectively. The $\left(x_{tx}, y_{tx}\right)$ pairs that satisfy the bottom line of eq. (2.14) are located on a hyperbola. Hence, the user's location is determined as a cross-section of two or more hyperboles (one for each pair of receivers). Owing to that, these techniques are often referred to as hyperbolic techniques. The TDOA approach to positioning is illustrated in Fig. 2-5.

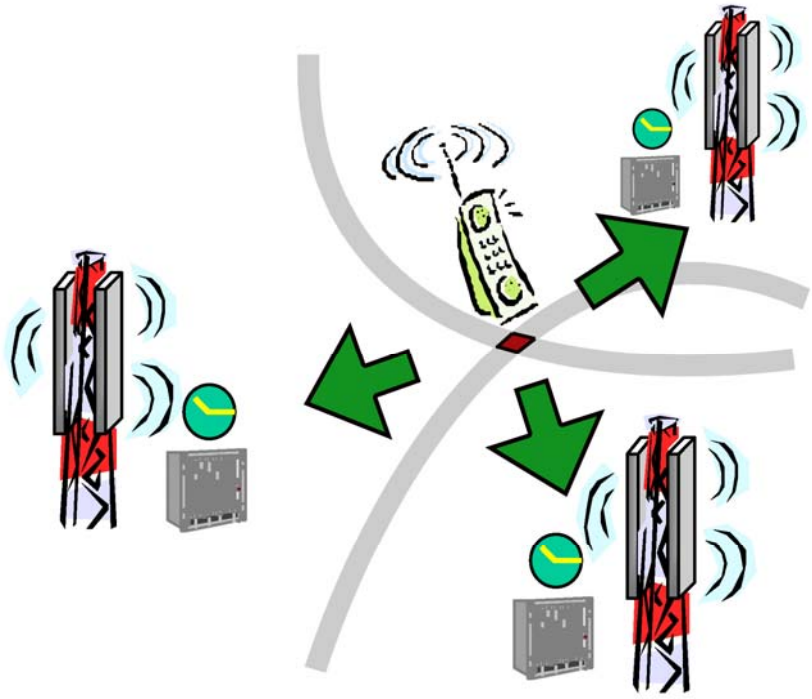

Fig. 2-5 Time Difference of Arrival Positioning Approach [2.1]

4) Based on the signal's angle of arrival (Angle of Arrival – AOA or Direction of Arrival – DOA) – The idea, with this approach, is to have directional antennas which can detect the angle of arrival of the signal with the maximal strength or coherent phase (Fig. 2-6). This procedure grants the spatial angle to a point where the signal originated (and whose location is determined). This approach is often implemented through the use of antenna arrays.

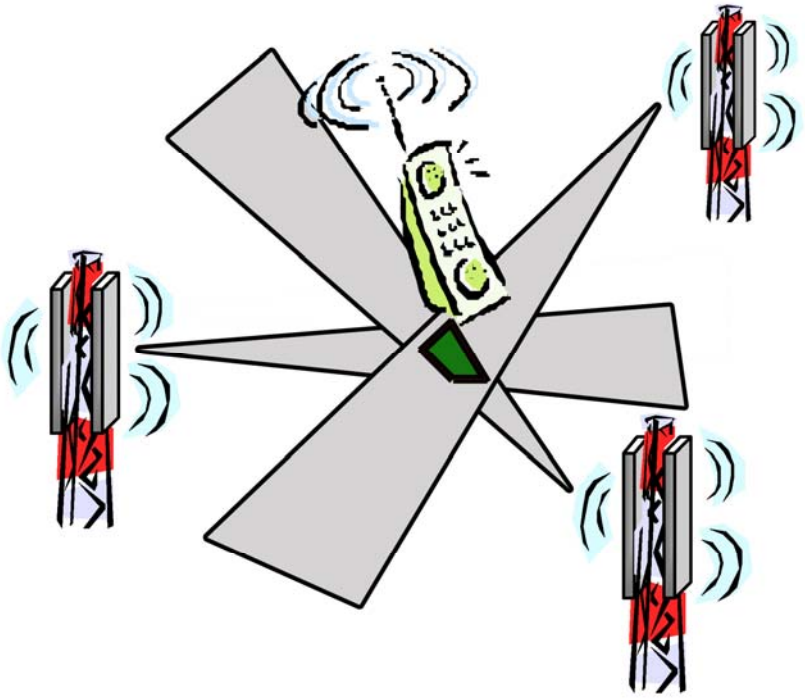

Fig. 2-6 Angle of Arrival Positioning Approach [2.1]

5) Based on the received signal strength (Received Signal Strength Indication – RSSI[2]) – The free space signal propagation is characterised with predictable attenuation dependent on the distance from the source. Moreover, in real conditions, the attenuation also largely depends on the obstacles and the configuration of the propagation path. That is why there are various mathematical models which describe the wave propagation for diverse surroundings and, ultimately, estimate the signal attenuation for the observed environment. This approach grants the distance of the entity whose position is being determined, to one or more transmitters.
6) Based on the fingerprint of the location (Database Correlation or Location Fingerprinting) – With this approach, the certain, location dependant, information is acquired in as many Reference Points (RPs) across the coverage area of the technique. This data is stored into so called Location Fingerprints Database. Afterwards, when the actual position determination process takes place, the information gathered at the unknown location is compared with the pre-stored data and the entity's position is

[2] In some communication systems (mostly outdoor), this parameter is also referred to as the Received Signal Strength or Received Level – Rx Lev. In this work, the RSS and RSSI notation will be used interchangeably.

estimated at a location of a pre-stored fingerprint from the database whose data are the "closest" to the measured data.

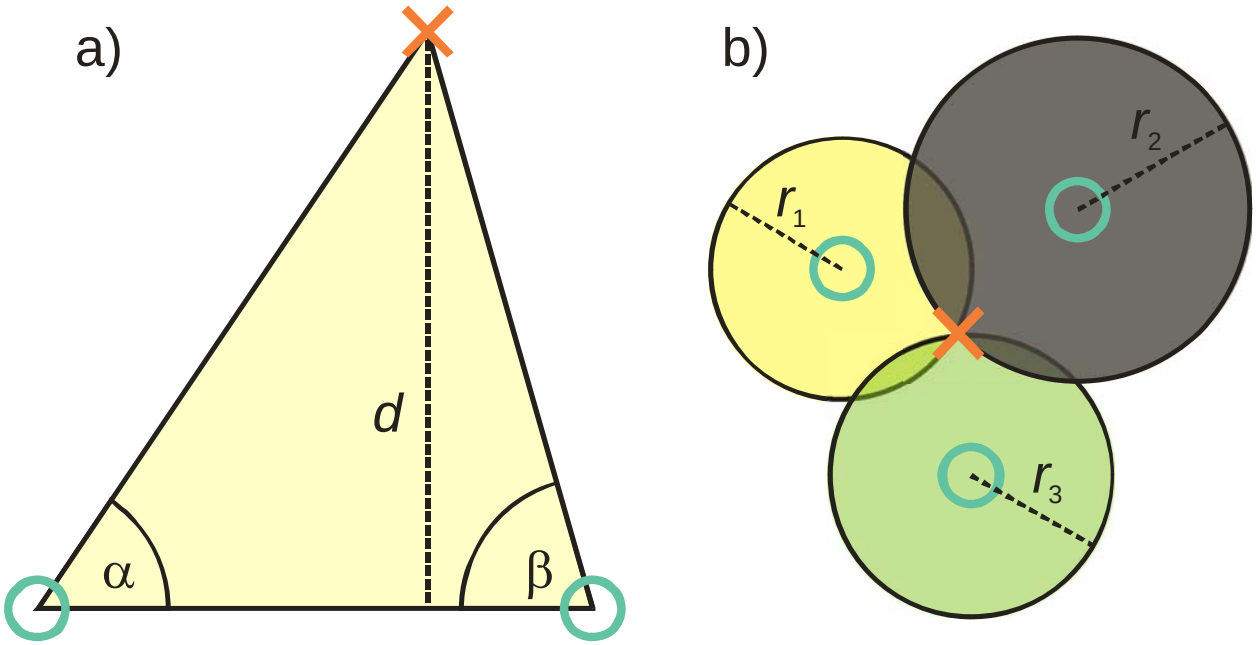

Fig. 2-7 The processes of estimating a user location: a) Angulation and b) Lateration (Green circles represent the known positions and the red cross stands for the estimated location)

Most often, the estimated position with TOA and RSSI approaches is determined by lateration. The process of lateration consists of determining the position of the entity when the distance between the entity and one or more points with identified positions is known. To uniquely laterate the position in *N*-dimensional space, the distances (or distance functions) to *N+1* points ought to be known. With TDOA approach, the estimated position is obtained as a cross-section of two or more hyperbolas in two-dimensional space, or three or more hyperbolic surfaces in case of three-dimensional space. The process of angulation is employed with AOA and DOA approaches. This process estimates the location of a user as a cross-section of at least two rays (half-lines) originating at known locations. The lateration and angulation processes are depicted in Fig. 2-7. As for the Location Fingerprinting approach, the estimated location is obtained by utilizing the correlation algorithm of some sort. This algorithm determines, following a certain metric, the "closeness" of the gathered data to the pre-stored samples from the location fingerprinting database.

Apart from these, basic, approaches, there are a number of other choices and hybrid techniques that combine the aforementioned approaches when determining the estimated position of the user.

2.4 Indoor Positioning

Cellular-based, Computer vision, IrDA (Infrared Data Association), ultrasound, satellite-based (Indoor GPS) and RF (Radio Frequency) systems can be used to obtain the user's position indoors. Positioning technologies, specific for indoor environment, such as computer vision, IrDA and ultrasound require deployment of additional infrastructural elements [2.6]. On the other hand, the performances of the satellite- and cellular-based positioning technologies are often unsatisfactory for typical LBSs in an indoor environment [2.6] – [2.8]. Due to the proliferation of IEEE 802.11 clients and infrastructure networks, and the fact that a broad scope of LBSs can be brought into an existing WLAN network without the need for additional infrastructure, WLAN positioning techniques are relevant and established subjects to intensive research.

2.4.1 IrDA Positioning Systems

IrDA technologies are based on devices with infrared light transceivers. This light occupies the part of spectrum between the visible light and the radio-waves (700nm – 1mm wavelengths). Upon encountering an obstacle, such as wall, the major part of the IR light's energy is being absorbed. Therefore, in order to communicate properly, two IR devices must have unobstructed Line of Sight (LoS) path between them. This poses a limitation for employing this technology in positioning purposes.

The most popular application of this technology for positioning use is the "Active Badge" technique [2.9]. The person or entity, whose position is being determined, possesses a device, badge alike, which periodically emits its ID code via IR transmitter. The IR sensors must be deployed in the coverage area (building). The position of the user is then determined based on the Cell-ID principle. With respect to the attributes of the IR light, the sensors must be deployed in every room in which the positioning feature is needed. Consequently, the accuracy of this technique is on a room level.

Other techniques based on this technology offer various accuracy and applications. The systems with greater number of IR receivers and transmitters on each device are proposed [2.10]. These systems are able to accurately estimate the position of a mobile communication device (e.g. PDA, laptop, digital camera, etc.) in order to allow them to automatically synchronise or perform other location dependent tasks. These activities are supposed to be performed on a flat, table alike surface. The obtained distance error is less than 20cm in more than 90% of the cases. On the other hand, there are systems that augment the "Active Badge" technique by using more IR sensors, micro VGA display and, optionally, video cameras. These systems provide so called Augmented Reality [2.11]. The typical application of an Augmented

Reality system would be for the museum environment, where the visitor would be, via micro display (in eyeglasses, for example), fed with the information related to the exhibit he is currently experiencing.

2.4.2 Ultrasound Positioning Systems

The term ultrasound is related to the high frequency sound waves, above the part of spectrum perceivable to the human ear (20kHz). Although the ultrasound is most frequently used in medicine, there are other areas of application such as: biomedicine, industry (e.g. flow-meters), chemistry, military applications (sonic weapon), etc. As for the positioning purposes, the greatest benefit of using the ultrasound positioning is the product of a fact that ultrasound propagates through the air at limited speed, which is by far smaller than the speed of light. Therefore, the implementation of techniques based on time of flight (i.e. TOA, TDOA) of the signal is very much facilitated. Moreover, the mechanic nature of sound waves grants ultrasound positioning techniques immunity to electromagnetic interference which could also be considered as an advantage. It ought to be pointed out that ultrasound waves do not penetrate, but rather reflect of walls. Therefore, the ultrasound receiver, in order to detect the signal, must be in the same room as transmitter but the LoS is not necessary.

Ultrasound positioning systems can be classified according to the number of ultrasound "base stations" (transmitters and/or receivers) in each room [2.12]. The basic ultrasound positioning technique comprises one receiver in each room, and an ultrasound emitting tag which is worn by the entity that needs to be positioned. In this case, the accuracy is on the level of the room. These systems are commercially available for some time now.

More sophisticated ultrasound positioning systems invoke the use of a greater number of transmitters in each room as well as the use of RF (seldom IR) signals for precise determining the time delay [2.13]. In this case, the controlling unit, which is connected to all the ultrasound emitters in one room as well as with RF transmitter, determines the exact time when each of the transmitters is about to send its chirps. Commonly, the RF signal is emitted first and then the chirps from all ultrasound transmitters are emitted separated by known time intervals. The receiver, knowing the separating time intervals and the propagation speed of RF and ultrasound waves, can now calculate, based on the time it received each of the chirps, the distance to each of the ultrasound emitters. The position is then determined by lateration. Consequently, for three-dimensional positioning at least four transmitters per room are required. The accuracy is in range of 10cm in 90% of the cases.

Furthermore, the system that eliminates the need for RF transmitter has been developed [2.14]. With this system, the processing power of the receiver can be reduced, and the whole system is

less complex. The transmitters are cyclically emitting chirps in constant time intervals whereas the receiver is employing an extended Kalman filter for resolving the chirp transmission and receipt times.

2.4.3 RF Positioning Systems

The RF (30 kHz – 300 GHz frequencies) positioning techniques employ different parts of the frequency spectrum. Some are implemented on existent short-range radio interfaces and serve as added services, while others are especially developed for positioning. The most common RF technologies which, through the use of these techniques, enable positioning are: RFID, UWB, Bluetooth and WLAN.

Being that the WLAN positioning is one of the main topics of the thesis, the positioning systems for this environment shell be explored in more details.

2.4.3.1 RFID (Radio-Frequency IDentification) Positioning Systems

The beginnings of this technology go far back to the time of the second World War. Over the recent years, due to the cheaper RFID components, the expansion of this technology is occurring.

RFID system consists of tags, reader with antenna and accompanying software. The tags are usually placed on entities whose position needs to be determined. The Line of Sight between the tag and a reader is usually not necessary. The tags can contain additional information apart from its ID code which broadens the usage of this technology.

There are three types of RFID tags:

- Passive tags do not have their own power supply. In order to operate, they use the energy, induced on their antenna, from the incoming radio wave from the reader. Using that energy, the passive tag replays by emitting its ID code and, optionally, additional information. Passive tags have very limited range (from a few cm up to a couple of meters). Their advantage is within the scope of cheap construction, compact size and cheap production.
- Active tags are encompassed with a power supply which enables them unrestrictive signal emission. This kind of tags are more reliable and immune to highly polluted RF environments. Their range can go up to a few hundreds of meters.
- Semi-active tags are equipped with battery power supply. Recent constructions enable a battery life span of more than 10 years.

RFID devices can operate in different frequency bands: 100 – 500 kHz, 10 - 15 MHz, 850 – 900 MHz, and 2.4 – 5.8 GHz [2.15].

RFID positioning techniques are based on knowing the position of the reader. When the tagged object enters the range of the reader, its position is assumed to be equal to the position of the reader (similar to Cell-ID). Correspondingly, it is possible to deploy tags across the coverage area. In that case the reader is mounted on the entity whose position is being determined. The accuracy depends on the density of deployed objects (tags/readers) across the coverage area. With active tags, the positioning accuracy can be upgraded with the RSSI information.

Most common application areas of RFID technology are in replacing the barcode readers, product tracking and management, personal documents identification, identification implants for humans and animals, etc. It is interesting to mention that the latter aforementioned application raises numerous ethical issues and there are organized groups worldwide opposing the implementation of this technology.

2.4.3.2 Bluetooth Positioning Systems

Bluetooth is a short-range, low-consumption radio interface for data and voice communication [2.16]. Initially conceived in the mid 90s by the Ericsson Mobile Communication as a technology that ought to replace the cable in personal communications, Bluetooth shortly gained significant popularity. Ericsson was joined by IBM, Microsoft, Nokia and Toshiba. They formed Bluetooth Special Interest Group (SIG) with an aim to standardize Bluetooth specifications. Independent group, called the Local Positioning Working Group, had a goal of developing the Bluetooth profile which would define the position calculation algorithm as well as the type and format of the messages that would enable Bluetooth devices to exchange position information.

The basic Bluetooth specification does not support positioning services *per se* [2.17], [2.18]. In absence of such support, various research efforts have produced diverse solutions. Bahl and Padmanabhan first used the RSSI information for in-building locating and tracking [2.19]. Patil introduced the concept of reference tags and readers [2.20]. He also investigated separately the cases when Bluetooth supports and does not give support to RSSI parameter. On the other hand, the research by Hallberg, Nilsson and Synnes goes to say that RSSI parameter is unreliable for positioning purposes and that its employment ought to be avoided with Bluetooth positioning systems [2.21].

In addition, there are ideas of exploiting other parameters than RSSI for positioning purposes. Link Quality and Bit Error Rate (BER) are the most commonly referred in this context. However, it should be stated that these solutions are still under development, and that the Link Quality is not uniquely defined and is therefore dependent on the equipment manufacturer. Also, BER parameter is not defined in the basic Bluetooth specifications and must be

extrapolated from the message received as a response to echo command supported at L2CAP layer. All in all, these parameters undoubtedly contain location dependent information, but the extraction of that information is still subject to research.

The accuracy of Bluetooth positioning systems is decreasing with the increase in the maximal range of the system [2.22]. That is, with the range increase, the positioning system uncertainty is increased as well, therefore the accuracy is worsened. The improvement of accuracy can be achieved through communicating with more than one Bluetooth nodes and possibly utilizing some of the aforementioned parameters (RSSI, Link Quality, BER). Finally, the major application of Bluetooth technology is expected in *ad-hoc* networks and the positioning techniques and LBS should be conceived and designed accordingly.

2.4.3.3 UWB (Ultra-WideBand) Positioning Systems

Ultra-wideband is a short-range high data throughput radio technology. The ultra-wideband signal is defined [2.23] as a radio-signal that occupies at least either 500MHz of frequency spectrum or 20% of the central frequency of the band. There are many ways in which the UWB signal can be generated. Two, most important from the positioning point of view, are:

1) Impulse UWB – By generating very short impulses, with sub nanosecond duration, that are mutually separated several tenths of nanoseconds. Clearly, this signal inherently possesses very wide band.
2) Frequency Hopped UWB – By generating the typical DSSS (Direct-Sequence Spread Spectrum) with the signal spectrum ranging from 10 to 20MHz which is then hopped around 1GHz frequency, applying between 10 and 100 thousands of hops per second.

Unlike conventional radio-signals, the impulse UWB signals are practically immune to multipath propagation problems. With conventional signals, the reflected component of the signal is, in its large part, overlapped with the component that is travelling the direct path. Hence, the direct and reflected component interfere at the receiver causing fading. Contrary to that, with the impulse UWB technology, due to the very short pulse duration, the reflected component is most often arriving at the receiver after the direct component has been completely received. With respect to this feature, the UWB positioning techniques utilising high resolution TOA approach come as the logical choice. Typically, the position accuracy of 1m in more than 95% of the cases is achievable.

Employing the mobile nods of the UWB network for accuracy improvement is also under research. Computer simulation [2.24] shows that the positioning error could be further reduced by employing a larger number of antennas with the beamforming capabilities.

Bearing in mind the amount of research in this area, the commercialisation of indoor UWB positioning systems can be expected in proximate future.

2.4.3.4 WLAN Positioning Systems

Positioning techniques in WLAN networks are becoming very popular. The reason for their popularity can be looked in-between the widespread of 802.11 networks and the fact that a broad scope of LBSs can be brought into an existing network without the need for any additional infrastructure. There are a number of approaches to the positioning problem in WLAN networks. Unquestionably, the most popular ones are based on the Received Signal Strength Information (RSSI). Nevertheless, there are other approaches that depend on timing measurements or require additional hardware but offer superior accuracy and/or faster implementation in return [2.25] – [2.27].

Positioning with the use of RSSI parameter can be, in its essence, regarded as the path loss estimation problem. The nature of the path loss prediction in an indoor environment is extremely complex and dependent on a wide variety of assumptions (e.g. type of the building, construction, materials, doors, windows, etc.)[2.28]. Even if these basic parameters are known, precise estimation of the path loss remains a fairly complex task.

Depending on the side on which the position calculation process takes place, positioning in WLAN networks with the use of RSSI parameter can be either network-based or client-based. Whereas the client-based solutions gather the RSSI vector from the radio-visible APs (Access Points), the network-based solutions have a central positioning engine which collects the client's signal strength vector from the APs and produces the position estimate. The network-based solutions do not require clients to have a specific software installed which is of great essence for security purposes. Moreover, the client does not need to be associated with the network – the positioning can be done solely based on the probe requests the client sends (in case of active scanning). Network-based solutions could also have an important advantage over the client-based ones when used in WLAN networks employing the Automatic Radio Management (ARM). This centralized mechanism is used to obtain the optimal radio coverage by changing the channel assignment and adjusting the output power and/or radiation pattern of the APs. Contrary to the client-based solutions, the network-based positioning engine could take into account the changes made by ARM mechanism while the ARM mechanism would present a setback for the client-based solutions. On the other hand, client's Network Interface Cards do not have to be consistent regarding the radiated power which may, depending on the positioning algorithm used, present an analogue problem for network-based solutions. In this

work, for explanatory purposes, usually the client-based solution will be presented. However, the reader should keep an open mind towards the analogue network-based option.

Regarding the approach used to determine the user's position, WLAN positioning techniques can be categorised as: propagation model based, fingerprinting based or hybrid.

- Propagation model based techniques rely on statistically derived mathematical expressions that relate the distance of an AP with the client's received signal strength. The estimated position of the user is then obtained by lateration. Therefore, if there are less than three radio-visible APs (for two-dimensional positioning) the estimated user's position is ambiguous. Also, the model derived for one specific indoor environment is usually not applicable to other indoor environments.
- Fingerprinting techniques are most commonly used for WLAN positioning. They are conducted in two phases: the off-line or training phase, and the on-line or positioning phase. The off-line phase comprises collecting the RSSI vectors from various APs and storing them, along with the position of the measurement, into a fingerprinting database. In the on-line phase, the estimate of the user's position is determined by "comparing the likeliness" of the RSSI vector measured during the on-line phase with the previously stored vectors in the database. The fingerprinting process is shown in Fig. 2-8. These techniques have yielded better performance than other positioning techniques, but are believed to have a longer set-up time.
- Hybrid techniques combine features from both propagation modelling and fingerprinting approaches, opting for better performances than propagation model techniques and shorter set-up time than fingerprinting techniques [2.29].

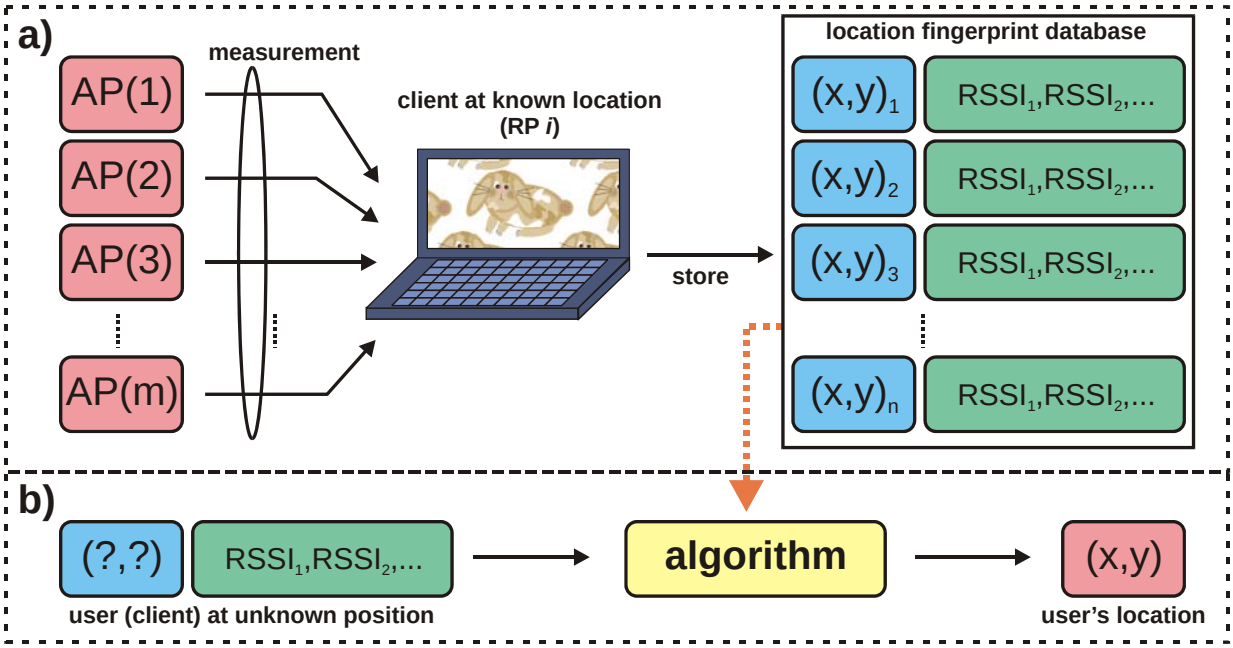

Fig. 2-8 Two phases of positioning: a) training phase – mobile client is recording RSSI vectors across RPs and stores them in fingerprint database, and b) positioning phase – based on the measured RSSI vector and database access, the algorithm estimates the user's location

The prospects of using RSSI parameter for indoor positioning were first systematically analysed in "RADAR" [2.19]. According to this research, it is better to use RSSI than SNR (Signal to Noise Ratio) for positioning purposes since the RSSI parameter is much more dependent on the client's position than SNR. Two algorithms to establish the user's location were proposed. The first one is the Nearest Neighbour (NN) algorithm which compares the RSSI vector of a mobile client against the RSSI vectors previously stored in the fingerprinting base. The performances of NN algorithm have been given in Table 2-I. For comparison, the authors also gave the performances of the Cell-ID like algorithm (the user is being assigned the location of the AP with the strongest RSSI) and the "random" algorithm which randomly gives the location estimates regardless of the inputs.

Table 2-I Accuracy performances summary of nearest neighbour empirical algorithm [2.19]

Method	25th percentile DE [m]	50th percentile DE [m]	75th percentile DE [m]
Empirical (NN)	1.92	2.94	4.69
Strongest (Cell-ID)	4.54	8.16	11.5
Random	10.37	16.26	25.63

An extension to the proposed NN algorithm was also considered: the estimated location is not identified as only one RP whose RSSI vector is closest to the observed RSSI vector, but

calculated as a "middle" point of k closest RPs (kNN algorithm). This analysis has shown that algorithm performance improved for $k = 2$ and $k = 3$. For larger k, the performance had started to decrease. The second algorithm is based on a simple propagation model with Rician distribution assumed. It ought to be emphasized that both approaches require a minimum of three radio visible access points (APs). The reported performances were 3m and 4.3m median errors for empirical kNN and propagation model approaches, respectively. The measuring campaign comprised 70 RPs. At each RP measurements were made for four orientations of the receiver, and each measurement was averaged from 20 samples.

To produce the maximum amount of information from the received RSSI vectors, the Bayesian approach was proposed [2.30]. This concept yields better results than the NN algorithm. The Bayes rule can be written as:

$$p\left(l_t \mid o_t\right) = p\left(o_t \mid l_t\right) p\left(l_t\right) N, \tag{2.15}$$

where l_t is location at time t, o_t is the observed RSSI vector at time t, while N is a normalizing factor that enables the sum of all probabilities to be equal to 1. In other words, at a given time t, the probability that a client is at location l_t, if the received RSSI vector is o_t, is equal to the product of the probability to observe RSSI vector o_t at location l_t and the probability that the client can be found at location l_t. The process of estimating client's location is based on calculating the conditional probability $p(l_t \mid o_t)$ for each RP. The estimated client's location is equal to the RP with the greatest conditional probability. To accomplish this task, two terms on the right hand side of Eq. (2.15) ought to be calculated. The first term, also referred to as the likelihood function, can be calculated based on the RSSI map (for all RP) using any approach that will yield probability density function of observation o_t for all RPs. As for the a priori probability $p(l_t)$, it ought to be calculated according to the client's habits. However, for most cases the assumption of uniform distribution across all RPs is valid. Using this approach, the authors managed to achieve the 2m median error. The measurements were made at 70 RPs. As with the previously discussed techniques, the measurements were made for four orientations of a receiver, and each measurement was averaged from 20 samples.

Another project, named Horus [2.31], [2.32], had the goal of providing high positioning accuracy with low computational demands. This is also a probabilistic approach in which time series of the received signal strength is modelled using Gaussian distribution. Due to the time dependence of the signal strength from an observed AP, the authors of this project have shown that the time autocorrelation between the time adjacent samples of signal strength can be as high as 0.9. To describe and benefit from such behaviour, they have suggested the following autoregressive model:

$$s_t = \alpha s_{t-1} + (1-\alpha)\upsilon_t, \quad 0 \le \alpha \le 1 \tag{2.16}$$

where υ_t is the noise process and s_t is a stationary array of samples from the observed AP.

Throughout the off-line phase, the value of parameter α is assessed at each RP and stored into the database along with Gaussian distribution parameters μ and σ. In the on-line phase, Gaussian distribution is modified according to the corresponding values of α retrieved from the fingerprinting database. Alike to the kNN algorithm, the Horus system estimates the client's location as a weight centre of *k* RPs with the highest probabilities. The principal difference to the kNN algorithm is that, in case of Horus system, the *k* most likely RP are multiplied with their corresponding probabilities. For verification purposes, the authors made measurements at 612 RPs, and each measurement was averaged from 110 samples. The attained median error was 2m.

More relevant information about the statistical modelling approach towards location estimation can be found in [2.33] and in the references found therein.

Battiti *et al.* [2.34] were the first to consider using Artificial Neural Networks (ANNs) for positioning in WLAN networks. This approach does not insist upon a detailed knowledge of the indoor structure, propagation characteristics, or the position of APs. A multilayer feedforward network with two layers and one-step secant training function was used. The number of units in the hidden layer was varied. No degradation in performance was observed when the number of units grew above the optimal number. For verification purposes, measurements were made at 56 RPs, and each measurement was averaged from 100 samples. This way, the median error of 1.69m was obtained. The authors also studied how the increasing number of measured RSSI samples in each RP impacts the accuracy. The obtained dependency is given in Fig. 2-9 and shows the increasing accuracy with the additional measured samples.

In most studies, WLAN positioning techniques are compared on the subject of their accuracy while other attributes of a positioning technique such as latency, scalability, and complexity are neglected (often enough even omitted). Another aspect that is seldom analyzed is the size of the environment in which the technique is implemented. The comparison of the WLAN positioning techniques regarding the accuracy and other available performance parameters will be given in Section 4.4.

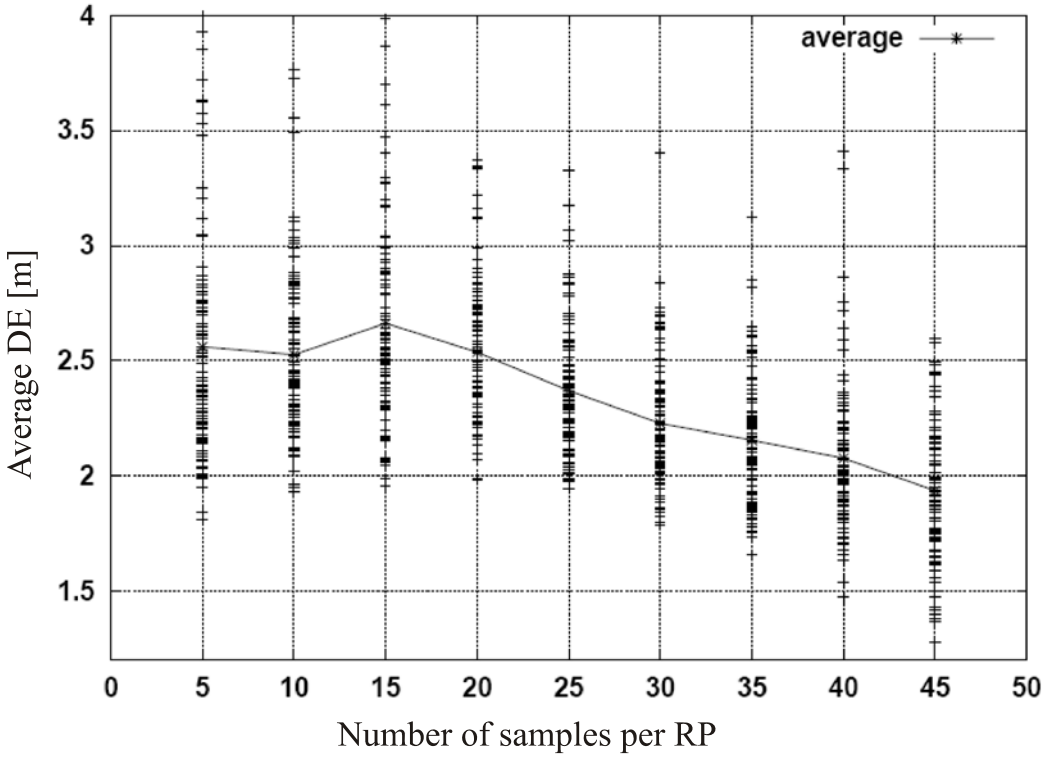

Fig. 2-9 Influence of the number of samples per RP on positioning accuracy [2.34]

It also ought to be pointed out that averaging the RSSI vectors in the on-line phase has an immense impact on the technique's latency, so the scope of location based services that could be utilized with such techniques might be significantly narrowed. Moreover, bearing in mind that all presented approaches had at least three radio-visible APs in each RP (which is seldom the case in most WLAN installations), feasibility of sound frequency planning is uncertain. Consequently, the degradation of packet data services is inevitable with respect to positioning in larger indoor areas (i.e. large number of APs is required). Enabling the radio-visibility of three APs across the indoor environment is usually constructively irrational and economically unjustified. Hence, the presented techniques cannot be applied to the majority of existing WLAN networks optimized for packet data services.

Finally, there are other studies that accompany the research for sophisticated positioning in WLAN networks. Other relevant research efforts comprise the impact of Network Interface Card on the RSSI parameter, compensation of small-scale variations of RSSI, clustering of locations to reduce the computational cost of positioning, use of spatial and frequency diversity, methods for generating a larger location fingerprinting database by interpolation, and unequal fusing of RSSI from different APs [2.35] – [2.41].

2.5 Outdoor Positioning

This section describes the positioning solutions that primarily aim at procuring location information in outdoor environment. Based on the network infrastructure, the satellite and cellular positioning systems are presented. Considering the scope of the thesis, the latter group of positioning systems has been granted significantly greater attention.

2.5.1 Satellite Positioning Systems

The present section focuses on the positioning systems that use a satellite infrastructure to determine the location of a mobile user. The systems considered in this chapter are GPS (and DGPS), GLONASS and Galileo.

2.5.1.1 Global Positioning System (GPS)

GPS is an Global Navigation Satellite System (GNSS) operated by the US Department of Defence and consists of a satellite infrastructure composed of at least 24 orbiting satellites (21 operational satellites and 3 active back-up satellites) and of a terrestrial infrastructure (1 Master Control Station in Colorado Springs and 5 other monitoring stations around the world).
Positioning is performed by a receiver that measures its distance to GPS satellites transmitting spread spectrum signals. This requires that the receiver knows the exact location of the satellites at the time the measurement is made.

- Distance measurement to at least four satellites enables three dimensional positioning and compensation of clock error.
- Distance measurement to three satellites enables two dimensional positioning and compensation of clock error.
- The accuracy of the location estimates obtained with GPS varies depending on the environment (GPS offers better performance in open areas than in areas where a large part of the sky may be masked, e.g. city centres).
- The average accuracy of GPS is contained between 10 m and 100 m depending on the environment.

The US Department of Defence has commissioned a new set of GPS satellites (so called Block II F group) whose deployment started in 2005. This upgraded GPS is not yet entirely available but, upon deployment, it should offer an accuracy of 2 m – 6 m.
The overall availability of GPS is very high except in areas where the visibility to satellites is low or null (e.g. urban canyons, indoors).
The Time to First Fix (TTFF) of a GPS receiver varies depending on the type of start:

- Cold start: no information is available in the receiver (almanac, ephemeris, time of Day, etc). Then, TTFF is generally included between 30s and 30 min.
- Warm start: time of day, almanac and last position are known by the receiver but the ephemeris is no longer valid (this corresponds to a situation where the receiver has not seen satellites for the past few hours). Then, TTFF ranges from a few seconds to 60 s.
- Hot start: this corresponds to the most favourable situation where all the necessary information is available in the receiver and the satellites have been seen during the last two hours. In such a case, the TTFF is under 20 s.

The main limitation of conventional GPS concerns its lack of availability in indoor or heavily masked environment.

New techniques for the acquisition, demodulation, decoding and interpretation of GPS signals could enable to determine positioning with a shorter latency, even in signal obstructed environments. This capability could be available to stand-alone GPS units or integrated into wireless devices such as mobile telephones and PDAs. In this latter case, this would enable to achieve A-GPS (Assisted-GPS) performance level without requiring any assistance from a third party (cellular network in this case). In particular, and contrary to A-GPS, the positioning would require no capacity, investment or operational modifications on cellular network.

This technology is readily available as there are many different GPS receivers available on the market and many applications and services based on GPS are currently deployed all around the world.

The performance of basic GPS can be improved through the use of augmentations to the basic system. Up to now, augmentations generally aimed at improving the accuracy and integrity performances. However, more and more studies and projects are addressing the possibility to improve availability in highly constrained environments.

The most significant improvement of accuracy is known as Differential GPS (DGPS). DGPS consists of broadcasting differential corrections obtained with a reference station. The reference station knows its exact location and compares it permanently with the calculated GPS position. This enables to calculate corrections that are broadcast continuously and can be used by GPS receivers to improve their own position determination.

2.5.1.2 GLONASS Positioning System

GLONASS is a Russian satellite positioning system based on a concept similar to the US GPS. Some receivers are able to decode both GPS and GLONASS signals, thus enabling to use an increased number of satellites compared with basic GPS. However it must be noted that these

dual receivers have not a wide diffusion and their cost is very high, thus making their use almost impossible for mass-market applications.

2.5.1.3 Galileo Positioning System

Galileo is also a GNSS currently being built by the European Union and European Space Agency (ESA). This project is an alternative and complementary to the U.S. Global Positioning System (GPS) and the Russian GLONASS. A reason given for Galileo as an independent system was that, though GPS is now widely used worldwide for civilian applications, it is a military system which as recently as 2000 had Selective Availability (SA) feature that could, if enabled, significantly decrease the performances in particular areas of coverage. Therefore Galileo's proponents argued that civil infrastructure, including aeroplane navigation and landing, should not be left relying solely upon GPS.

The Galileo fully deployed system should consist of 30 satellites in Medium Earth Orbit (MEO) and should be operational by 2013 but later press releases suggest it was delayed to 2014 [2.42].

When in operation, it will have two ground operations centres, one near Munich, Germany, and another in Fucino, Italy.

Galileo is intended to provide more precise measurements than those available through GPS or GLONASS (Galileo will be accurate down to the metre range) including the height (altitude) above sea level, and a better positioning services at high latitudes.

Like with GPS, use of basic (open) Galileo services will also be free for everyone. However, more qualified services will be accessible with pecuniary or military restrictions.

2.5.2 Cellular Positioning Systems

GSM (Global System for Mobile Communications) is the most popular standard for PLMN in the world. This second generation system introduced digital communication and thereby significantly improved the quality of experience for mobile telephony users. Moreover, GSM pioneered short text messages and packet data services. The GSM Association, estimates that 80% of the global mobile market uses the standard [2.43].

Universal Mobile Telecommunications System (UMTS), the successor of GSM, is one of the third-generation (3G) cellular technologies. The most common form of UMTS uses W-CDMA (Wideband Code Division Multiple Access) as the underlying air interface. It is standardized by the 3GPP, and is the European answer to the ITU IMT-2000 requirements for 3G cellular radio systems.

The popularity and widespread of GSM and UMTS had made researchers to turn their focus towards finding a superior positioning technique for this technologies.

Location techniques, proposed in the Access Networks, GSM (ETSI) and UMTS (3GPP) standards are:

GSM [2.44]

- Cell Id + Timing Advance (TA),
- Time of Arrival (TOA) based on handover measurements at different BTS,
- Enhanced Observed Time Difference (E-OTD) based on BCCH timing measurements from different cells at target MS (Mobile Station), and
- Assisted Global Positioning System (A-GPS).

UMTS [2.45]

- Cell Id + Round Trip Time (RTT) - similar to GSM Cell Id + TA method,
- Angle of Arrival (AOA),
- Observed Time Difference of Arrival (OTDOA) - similar to GSM E-OTD method, and
- Assisted-GPS - similar to GSM's A-GPS.

Cell ID + TA (RTT in UMTS) – The position of a target mobile station (or UE - User Equipment in UMTS) is estimated with the knowledge of its serving cell. The accuracy varies according to the size of the cell. The radius of a cell may vary from less than a 100m to 35 km (for GSM). Accuracy is generally greater in urban areas with a dense network of smaller cells than in rural areas where there are fewer BTSs (Node-B stations in UMTS). The TA (RTT) parameter is an estimate of the time needed for signal to propagate from the serving BTS (Node B) to the MS (UE) and back. It is used to synchronize the bursts arriving from mobile handset to BTS (Node-B).

Drawbacks:

- Low accuracy varying from 100 - 1100 m.

Advantages:

- No modifications to handset. Requires only MLC (Mobile Location Centre) in the network. Low cost,
- Usable for all existing equipment and across networks, and
- Fast response, approximately 1 sec.

Observed Time Difference of Arrival - Idle Period Down Link (OTDOA - IPDL) – This method is quite similar to TOA in GSM, except that the UE also performs the calculations. OTDOA is a time-based method, whereby the handset measures the arrival of time of signals transmitted from the 3+ Node-Bs and this requires new function in handset. In UE-assisted OTDOA, the timing measurements are transferred from UE to the SRNC (Serving Radio

Network Controller) using standardized LBS signalling. The position of the UE is estimated using trilateration and this also requires the accurate position of each Node-B. In UE-based OTDOA, the handset performs the position calculation and the information is returned to the SRNC. For unsynchronized networks, the real time difference between the Node-Bs must be measured using a fixed Location Measurement Unit (LMU) whose location is known. LMU receives the signals between pair of Node-Bs to perform measurements and return them to SRNC. LMU can be avoided by synchronizing Node-Bs with GPS.

Drawbacks:

- Average accuracy between 50-200 m,
- Added software required in the handset and high impact on the network - high cost,
- For roaming, implementation of E-OTD requires major modifications since the roamed-to network must have LMUs, and
- Non resistant to multi-path propagation.

Advantages:

- Fast response – approximately 5 s, depending on the network latency.

Angle of Arrival (AOA) – The angle of arrival method requires the installation of directional antennas or antenna arrays. The method determines location of the MS based on angulation. The intersection of two directional lines each formed by a radial from a Node-B defines a unique position for the UE. This method requires the UE to have knowledge of a minimum of two Node-Bs (or one pair). If available, more than one pair can be used (most common is three Node-Bs which yields two pairs). The method also requires LoS to the involved Node-Bs for the position estimate to be accurate.

Drawbacks:

- Susceptible to multipath interference,
- Relatively low accuracy (approx. 300 m), and
- Larger infrastructure costs for installation of additional directional antennas.

Advantages:

- No modification to handset necessary, and
- Requires only a minimum of 2 cells sites to determine a user's location.

Assisted Global Positioning System (A-GPS) – The assisted GPS is a time-based method, whereby the handset measures the arrival time of signals transmitted from 3+ GPS satellites, to determine its position. Adding GPS functionality has high impact on the handset with new hardware (GPS receiver) and software required. The impact on the network is low, requiring only support from the SRNC. The conventional GPS might normally require few minutes to obtain a first position and the time is too long. In A-GPS, the assistance information is sent

from the reference GPS receiver in the network (SRNC) to reduce that time. The wireless network, based on the approximate location of the handset (generally the location of the closest cell site), determines which GPS satellites should be relevant for calculating its position. This additional information is provided to the UE. The handset then takes a reading of the proper GPS signals, calculates its distance from all satellites in view and sends this information back to the network. There are two implementations of A-GPS. UE assisted, whereby the measurements are passed back to the network for position calculation and UE based, where the position is calculated in the handset. A-GPS implementation mainly impacts UE and SRNC and has low dependency on Radio Access Network.

Drawbacks:

- Heavy battery-use of handset,
- Initial response time slow compared to other technologies,
- Integration of GPS receiver required in handset – high impact, and
- Low availability in indoor environments.

Advantages:

- High accuracy (10-50 m),
- Proven technology,
- Avoids expensive modifications to the network, and
- Roaming can be supported easily.

From the aforementioned, it is obvious that there is no ideal positioning solution for UMTS users and that there is much more space for further improvement left. Due to the fact that UMTS networks are seldom found without collocated GSM networks and that most of the techniques standardized for UMTS have evolved from similar GSM positioning techniques, the research presented herein will address positioning techniques that use the information available from both the UMTS and GSM networks.

Basically, all the standardised positioning techniques come with a few drawbacks as well. That is why there is no unique solution widely accepted by the network operators. On the other hand, the same reasons induced an increasing part of research community to work on improving the aforementioned positioning solutions by adding various tricks of trade. Usually, they depend on additional signal processing [2.46] in order to improve on positioning performances.

The most basic techniques are founded on serving cell identification (Cell-ID) [2.47]. In this way, the MS can be located with the accuracy given by the cell radius. Bearing in mind that the cell radius can be extended beyond 35km (in case of GSM), it becomes obvious that this technique does not grant preferable accuracy. On the other hand, it is considered to be the

simplest technique within PLMN based positioning systems. Various non-standardized augmentations to this plain technique have been made. Adaptive enhanced Cell-ID is a self learning method that uses precise position results of opportunity, together with fingerprinting radio measurements to populate the fingerprinting database. The method can also make use of other information like signal strength and time measurements. This approach has yielded a 20-50% reduction in the size of the area where the user equipment is located. The paper [2.48] reports this method's field results.

Most of the other positioning algorithms enrich the Cell-ID information with RSS (Received Signal Strength) measurements. Simulation results using statistical modelling of RSS [2.49] achieved accuracy of 320m with 67% confidence (320m | 67%) which is 70 – 75% better than basic Cell-ID technique's performances. Accuracy performances of this approach are summarized in Table 2-II.

Table 2-II Summary statistics for the simulation of Statistical Modelling Approach [2.49]

DE	Statistical Modelling Approach	Cell-ID
Average DE [m]	279	1092
Median DE [m]	237	773
67^{th} percentile DE[m]	320	1262
95^{th} percentile DE [m]	620	3108
Maximum DE [m]	1930	5015

Genetic algorithms are an optimisation technique that was tried-out for positioning. Their employment in the UMTS network [2.50] resulted in accuracy of 450m | 72%. The parameters that were used for genetic algorithms optimisation technique are shown in Table 2-III. There is an additional issue with using the genetic algorithms for positioning. Namely, with each positioning request the whole population/selection simulation has to be rerun. Therefore, their latency, is usually unsustainable for a broad number of LBS. In this study, the reported computing time (latency) was 7s.

Table 2-III Parameters of genetic algorithms used for positioning [2.50]

Fitness Function	Cumulative Error
Population Size	100

Parent Size	20
Selection Algorithm	Tournament Selection
Number of Generations	50
Ratio of Elite, Crossover & Mutation Children	4:80:16

When regarding the Database Correlation Method (DCM) with RSS, the fingerprinting database can be constructed two-fold: from actual field measurements, or from RSS estimates obtained by some form of propagation model. The first approach produces more accurate fingerprinting database, however, it consumes significantly more time for measurement campaign. In [2.51], the DCM was used on a fingerprinting database obtained with commonly used propagation models. For correlation metrics the following equation was used:

$$d(k) = \sum_i \left(f_i - g_i(k) \right)^2 + p(k) \tag{2.17}$$

where f_i is the RSS measured by the MS on the *i*-th channel, $g_i(k)$ is the RSS of the *k*-th database fingerprint on the same channel, *i* refers to the number of selected cells or channels, and $p(k)$ is the penalty term contributed by the channels that are radio-visible in only one of the fingerprints. Actual field RSS measurements were used to verify the accuracy performances. The method achieved an accuracy of 483m | 67% in the urban environment. Other accuracy performances of this method are presented in Table 2-IV.

Table 2-IV Accuracy summary for RSS DCM positioning technique

DE	Rural	Suburban	Urban
Minimum DE [m]	168	204	198
Maximum DE [m]	906	782	1008
Average DE [m]	475	371	653

Another course in PLMN positioning uses timing parameters, such as Timing Advance (TA) parameter in GSM, or Round Trip Time (RTT) and the Rx-Tx observed time difference in UMTS. It should be noted that these parameters can only estimate the distance between the mobile terminal and the serving base station (or Node B in case of UMTS). Only in the case when there are more than two Nodes B in the active set (Node Bs involved in a soft handover

procedure) can the location estimate be obtained through the process of multilateration. It ought to be pointed out that this situation occurs seldom. In case of GSM the situation is even less favourable. At any given time there is only one TA parameter available. Therefore, this type of information by itself is generally insufficient for precise positioning and is, most often, combined with RSS measurements. Moreover, the RTT parameter is not even available in all UMTS networks.

In [2.52], a simulation of the database correlation method using RTT and power delay profile yielded a 15m median DE, 25m | 67%, and 135m | 95% accuracy. Similar accuracy performances (15m median DE, 20m | 67%, and 115m | 95%) were recorded in [2.53] where a novel selection criterion was used to choose the three optimal RTT values (in non-line-of-sight conditions) for subsequent trilateration. Nevertheless, none of the studies involving real measurements endorse such superb accuracy.

Note that none of the presented techniques offers straightforward precise positioning in PLMN. Positioning based on timing measurements (TDOA based) require additional network components. RSS and hybrid RSS + TA (RTT) solutions have not shown sufficient accuracy thus far. Even if the satellite based techniques are included, they up to date fail to provide seamless indoor-outdoor positioning and the handset impact in terms of price and battery consumption remains an issue.

The initial location estimate can further be improved if consecutive estimations can be obtained. In this case the algorithm is referred to as the “tracking algorithm”. Kalman filter [2.54], post filtering using a state-space model [2.55] and probabilistic approaches [2.56] can be used as tracking algorithms. Moreover, the initial location estimate can be improved by a map matching process which coerces the estimated location to a specific area on the map [2.57]. Nevertheless, this work investigates only the initial location determination stage and overlaid algorithms fall outside its scope.

2.6 References

[2.1] Collomb Frédéric, Location Service Study Report (Loc_Serv_Study_Rep_PU.doc), Mobile and Vehicles Enhanced Services, 2002.

[2.2] Basic Statistical Definitions. http://www.weibull.com/AccelTestWeb/basic_statistical_definitions.htm Retrieved on 2010-09-22.

[2.3] Weisstein, Eric W. "Rayleigh Distribution." From MathWorld--A Wolfram Web Resource. http://mathworld.wolfram.com/RayleighDistribution.html Retrieved on 2010-09-22.

[2.4] The FCC, ”Fact Sheet—FCC Wireless 911 Requirements,” FCC, (January 2001).

[2.5] Coordination Group on Access to Location Information for Emergency Services (CGALIES), ”Final report. Report on implementation issues related to access to location information by emergency services (E112) in the European Union,” (2002). http://ec.europa.eu/environment/civil/pdfdocs/cgaliesfinalreportv1_0.pdf Retrieved on 2010-09-22.

[2.6] Gu, Y., Lo, A., Niemegeers, I.: A survey of indoor positioning systems for wireless personal networks. Communications Surveys & Tutorials, IEEE, Volume 11, Issue 1, pp. 13 – 32 (First Quarter 2009)

[2.7] van Diggelen, F.: Indoor GPS theory & implementation. Position Location and Navigation Symposium, 2002 IEEE pp. 240 – 247 (April 2002)

[2.8] Ahonen, S., Eskelinen, P.: Mobile terminal location for UMTS. Aerospace and Electronic Systems Magazine, IEEE Volume 18, Issue 2, pp. 23 – 27 (Feb. 2003)

[2.9] Roy Want, Andy Hopper, Veronica Falcao, and Jon Gibbons, „The Active Badge location system“, ACM Transactions on Information Systems, 10(1):91–102, January 1992.

[2.10] Krohn, A. Beigl, M. Hazas, M. Gellersen, H.-W, „Using fine-grained infrared positioning to support the surface-based activities of mobile users“, Distributed Computing Systems Workshops, 2005. 25th IEEE International Conference on, Telecooperation Office, Karlsruhe Univ., Germany.

[2.11] Masaki Maeda, Takefumi Ogawa, Takashi Machida, Kiyoshi Kiyokawa, Haruo Takemura, „Indoor Localization and Navigation using IR Markers for Augmented Reality“, HCI International 2003 Interactive demo

[2.12] Esko O. Dijk, „Indoor ultrasonic position estimation using a single base station“, Technische Universiteit Eindhoven, 2004. October 6, 2004, p44-45

[2.13] Mike Fraser, „Mobile and Ubiquitous Computing: Sensing Location Indoors.“, COMSM0106, 2006.

[2.14] Michael R. McCarthy, Henk L. Muller, „RF Free Ultrasonic Positioning“, University of Bristol, 7th International Symposium on Wearable Computers, October 2003.

[2.15] Hae Don Chon, Sibum Jun, Heejae Jung, Sang Won An, „Using RFID for Accurate Positioning“, Journal of Global Positioning Systems, 2004, Vol. 3, No. 1-2: 32-39.

[2.16] Muller N., „Bluetooth Demystified“, McGraw-Hill, New York, 2001.

[2.17] Bluetooth Special Interest Group (2001). Specification Volume 1, Specification of the Bluetooth System, Core. Version 1.1, February 22, 2001.

[2.18] Bluetooth Special Interest Group (2001). Specification Volume 2, Specification of the Bluetooth System, Profiles. Version 1.1, February 22, 2001.

[2.19] Bahl, P. & Padmanabhan, V. (2000). „Radar: An in-building RF_based user location and tracking system“, Proceedings of the IEEE Infocom 2000, Tel-Aviv, Israel, vol. 2, Mar. 2000, pp. 775-784.

[2.20] Patil, A., „Performance Of Bluetooth Technologies And Their Applications To Location Sensing“, Michigan State University, 2002.

[2.21] K. Thapa, S. Case, „An indoor positioning service for Bluetooth Ad Hoc networks“, in: MICS 2003, Duluth, MN, USA.

[2.22] Hallberg, Nilsson, Synnes, „Positioning with Bluetooth“, Telecommunications, 2003. ICT 2003. 10th International Conference on, Volume 2, Issue, 23 Feb.-1 March 2003 Page(s): 954 - 958 vol.2

[2.23] Dave Harmer, „Ultra Wide-Band (UWB) Indoor Positioning“, Thales Research and Technology UK Ltd. ARTES 4 Project. ESTEC December 2004.

[2.24] Eltaher, Th. Kaiser, „A Novel Approach based on UWB Beamforming for Indoor Positioning in None-Line-of-Sight Environments“, RadioTeCc, October 26-27, 2005, Berlin, Germany.

[2.25] Llombart, M., Ciurana, M., Barcelo-Arroyo, F.: On the scalability of a novel WLAN positioning system based on time of arrival measurements. 5th Workshop on Positioning, Navigation and Communication, 2008. WPNC 2008, pp. 15 – 21 (March 2008)

[2.26] King, T., Kopf, S., Haenselmann, T., Lubberger, C., Effelsberg, W.: COMPASS: A Probabilistic Indoor Positioning System Based on 802.11 and Digital Compasses. University of Mannheim, D-68159 Mannheim, Germany, TR-2006-012

[2.27] Sayrafian-Pour, K., Kaspar, D.: Indoor positioning using spatial power spectrum. IEEE PIMRC 2005. Volume: 4, pp. 2722- 2726 (Sept. 2005)

[2.28] Nešković, N. Nešković, Đ. Paunović, „Indoor Electric Field Level Prediction Model Based on the Artificial Neural Networks“, IEEE Communications Letters, vol. 4, No. 6, June 2000.

[2.29] Wang, H., Jia, F.: A Hybrid Modeling for WLAN Positioning System. International Conference on Wireless Communications, Networking and Mobile Computing, 2007. pp.2152 - 2155 (Sept. 2007)

[2.30] Li, B., Salter, J., Dempster, A., Rizos, C.: Indoor Positioning Techniques Based on Wireless LAN. AusWireless '06, Sydney (March 2006)

[2.31] Youssef, M., Agrawala, A.: The Horus WLAN Location Determination System. Int. Conf. on Mobile Systems, Applications And Services, pp.205–218 (2005)

[2.32] Eckert, K.: Overview of Wireless LAN based Indoor Positioning Systems, Mobile Bussines Seminar, University of Mannheim, Germany, (2005)

[2.33] Roos, T., Myllymaki, P., Tirri, H.: A statistical modeling approach to location estimation. Mobile Computing, IEEE Transactions on, Volume 1, Issue 1, pp.59 – 69, (First Quarter 2002)

[2.34] Battiti, R., Nhat, T. L., Villani, A.: Location-aware Computing: A Neural Network Model For Determining Location in Wireless LANs. Technical Report # DIT-02-0083 (Feb. 2002)

[2.35] Kaemarungsi, K.: Distribution of WLAN received signal strength indication for indoor location determination. 1st International Symposium on Wireless Pervasive Computing, 2006. pp.6 (Jan. 2006)

[2.36] Youssef, M., Agrawala, A.: Small-scale compensation for WLAN location determination systems. Wireless Communications and Networking, 2003. Volume 3, 20-20 pp.1974 – 1978 (March 2003)

[2.37] Youssef, M.A., Agrawala, A., Shankar, A. U.: WLAN location determination via clustering and probability distributions. Proceedings of the First IEEE International Conference on Pervasive Computing and Communications. pp.143 – 150 (March 2003)

[2.38] Ramachandran, A., Jagannathan, S.: Spatial Diversity in Signal Strength based WLAN Location Determination Systems. 32nd IEEE Conference on Local Computer Networks, 2007. pp. 10 - 17 (Oct. 2007)

[2.39] Ramachandran, A., Jagannathan, S.: Use of Frequency Diversity in Signal Strength based WLAN Location Determination Systems 32nd IEEE Conference on Local Computer Networks, 2007. pp.117 - 124 (Oct. 2007)

[2.40] Li, B., Wang, Y., Lee, H.K., Dempster, A., Rizos, C.: Method for yielding a database of location fingerprints in WLAN. Communications, IEE Proceedings-Volume 152, Issue 5, pp.580 - 586 (Oct. 2005)

[2.41] Zhang, M., Zhang, S., Cao, J.: Fusing Received Signal Strength from Multiple Access Points for WLAN User Location Estimation. International Conference on Internet Computing in Science and Engineering, 2008. pp.173 - 180 (Jan. 2008)

[2.42] http://europa.eu/rapid/pressReleasesAction.do?reference=IP/10/7&language=en Retrieved 2010-09-22.

[2.43] GSM Association. 2010. http://www.gsmworld.com/newsroom/market-data/market_data_summary.htm. Retrieved 2010-06-08.

[2.44] 3GPP TS 43.059, release 8 (v8.0.0), GSM/EDGE Radio Access Network, Functional stage 2 description of Location Services (LCS) in GERAN, 2007. http://www.3gpp.org/ftp/Specs/archive/43_series/43.059. Retrieved 2010-09-22.

[2.45] 3GPP TS 25.305, release 8 (v8.0.0), Stage 2 Functional specification of UE positioning in UTRAN, 2007. http://www.3gpp.org/ftp/Specs/archive/25_series/25.305. Retrieved 2010-09-22.

[2.46] G. Sun, J. Chen, W. Guo, K.J.R. Liu, "Signal processing techniques in network-aided positioning—A survey of state-of-the-art positioning designs," IEEE Signal Processing Magazine, vol. 22, No 4, pp. 12–23 (July 2005).

[2.47] 3GPP TS 23.271, release 7 (v7.2.0), Functional Stage 2 Description of Location Services (LCS), Sep. 2005. [Online]. Available: http://www.3gpp.org/ftp/Specs/html-info/23271.htm

[2.48] L. Shi and T. Wigren, "AECID fingerprinting positioning performance," Proc. Globecomm 2009, Honolulu, USA, pp. 2767-2772, (2009)

[2.49] T. Roos, P. Myllymäki, H. Tirri, "A statistical modeling approach to location estimation," IEEE Transactions on Mobile Computing, vol. 1, No 1, pp. 59-69 (January-March 2002).

[2.50] M.J. Magro, C.J. Debono, "A Genetic Algorithm Approach to User Location Estimation in UMTS Networks." Int. Conf. on Computer as a Tool, 2007, pp. 1136 – 1139

[2.51] C.J. Debono, C. Calleja, "The application of database correlation methods for location detection in GSM networks," 2008. 3rd International Symp. on Comm., Control and Signal Processing, pp. 1324–1329

[2.52] S. Ahonen, H. Laitinen, "Database correlation method for UMTS location," The 57th IEEE Semiannual Vehicular Technology Conference, Vol. 4, 2003 pp. 2696-2700

[2.53] S. Bartelmaos, K. Abed-Meraim, E. Grosicki, "General Selection Criteria for Mobile Location in NLoS Situations," IEEE Trans. on Wireless Comms, Vol. 7 (2008), pp. 4393 - 4403

[2.54] S. Knedlik, P. Ubolkosold, O. Loffeld, “A Data Fusion Approach for Improved Positioning in GSM Networks,” IEEE/ION Position, Location, And Navigation Symp, 2006 pp. 218-222

[2.55] D. Catrein, M. Hellebrandt, R. Mathar, “Location tracking of mobiles: A smart filtering method and its use in practice” Proc. IEEE Veh.Technol. Conf., 2004, pp. 2677–2681

[2.56] R. Haeb-Umbach, S. Peschke, “A Novel Similarity Measure for Positioning Cellular Phones by a Comparison With a Database of Signal Power Levels,” IEEE Trans. on Vehicular Technology, Vol. 56, Issue 1, 2007 pp. 368–372

[2.57] H. Laitinen, J. Lähteenmäki, T. Nordström, “Database correlation method for GSM location,” in Proc. IEEE Veh. Technol. Conf., Greece, May 2001, pp. 2504–2808.

3 Artificial Neural Networks (ANN)

3.1 Introduction

Artificial Neural Networks (ANNs) are computational models inspired by biological networks of neurons. They are based on closely interconnected groups of artificial neurons. Essential characteristic of these networks is their adaptive nature, which grants them the ability to model complex relations between inputs and outputs by changing their inner structure during the *learning phase*. When compared to other approaches, this ability gives the ANNs notable advantage in cases when there is not enough knowledge of the problem or the problem cannot be entirely understood. On the other hand, in order to make use of ANN, sufficient amount of *training* data must be made available. The extent of ANN efficiency is exceptionally high concerning the implementations on systems with parallel architecture as well as direct hardware implementations.

The ANNs, as suitable computational systems, can be used to solve a large number of problems where, due to the complexity of data or functions, other models fail to adequately perform. Some of the typical applications of ANNs include: pattern recognition, speech recognition and synthesis, adaptive interfaces between human and complex physical systems, function approximation, financial applications, diagnostics in medicine, spam filters for e-mail, image compression, associative memories, prediction, optimisation, modelling of non-linear systems, unmanned vehicle control, etc.

The application of ANNs for positioning purposes has been the subject of many recent studies. However, there is still opportunity for further improvement. For that matter, the overview of fundamental theoretical knowledge given in this section has the purpose to facilitate the understanding of the ANNs application on positioning problem in current radio systems. Additionally, the *feedforward* ANNs, which are known to efficiently solve the electric field level prediction problem [3.1], have been described in more detail. More details on theoretical foundation and ANN application analysis can be found in [3.1].

3.2 ANN Architecture Analysis

3.2.1 The Model of Computational Neuron

The "artificial neuron" is the atom of an ANN. It translates several inputs into a single output. The basic transfer function of an artificial neuron was initially proposed by McCulloch and Pitts in 1943 [3.2]. They suggested a Linear Threshold Gate – LTG as a computational neuron model (Fig. 3-1). The basic task of LTG is to classify the input vector ***x*** into one of the two possible values of the output, *y*. The LTG's transfer function is given as:

$$y = \begin{cases} 1, & \text{if} \quad \mathbf{w}^T\mathbf{x} = \sum_{i=1}^{n} w_i x_i \geq T \\ 0, & \text{otherwise} \end{cases}, \tag{3.1}$$

where $\mathbf{x}=[x_1 x_2 ... x_n]^T$ and $\mathbf{w}=[w_1 w_2 ... w_n]^T$ are input and weight column vectors, respectively, while *T* is the threshold value.

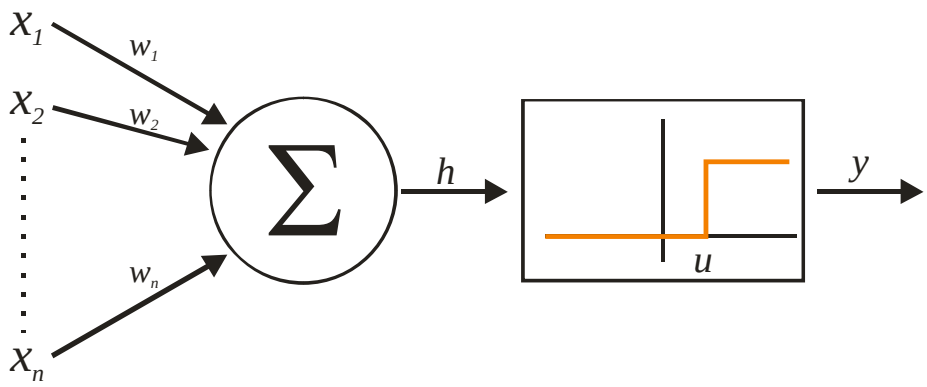

Fig. 3-1 McCulloch-Pitts neuron model [3.1]

To simplify the notation, the threshold value *T* is usually expressed through an additional neuron input as $w_0 = -T$, and $x_0 = 1$.

As the areas of ANN application grew, there has been several modifications of McCulloch-Pitts neuron. Perhaps the most significant one is related to the change in activation function (threshold function – *f*). Besides the LTG, activation function can be implemented in form of piecewise linear, sigmoid or Gaussian functions as depicted in Fig. 3-2. The sigmoid activation function is used most commonly and will be discussed in more details in the forthcoming sections.

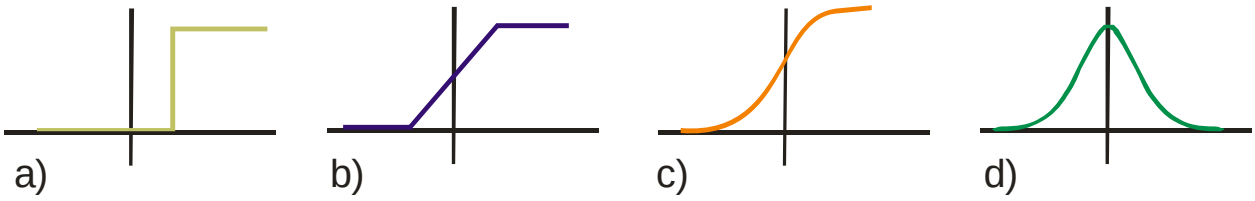

Fig. 3-2 Activation functions: a) threshold, b) piecewise linear, c) sigmoid, and d) Gaussian

3.2.2 ANN Architectures

If ANNs are observed as directed graphs, neurons become the vertices and the connections between the neurons (with weight coefficients) become directed edges. Based on the analysis of topology of such graphs, the ANNs can be split into two main categories:

- feedforward networks – associated graph has no recurrent edges, and
- recurrent or feedback networks – associated graph has recurrent edges.

One of the most significant families of feedforward networks is a multilayer perceptron network. With the networks of this architecture, the neurons are organized in at least three layers and the activation function is non-linear. By using the multilayer perceptron ANN it is possible to solve the problem of non-linear data classification (line in case of 2D, plane in case of 3D and hyperplane in case of multidimensional problem). Multilayer perceptron ANN as well as other commonly used ANN architectures are shown in Fig. 3-3.

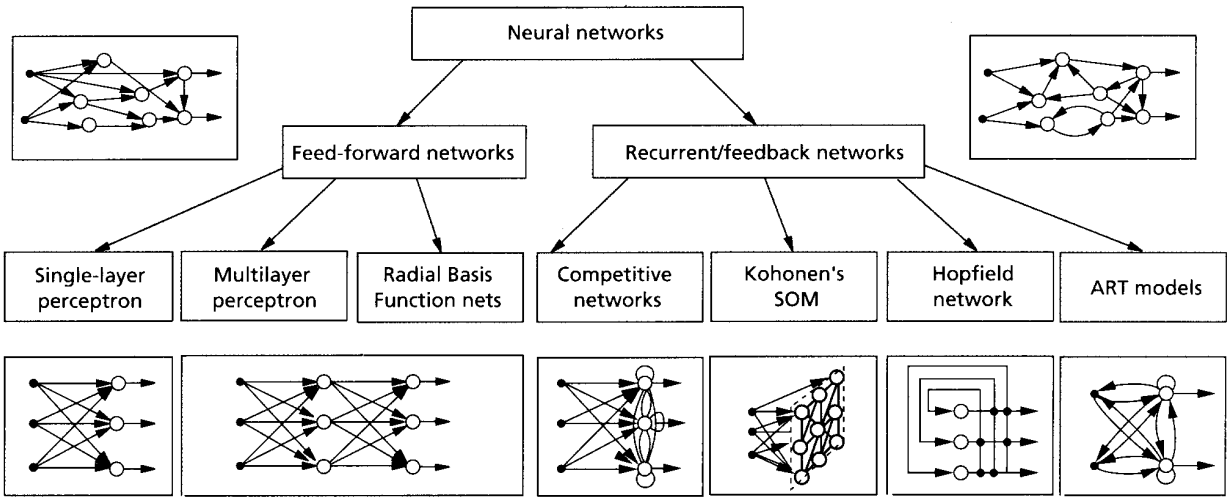

Fig. 3-3 Feedforward and recurrent/feedback ANN architectures [3.1], [3.3]

The characteristics of ANNs are mostly dependent on the manner the vertices are interconnected. Generally, feedforward networks are of static nature [3.1]. As opposed to recurrent networks, they have no memory and, therefore, for a single input set always produce the same output. On the other hand, recurrent/feedback networks are dynamic systems where the output of the network depends not only on its current input but on the state the network is

in. Consequently, new input set changes not only the outputs, but also the current state of the network.

3.2.3 Learning Rule

Fundamental and the most important feature of an ANN is *learning* based on the network's inputs. The learning process in neural networks is based on a defined procedure called the learning rule. This process consists of the gradual adaptation of the weight coefficients with the goal of reducing the predefined error.

In the ANN context, the learning process can be best observed as an optimization procedure. More precise, the learning process can be comprehended as "searching" for the extreme of the *criterion function* in the multidimensional parameter space (the weight coefficient space).

There are three essential learning rules: *supervised learning*, *unsupervised learning*, and *reinforcement learning*. In general, any of these learning rules can be applied to any of the ANN architectures. With supervised learning, for each set of input data, the network is supplied with a desired network output. That way, the network, going through the learning process, adapts its weight coefficients so as to minimize the cost (difference) function between the outputs and the desired (genuine) values. The most commonly used cost function is the mean-square error. On the other hand, with reinforced learning rule, the network is given the assessment of the produced outputs rather than the exact outputs. Finally, unsupervised learning rule does not require the knowledge of the each output value. The function network should perform is defined through criterion function. This learning rule is suitable for detecting the structures in data, data mining and classification.

3.2.4 ANN Architecture Suitable for Positioning

If the problem of positioning a user in mobile radio systems based on the received signal strength is taken into consideration, for a given number of inputs there are usually only two or three outputs (i.e. the coordinates of a user). Based on that, and the aforementioned overview of neural network architectures and learning rules, it is fair to assume that the positioning problem would be best solved by the feedforward neural network architecture. Recurrent or feedback networks better model dynamic problems, where the outputs of the network depend not only on its inputs, but on its previous state. There are research efforts invested in overlaid tracking algorithms, used to improve the initial position estimation by consecutive localization requests. For such applications, recurrent networks may find their use. However, the herein presented work is restrained only to initial positioning which is, in its nature, a different type of problem. The position determination based on received signal strength may be regarded as the electric field level estimation problem. If the initial positioning is observed, the localization is

usually performed for mutually uncorrelated cases. Therefore, this problem can be labelled as static, i.e. given inputs invoke unambiguous outputs, which can be best achieved by using the feedforward network architecture.

Being that the position estimation of a user in a multidimensional space does not belong to a linear class of problems, a simple single-layer perceptron network architecture cannot provide the adequate solution. Hence, the appropriate ANN architecture should be looked in-between multilayer perceptron and Radial Basis Function (RBF) networks.

In the context of prediction and function approximation, both the multilayer perceptron and RBF networks have performed well [3.4]. Generally, multilayer perceptron networks have shown better performances in cases when the training set is difficult to generate (or, likewise, not economically justified) or when the execution speed is important (which is the case for positioning application) [3.1].

It has been shown that multilayer perceptron networks perform global optimisation on the training data. This feature translates to superior generalisation characteristics in comparison to RBF networks. Moreover, the multilayer perceptron networks have shown better extrapolation properties [3.1] (which may be significant for positioning application). This comes as a consequence of a fact that multilayer perceptron networks with sigmoid activation functions in hidden layer perceptrons perform not only approximation of the function, but its derivative as well. Although the RBF networks have considerably shorter training times, bearing in mind the processing power of modern computers, this advantage comes with a limited relevance. On the other hand, with multilayer perceptron networks, all network weights are adjusted in each epoch of the training process. For the type of application where the training data is easily collectable and/or the on-line training is required (e.g. for some adaptive processes), the RBF network would be superior. However, in the positioning context, where collecting the training data is sometimes a highly time consuming task (e.g. indoor environment where no automated reference positioning is available) and the training process is seldom performed, multilayer perceptron networks have considerable advantages compared to RBF and other investigated ANN architectures. Forthcoming sections give details on the fundamentals of multilayer perceptron networks operation and learning processes.

3.2.5 Multilayer Feedforward Networks

This section describes one of the most commonly used neural network architectures – multilayer feedforward neural network. Fig. 3-4 shows an example of multilayer feedforward network with two hidden layers.

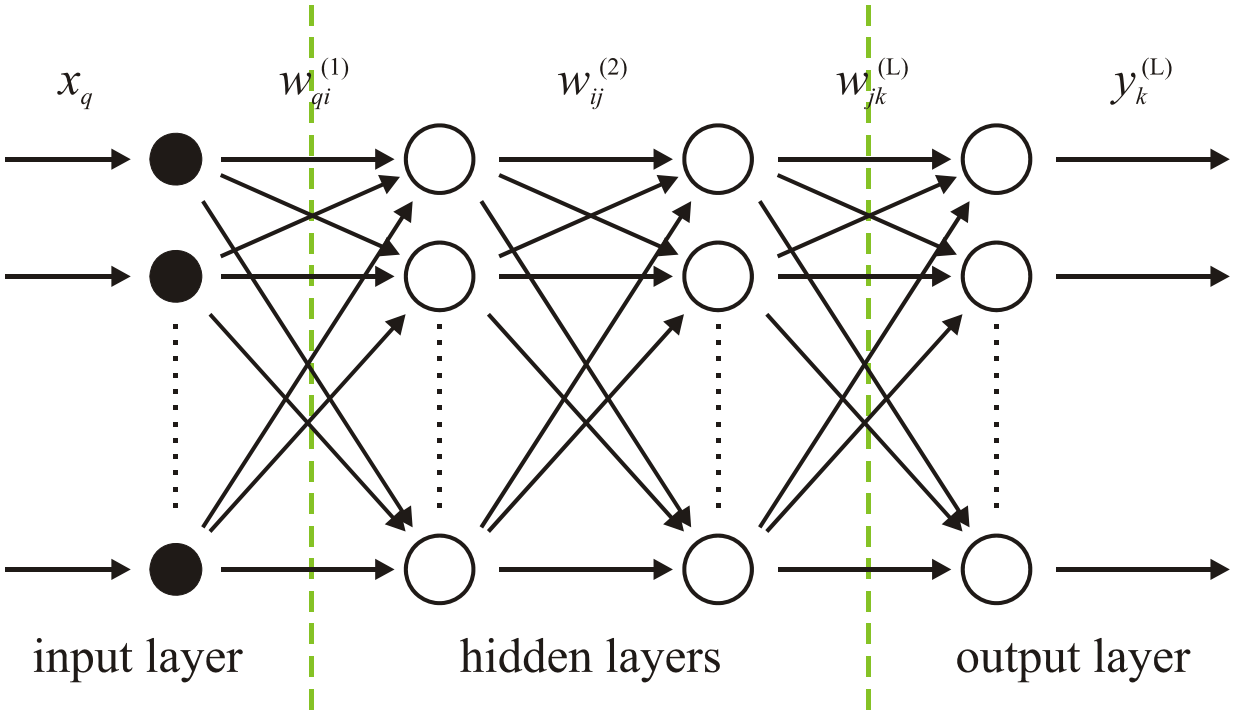

Fig. 3-4 Typical three-layer feedforward neural network architecture

In more general notation, typical feedforward network with L layers implies an input layer (which is not counted in the total number of layers because it only stores the input data without multiplying them with weight coefficients), L-1 hidden layers and an output layer. Layers consist of neural units (vertices of the network), interconnected according to the aforementioned feedforward principle. The edges (links) between the units of the same layer, the units of non-adjacent layers and recurrent links do not exist. This type of networks is commonly coupled with the supervised learning paradigm. The introduction of the *error backpropagation* learning rule has made multilayer feedforward neural network one of the most commonly applied ANNs.

3.2.6 Error Backpropagation Learning Rule

Error backpropagation or just backprop defines an efficient numerical method for altering the weight coefficients in feedforward networks with differentiable neuron activation functions. This method is suitable for use with supervised learning and has been successfully applied onto solving diverse non-linear problems such as: shape recognition, function approximation, non-linear system modelling, electric field level prediction, image compression and reconstruction, etc.

Fig. 3-5 depicts a two-layer feedforward network architecture. Network inputs are denoted as $\{x_0,x_1,x_2,...,x_n\}$, where x_0=1. This set of data forms an input vector $\mathbf{x}\in\mathbf{R}^{n+1}$. The layer which gathers the input data is referred to as the first hidden layer (in this case also the only one). The

hidden layer in Fig. 3-5 has J neurons. The output of the hidden layer is $(J+1)$-dimensional real vector $\mathbf{z}=[z_0,z_1,z_2,...,z_J]^T$, where $z_0=1$. The outputs of the hidden layer, vector $\mathbf{z}$, are, at the same time inputs of the output layer consisted of L neurons. The output layer generates L-dimensional vector $\mathbf{y}$ which corresponds to the input vector $\mathbf{x}$. If the network is optimally trained, the output vector should be close to the "desired" output vector $\mathbf{d}$.

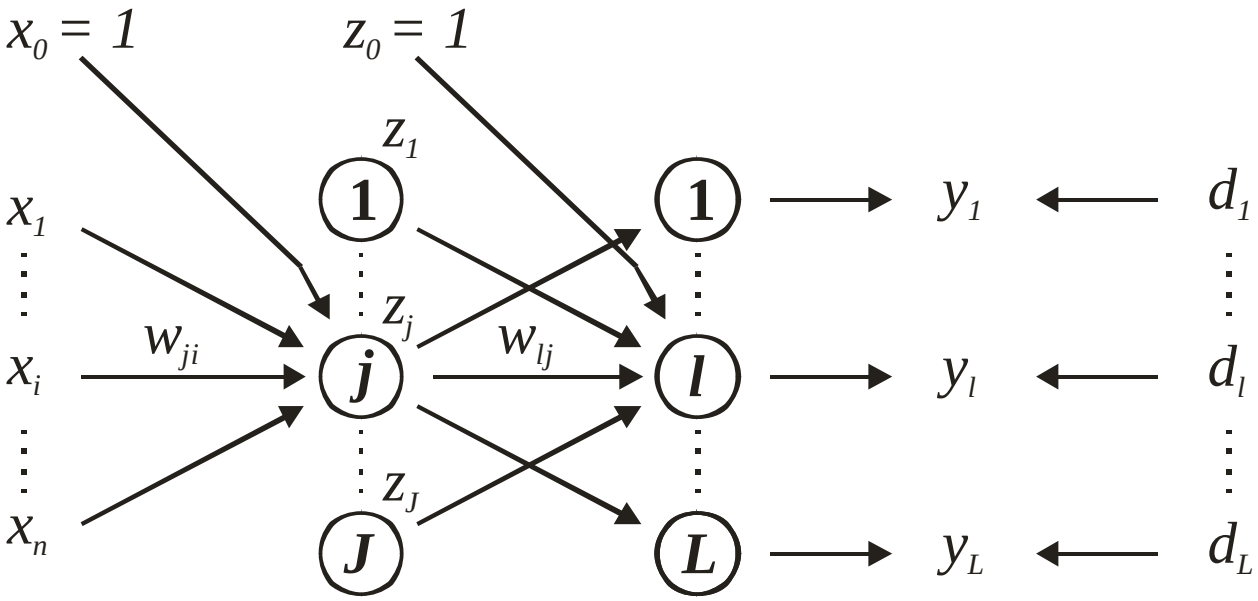

Fig. 3-5 Two-layer fully connected feedforward network [3.1]

For further analysis, the neurons in hidden layers are assumed to have differentiable activation functions – f_h. Typically, f_h is defined either as a logistic function – $f_h(net)=1/(1+e^{-\lambda \cdot net})$, or as a hyperbolic tangent – $f_h(net)=\tanh(\beta \cdot net)$, where λ and β are close to 1. The sigmoid activation function is a special case of logistic function. Another assumption made is that all neurons in output layer have the same activation functions f_o. The form of f_o is determined based on properties of the output signal. For example, if the output signal is a real value (function approximation) then the linear activation function $f_o(net)=\lambda \cdot net$ may be used. On the other hand, if the network is used to implement the classification procedure with binary outputs, usually the non-linear function similar to f_h is used. Finally, the weight coefficient of the j-th hidden neuron associated with the x_i input signal will be noted as w_{ji}. Likewise, w_{lj} will stand for the weight coefficient of the l-th output neuron associated with the hidden signal z_j.

Let us assume the set of m input/output pairs $\{\mathbf{x}^k,\mathbf{d}^k\}$, where $\mathbf{d}^k$ is L-dimensional vector representing the known outputs of the network for given inputs $\mathbf{x}^k$. Based on this set of input/output parameters, $J(n+1)+L(J+1)$ weight coefficients should be determined in order for

network to adequately learn the given training set. Being that the network outputs are known, the cost function, measuring the extent of achieved approximation for a given set of weight coefficients, can be defined. Often, the Root Mean Square (RMS) function is taken as a cost function. Once the cost function is defined, the learning process can be observed as the process of optimisation. For example, if the differentiable criterion function is chosen, the gradient of such function may inherently lead to a learning rule. This idea was independently conceived by Amari (1967, 1968) [3.5], [3.6], Bryson and Ho (1969) [3.7], Werbos (1974) [3.8] and Parker (1985) [3.9]. Let us assume that the cost function that needs to be minimized based on the training data set is defined as:

$$E(\mathbf{w}) = \frac{1}{2}\sum_{l=1}^{L}\left(d_l - y_l\right)^2, \tag{3.2}$$

where **w** is the set of all weight coefficients in the network.

Being that the set of input/output parameters is known, the so called "delta" rule for adjusting the weight coefficients w_{lj} can be directly applied:

$$\Delta w_{lj} = w_{lj}^{new} - w_{lj}^{c} = -\rho_0 \frac{\partial E}{\partial w_{lj}} = \rho_0 \left(d_l - y_l\right) f_0'\left(net_l\right) z_j, \tag{3.3}$$

where l=1,2,...,L, j=0,1,...,J, ρ_o is the *learning speed*, $net_l = \sum_{j=0}^{J} w_{lj} z_j$ is the weighted sum for l-th output neuron, f_o' is the derivative of f_o with respect to *net*, whereas w_{lj}^{new} and w_{lj}^{c} are new and current values of the weight coefficient, respectively. z_j values are obtained by propagating the input vector **x** through the hidden layers:

$$z_j = f_h\left(\sum_{i=0}^{n} w_{ji} x_i\right) = f_h\left(net_j\right), \quad j = 1, 2, \ldots, J. \tag{3.4}$$

The learning rule for weight coefficients of the hidden layer is not so evident due to the lack of defined values at the outputs of the neurons from hidden layers. However, the learning rule for the hidden units can be obtained by minimizing the error of the output layer. In other words, by propagating the error (d_l-y_l) backwards from the outputs to hidden layers, the "dynamic" desired values for hidden units can be obtained. This learning rule is called the error backpropagation learning rule. To define the rule for changing the weight coefficients of the hidden units, alike to the procedure with the output layer, it is necessary to define the gradient of the criterion function, eq. (3.2), with respect to the weight coefficients of the hidden layer:

$$\Delta w_{ji} = -\rho_h \frac{\partial E}{\partial w_{ji}}, \quad j = 1, 2, \ldots, J; \quad i = 1, 2, \ldots, n; \tag{3.5}$$

where the partial derivative is calculated for the current value of the weight coefficients. The partial derivative (3.5) can be expressed as:

$$\frac{\partial E}{\partial w_{ji}} = \frac{\partial E}{\partial z_j}\frac{\partial z_j}{\partial net_j}\frac{\partial net_j}{\partial w_{ji}}, \tag{3.6}$$

where

$$\frac{\partial net_j}{\partial w_{ji}} = x_i, \tag{3.7}$$

$$\frac{\partial z_j}{\partial net_j} = f_h'\left(net_j\right), \tag{3.8}$$

$$\begin{aligned}\frac{\partial E}{\partial z_j} &= \frac{\partial}{\partial z_j}\left\{\frac{1}{2}\sum_{l=1}^{L}\left[d_l - f_o\left(net_l\right)\right]^2\right\} \\ &= -\sum_{l=1}^{L}\left[d_l - f_o\left(net_l\right)\right]\frac{\partial f_o\left(net_l\right)}{\partial z_j}. \\ &= -\sum_{l=1}^{L}\left(d_l - y_l\right) f_o'\left(net_l\right) w_{lj}\end{aligned} \tag{3.9}$$

Inserting the equations (3.7), (3.8) and (3.9) into equation (3.6) and using the equation (3.5), the aforementioned learning rule is obtained:

$$\Delta w_{ji} = \rho_h\left[\sum_{l=1}^{L}\left(d_l - y_l\right) f_o'\left(net_l\right) w_{lj}\right] f_h'\left(net_j\right) x_i. \tag{3.10}$$

Comparing the eq. (3.10) with eq. (3.3) the "estimated desired value" d_j for j-th hidden neuron can be defined through the cost function:

$$d_j - z_j \;\square\; \sum_{l=1}^{L}\left(d_l - y_l\right) f_o'\left(net_l\right) w_{lj}. \tag{3.11}$$

Quite often, it is possible to express the derivatives of the activation function, from eq. (3.3) and (3.10), as a function of the activation functions themselves. For example, for logistics activation function,

$$f'\left(net\right) = \lambda f\left(net\right)\left[1 - f\left(net\right)\right] \tag{3.12}$$

and for hyperbolic tangent

$$f'\left(net\right) = \beta\left[1 - f^2\left(net\right)\right] \tag{3.13}$$

The previously defined learning rules can be expanded to the feedforward neural networks with more than one hidden layer. The following text shows the complete procedure for changing the

weight coefficients for two-layer network architecture given in Fig. 3-5 [3.1]. This procedure defines the learning rule known as incremental error backpropagation learning rule:

1) Initialize all weight coefficients and label them as current weight coefficients w_{lj}^{c} and w_{ji}^{c}.

2) Assume small, positive values for learning speeds ρ_o and ρ_h (close to 0.1).

3) Assume (randomly) one input set $\mathbf{x}^k$ from input/output training data set and let it propagate through the network. That way, the outputs of the hidden and output neurons, based on current values of the weight coefficients, are generated.

4) Based on the output of the network and the desired output $\boldsymbol{d}^k$ associated to the chosen input $\boldsymbol{x}^k$, using the eq. (3.3), calculate the correction of the weight coefficients of the output layer units – Δw_{lj}.

5) Using the eq. (3.10) calculate the correction of all weight coefficients for hidden layer units Δw_{ji}. In these steps, use the current values of the weight coefficients. Generally, greater error correction (i.e. faster convergence) can be achieved if the calculation uses the newly obtained output layer neurons weight coefficients $w_{lj}^{new}=w_{lj}^{c}+\Delta w_{lj}$. On the other hand, this invokes recalculating y_l and $f_o'(net_l)$.

6) Calculate the new weight coefficients $w_{lj}^{new}=w_{lj}^{c}+\Delta w_{lj}$ and $w_{ji}^{new}=w_{ji}^{c}+\Delta w_{ji}$ for the output and the hidden layer, respectively.

7) Test the convergence. This may be achieved by checking the value of the previously defined cost function. If the obtained value is below the defined threshold, the process is halted. Otherwise, the $w_{lj}^{c}=w_{lj}^{new}$ and $w_{ji}^{c}=w_{ji}^{new}$ are set and the procedure is repeated from step 3). Commonly, the test function is chosen in form of RMS function given as $\sqrt{2E_r/(mL)}$, where E_r is given by eq. (3.14). To test the convergence, a much more sophisticated test, called the cross-validation, may be used. It should be noticed that the backprop learning rule may fail to find the solution which satisfies the convergence test. In this case, the re-initialisation of the network, readjustment of the leaning parameters or adding the hidden neurons may improve the results.

The previously described procedure is based on "incremental" learning, i.e. weight coefficients of the network are changed after consideration of each input/output training pair. The alternative is so called "batch" learning, where the weight coefficients are corrected only after all available input/output pairs are considered. Batch learning rule is formally obtained by adding the right hand sides of the eq. (3.3) and (3.10) for all input/output pairs. This is equivalent to the application of the gradient onto the following criterion function:

$$E(\mathbf{w})=\frac{1}{2}\sum_{k=1}^{m}\sum_{l=1}^{L}\left(d_l-y_l\right)^2. \tag{3.14}$$

The correction of the weight coefficients according to the batch learning rule moves the **w** in the direction of the calculated gradient for each epoch of the training process.

Incremental rule has the following advantages: it consumes less memory, and the obtained path in the weight coefficient space is stochastic (with each step the input/output pair is selected randomly), which enables covering the wider space and, potentially, obtaining better solution [3.1].

In cases when the backprop is converging, it converges towards a local criterion function minimum [3.10]. Using the stochastic approximate theory [3.11], [3.12] it can be shown that for "very low" learning speeds (which converge to zero), incremental backprop and batch backprop approaches, basically, provide the same results. However, for small but constant learning speeds the stochastic nature in the training process becomes negligible, rendering the process unable to avoid the shallow local minima. That is why the solutions obtained by using the incremental learning are usually better. The local minima problem can be further reduced heuristically, by adding the random noise to the weight coefficients [3.13] or by adding the noise to the training inputs [3.14]. In both cases, as the process advances, some of the procedures to dynamically decrease the added noise must be applied.

3.2.7 Procedures for improving the solution

The backprop learning process is, in its essence, slow [3.15]. This, most commonly, comes as a consequence of the cost function form which has flat and steep regions. In the search direction, usually there are many flat regions in which the learning process is slow. This problem is more evident in cases when the training set is limited in volume [3.16].

Many studies suggested (and still suggest) improvements and variations of the backprop learning rule in order to enhance the obtained solution. Most commonly, these improvements and variations are performed heuristically with the goal of increasing the speed of convergence, avoid local minima and/or boost the generalization capacities of the network. Such studies include:

- changing the weight coefficients initialisation strategy [3.17]–[3.20],
- defining the optimal strategy for learning speed determination [3.21]–[3.33],
- speeding up of convergence by introducing the momentum [3.21], [3.34]–[3.48],
- dealing with flat-spot problem by modifying the activation function [3.35], [3.49]–[3.60],
- reducing the size of the network to an optimal number of neurons [3.21], [3.61]–[3.65],

- strategies for increasing the generalisation capacities of the network [3.62], [3.66]–[3.68],
- optimal choice of criterion function [3.69]–[3.71], and
- optimal incremental learning rule selection strategy [3.72]–[3.74].

3.3 Practical guidelines used for designing ANN positioning models

For the benefit of a broad scope of built-in functions for creating, initializing, training and simulation of neural networks, the herein given ANN based models were implemented in *Matlab*. For training purposes, the *traingda* – gradient descent training function with adaptive learning rate was selected. All neural units (perceptrons) use the hyperbolic tangent sigmoid transfer function (except from the output ones which had a linear transfer function). Being that the input probability distribution function of RSSI values is shown to be near Gaussian, the Mean Square Error (MSE) was selected as a criterion function [3.71].

Regarding the purpose that ANN models are intended for and, moreover, the nature of the problem, the multilayer feedforward neural networks with error backpropagation have substantial advantages in comparison to other structures [3.4]. Multilayer feedforward networks can have one or more hidden layers with perceptron units. The hidden layers with corresponding perceptron units form the inner structure of the ANN. There is no exact analytical method for determining the optimal inner structure of the network. However, there are algorithms that, starting with an intentionally oversized network, reduce the number of units and converge to the optimal network structure [3.4]. Also, there are other algorithms, such as the Cascade-Correlation Learning architecture [3.75], that build the network towards the optimal structure during the training process. However, being aware of the fact that these procedures can be complex and that determining the most optimal structure was not the central scope of this research, the networks' inner structures have been slightly oversized knowing that an oversized network will not yield degradation in performance. There is also an advantage to slightly over-sizing the network due to the fact that, in general, more unknown parameters (weights) induce more local and global minima in the error surface, making it easy for a local minimization algorithm to find a global or nearly global minimum [3.76]. The stance that the first hidden layer ought to have more perceptrons than the input layer so that the input information is quantified and fragmented into smaller pieces was also adopted [3.77]. The

number of perceptrons in the following hidden layers ought to decrease, converging to the number of perceptrons in the output layer.

The general ANN structure used in all models consists of an input layer, three hidden layers and an output layer. The number of perceptron units per layer is changed to accommodate the previously stated guidelines and the network's number of inputs and outputs.

The outer interfaces of the ANN must equal the number of the RSS values used, on the input side, and the number of values that are expected as a result on the output side of the ANN (e.g. two outputs if the model is used for two-dimensional positioning).

The aforementioned rules were applied to all of the following models based on ANNs.

3.4 References

[3.1] Nešković, "New electric field level prediction models based on artificial neural networks", PhD Thesis, Belgrade, 2002.

[3.2] McCulloch J. L., Pitts W., „A logical calculus of ideas immanent in nervous activity", Bulletin of Mathematical Biophysics, 5, pp. 115-133, 1943.

[3.3] Jain K. A., Jianchang M., Mohiuddin K. M. „Artificial Neural Networks: A Tutorial", COMPUTER, IEEE Computer Society, pp. 31-44, March 1996.

[3.4] Hasoun H. M., „Fundamentals of Artificial Neural Networks", Massachusetts Institute of Technology, 1995.

[3.5] Amari S. I., „Theory of adaptive pattern classifiers", IEEE Trans. On Electronic Computers, EC-16, pp. 299-307, 1967.

[3.6] Amari S. I., „Geometrical Theory of Information", Kyoritsu-Shuppan, Tokyo, 1968.

[3.7] Bryson A. E., Ho Y. C., „Applied Optimal Control", Blaisdell, New York, 1969.

[3.8] Werbos P., „Beyond regression: New Tools for Prediction and Analysis in the Behavioral Sciences", Ph.D. dissertation, Commitee on Applied Mathematics, Hardvard University, Cambridge, Massachusetts, 1974.

[3.9] Parker D. B., „Learning Logic", Technical Report TR-47, Center for Computational Research in Economics and Management Science, Massachusetts Institute of Technology, Cambridge, 1985.

[3.10] McInerny J. M., Haines K. G., Biafore S., Hecht-Nielsen R., „Backpropagation error surfaces can have local minima", International Joint Conference on Neural Networks (Washington 1989), vol. II, pp.627, IEEE, New York, 1989.

[3.11] Finnoff W., „Diffusion Approximations for the Constant Learning Rates Backpropagation Algorithm and Resistance to Local Minima", Advances in Neural Information Processing Systems 5 (Denver, 1992), (editors: Hanson S. J., Cowan J. D., Giles C. L.), pp. 459-466, Morgan Kaufmann, San Mateo, California, 1993.

[3.12] Finnoff W., „Diffusion Approximations for the Constant Learning Rates Backpropagation Algorithm and Resistance to Local Minima", Neural Computation, vol. 6, No. 2, pp. 285-295, 1994.

[3.13] von Lehman A., Paek E. G., Liao P. F., Marrakhci A., Patel J. S., „Factors Influencing Learning by Backpropagation", IEEE International Conference on Neural Networks (San Diego, 1988), vol. I, pp. 335-341, IEEE, New York, 1988.

[3.14] Sietsma J., Dow R. J. F., „Neural Net Pruning - Why and How", IEEE International Conference on Neural Networks (San Diego, 1988), vol. I, pp. 325-333, IEEE, New York, 1988.

[3.15] Huang W. Y., Lippmann R. P., „Neural Nets and Traditional Classifiers", Neural Information Processing Systems (Denver, 1987), (editor Anderson D. Z.), pp. 387-396, American Institute of Physics, New York, 1988.

[3.16] Hush D. R., Salas J. M., Horne B., „Error Surfaces for Multi-layer Perceptrons", International Joint Conference on Neural Networks (Seatle 1991), vol. I, pp.759-764, IEEE, New York, 1991.

[3.17] Kolen J. F., Pollack J. B., „Backpropagation is Sensitive to Initial Conditions", Advances in Neural Information Processing Systems 3 (Denver, 1990), (editors: Lippmann R. P., Moody, Touretzky D. S.), pp. 860-867, Morgan Kaufmann, San Mateo, California, 1991.

[3.18] D. E. Rumelhart, G. E. Hinton, and R. J. Williams, „Learning internal representations by error propagation", in Rumelhart D.E., and McClelland J.L. [Eds], Parallel Distributed Processing: Explorations in the Microstructure of Cognition, pp. 318-362, MIT Press, Cambridge MA, 1986.

[3.19] Lee Y., Oh S. H., Kim M. W., „The Effect of Initial Weights on Premature Saturation in Backpropagation Learning", International Joint Conference on Neural Networks (Seatle 1991), vol. I, pp. 765-770, IEEE, New York, 1991.

[3.20] Wessels L. F. A., Bernard E., „Avoiding False Local Minima by Proper Initialization of Connections", IEEE Trans. On Neural Networks, vol. 3, No. 6, pp. 899-905, 1992.

[3.21] Plaut D. S., Nowlan S., Hinton G., „Experiments on Learning by Backpropagation", Technical Report CMU-CS-86-126, Department of Computer Science, Carnegie-Mellon University, Pittsburg, 1986.

[3.22] Tesauro G., Janssens B., „Scaling Relationships in Backpropagation Learning", Complex Systems, vol. 2, pp. 39-44, 1988.

[3.23] Le Cun Y., Kanter I., Solla S. A., „Second Order Properties of Error Surfaces: Learning Time and Generalization", Advances in Neural Information Processing Systems 3 (Denver, 1990), (editors: Lippmann R. P., Moody, Touretzky D. S.), pp. 918-924, Morgan Kaufmann, San Mateo, California, 1991.

[3.24] Le Cun Y., Simard P. Y., Pearlmutter B., „Automatic Learning Rate Maximatization by On-line Estimation of the Hessian's Eigenvectors", Advances in Neural Information Processing Systems 5 (Denver, 1992), (editors: Hanson S. J., Cowan J. D., Giles C. L.), pp. 156-163, Morgan Kaufmann, San Mateo, California, 1993.

[3.25] Chan L. W., Fallside F., „An Adaptive Training Algorithm for Backpropagation Networks", Computer Speech and Language, vol. 2, pp. 205-218, 1987.

[3.26] Jacobs R. A., „Increased Rates of Convergence through Learning Rate Adaptation", Neural Networks, vol. 1, No. 4, pp. 295-307, 1988.

[3.27] Franzini M. A., „Speech Recognition with Back Propagation", Proceedings of the Ninth Annual Conference of the IEEE Engineering in Medicine and Biology Society (Boston, 1987), pp. 1702-1703, IEEE, New York, 1987.

[3.28] Cater J. P., „Successfully Using Peak Learning Rates of 10 (and greater) in Back-propagation Networks with Heuristic Learning Algorithm", Proceedings of the IEEE First International Conference on Neural Networks (San Diego 1987), (editors: Caudill M., Butler C.), vol. II, pp. 645-651, IEEE, New York, 1987.

[3.29] Silva F. M., Almeida L. B., „Acceleration Tehniques for the Backpropagation Algorithms", Neural Networks, Europe Lecture Notes in Computer Scence, (editors: Almeida L. B., Wellekens), pp. 110-119, Springer-Verlag, Berlin, 1990.

[3.30] Vogl T. P., Manglis J. K., Rigler A. K., Zink W. T., Alkon D. L., „Accelerating the Convergence of the Back-propagation Method", Biological Cybernetics, vol. 59, pp. 257-263, 1988.

[3.31] Pflug G Ch., „Non-asymptotic Confidence Bounds for Stohastic Approximation Algorithms with Constant Step Size", Mathematik, vol. 110, pp. 297-314, 1990.

[3.32] Ljung L., „Analysis of Recursive Stochastic Aproximation Algorithm", IEEE Trans. On Automatic Control, vol. 22, No. 4, pp. 551-575, 1977.

[3.33] Darken C., Moody J., „Towards Faster Stohastic Gradient Search", Neural Information Processing Systems 4 (Denver, 1991), (editors: Hanson S. J., Moody J. E., Lippmann R. P.), pp. 1009-1016, Morgan Kaufmann, San Mateo, California, 1992.

[3.34] Wegstein J. H., „Accelerating Convergence in Iterative Processes", ACM Communications, vol. 1, No. 6, pp. 9-13, 1958.

[3.35] Fahlman S. E., „Fast Learning Variations on Back-propagation: An empirical study", Proceeding of the 1988 Connectionist Models Summer School (Pittsburgh, 1988), (editors: Touretzky D., Hinton G., Sejnowski T.), pp. 38-51, Morgan Kaufmann, San Mateo, California, 1989.

[3.36] Dennis J. E. Jr., Schnabel R. B., „Numerical Methods for Unconstrained Optimization and Nonlinear Equations", Prentice-Hall, Englewood Clifs, N.J., 1983.

[3.37] Parker D. B.ater J. P., „Optimal Algorithms for Adaptive Networks: Second Order Backprop, Second Order Direct Propagation, and Second Order Hebbian Learning", IEEE First International Conference on Neural Networks (San Diego 1987), (editors: Caudill M., Butler C.), vol. II, pp. 593-600, IEEE, New York, 1987.

[3.38] Riccoti L.P., Ragazzini s., Martinelli G., „Learning of Word Stress in a Sub-optimal Second Order Backpropagation Neural Networks", IEEE First International Conference on Neural Networks (San Diego 1987), (editors: Caudill M., Butler C.), vol. I, pp. 355-361, IEEE, New York, 1987.

[3.39] Becker S., Le Cun Y., „Improving the Convergence of Backpropagation Learning with Second Order Methods", Proceeding of the 1988 Connectionist Models Summer School (Pittsburgh, 1988), (editors: Touretzky D., Hinton G., Sejnowski T.), pp. 29-37, Morgan Kaufmann, San Mateo, California, 1989.

[3.40] Bishop C., „Exact Calculations of the Hessian Matrix for the Multilayer Perceptron", Neural Computation, vol. 4, No. 4, pp. 494-501, 1992.

[3.41] Yu X., Loh N., K., Miller W. C., „A New acceleration technique for the backpropagation algorithm", IEEE International Conference on Neural Networks (San Francisco, 1993), vol. III, pp. 1157-1161, IEEE, New York, 1993.

[3.42] Polak E., Ribiere G., „Note sur la convergence de methods de directions conjugies", Revue Francaise d'Informatique et Recherche Operationnalle, vol. 3, pp. 35-43, 1969.

[3.43] Press W. H., Flannery B. P., Teukolsky, S. A., Vetterling W. T., „Numerical Recipes: The Art of Scientific Computing", Cambridge University Press, Cambridge, England, 1986.

[3.44] Kramer A. H., Sangiovanni-Vicentelli A., „Efficient Parallel Learning Algorithms for Neural Network", Advances in Neural Information Processing Systems 1 (Denver, 1988), (editor: Touretzky D. S.), pp. 44-48, Morgan Kaufmann, San Mateo, California, 1989.

[3.45] Makram-Ebeid S., Sirat J. A., Viala J. R., „A Rationalized Backpropagation Learning Algorithm", International Joint Conference on Neural Networks (Washington 1989), vol. II, pp.373-380, IEEE, New York, 1989.

[3.46] van der Smagt P. P., „Minimization Methods for Training Feedforward Neural Networks", Neural Networks, vol. 7, No. 1, pp. 1-11, 1994.

[3.47] Moller M. F., „A Scaled Conjugate Gradient Algorithm for Fast Supervised Learning", Technical Report PB-339, Computer Science Department, University of Aarhus, Aarhus, Denmark, 1990.

[3.48] Gorse D., Shepherd A., „Adding stohastic search to conjugate gradient algorithms", Proceedings of 3rd International Conference on Parallel Applications in Statistics and Economics, Tiskarenfke Zacody, Prague.

[3.49] Hinton G. E., „Connectionist Learning Procedures", Technical Report CMU-CS-87-115, Department of Computer Science, Carnegie-Mellon University, Pittsburg, 1987.

[3.50] Yang L., Yu W., „Backpropagation with Homotopy", Neural Computation, vol. 5, No. 3, pp. 363-366, 1993.

[3.51] Tawel R., „Does the Neuron "Learn" like the synapse?", Advances in Neural Information Processing Systems 1 (Denver, 1988), (editor: Touretzky D. S.), pp. 169-176, Morgan Kaufmann, San Mateo, California, 1989.

[3.52] Kufudaki O., Horejs. J., „PAB: Parameters Adapting Backpropagation", Neural Network World, vol. 1, pp. 267-274, 1990.

[3.53] Rezgui A., Tepedelenlioglu N. „The Effect of the Slope of the Activaction Function on Backpropagation Algorithm", Proceedings of the International Joint Conference on Neural Networks (Washington 1990), vol. I, pp.707-710, IEEE, New York, 1990.

[3.54] Kruschke J. K., Movellan J. R., „Benefits of Gain: Speeded Learning and Minimal Hidden Layers in Backpropagation Networks", IEEE Trans. On Systems, Man and Cybernetics, vol. SMC-21, No. 1, pp. 273-280, 1991.

[3.55] Sperduti A., Stratia A., „Extensions of Generalized Delta Rule to Adapt Sigmoid Functions", Proceedings of the 13th Annual International Conference IEEE/EMBS, pp. 1393-1394, IEEE, New York, 1991.

[3.56] Sperduti A., Stratia A., „Speed up Learning and Network Optimization with Extended Back Propagation”, Neural Networks, vol. 6, No. 3, pp. 365-383, 1993.

[3.57] Robinson A. J., Niranjan M., Fallside F., „Generalizing the Nodes of the Error Propagation Network”, Proceedings of the International Joint Conference on Neural Networks (Washington 1989), vol. II, pp.582, IEEE, New York, 1989.

[3.58] Moody J., Yarvin N., „Networks with Learned Unit Response Functions”, Advances in Neural Information Processing Systems 4 (Denver, 1991), (editors: Hanson S. J., Moody J. E., Lippmann R. P.), pp. 1048-1055, Morgan Kaufmann, San Mateo, California, 1992.

[3.59] Schumaker L. L., „Spline Functions: Basic Theory”, Wiley, New York, 1981.

[3.60] Hornik K., Stinchcombe M., White H., „Univesal Approximation of an Unknown Mapping and Its Derivates Using Multilayer Feedforward Network”, Neural Networks, vol. 3, No. 5, pp. 551-560, 1990.

[3.61] Hinton G. E., „Learning Distributed Representations of Concepts”, Proceedings of the 8th Annual Conference on Cognitive Science Society (Amherst, 1986), pp. 1-12, Erlbaum, Hillsdale, N.J., 1986.

[3.62] Weigend A. S., Rumelhart D. E., Huberman B. A., „Generalization by Weight-elimination with Application to Forecasting”, Advances in Neural Information Processing Systems 3 (Denver, 1990), (editors: Lippmann R. P., Moody, Touretzky D. S.), pp. 875-882, Morgan Kaufmann, San Mateo, California, 1991.

[3.63] Hanson S. J., Pratt L., „A Comparison of Different Biases for Minimal Network Construction with Backpropagation”, Advances in Neural Information Processing Systems 1 (Denver, 1988), (editor: Touretzky D. S.), pp. 177-185, Morgan Kaufmann, San Mateo, California, 1989.

[3.64] Chauvin Y., „A Backpropagation with Optimal Use of Hidden Units”, Advances in Neural Information Processing Systems 1 (Denver, 1988), (editor: Touretzky D. S.), pp. 519-526, Morgan Kaufmann, San Mateo, California, 1989.

[3.65] Hassoun M. H., Song J., Shen S. M., Spitzer A. R., „Self-organizing Autoassociative Dynamic Multiple-layer Neural Net for the Decomposition of Repetitive Superimposed Signals”, Proceedings of the International Joint Conference on Neural Networks (Washington, 1990), vol. I, pp. 621-626, IEEE, New York, 1990.

[3.66] Morgan N., Bourlard H., „Generalization and Parameter Estimation in Feedforward Nets: Some Experiments”, Advances in Neural Information Processing Systems 2 (Denver, 1989), (editor: Touretzky D. S.), pp. 630-637, Morgan Kaufmann, San Mateo, California, 1990.

[3.67] Wang C., Venkatesh S. S., Judd J. S., „Optimal Stopping and Effective Machine Complexity in Learning", Advances in Neural Information Processing Systems 6 (Denver, 1993), (editors: Cowan J. D., Tesauro G., Alspector J.), pp. 303-310, Morgan Kaufmann, San Francisco, 1994.

[3.68] Stone M., „Cross-validation: A Review", Mathematische Operationsforschung Statistischen, vol. 9, 127-140.

[3.69] Baum E. B., Wilczek F., „Supervised Learning of probability Distributions by Neural Networks", Neural Information Processing Systems (Denver, 1987), (editor Anderson D. Z.), pp. 52-61, American Institute of Physics, New York, 1988.

[3.70] Solla S. A., Levin E., Fleisher M., „Accelerated Learning in Layered Neural Networks", Complex Systems, vol. 2, pp. 625-639, 1988.

[3.71] Hanson S. J., Burr D. J., „Minkowski-r Backpropagation: Learning in Connectionist Models with non-Euclidean Error Signals", Neural Information Processing Systems (Denver, 1987), (editor Anderson D. Z.), pp. 348-357, American Institute of Physics, New York, 1988.

[3.72] Heskes T., Wiegernick W., „A Theoretical Comparison of Batch-Mode, On-Line, Cyclic and Almost-Cyclic Learning", IEEE Trans. On Neural Networks, vol. 7, No. 4, pp. 919-924, July 1996.

[3.73] Heskes T., Slijpen E., Kappen B., „Learning in Neural Networks with Local Minima", Phys. Rev. A, vol. 46, pp. 5221-5231, 1992.

[3.74] Barnard E., „Optimization for Neural Nets", IEEE Trans. On Neural Networks, vol. 3, pp. 232-240, 1992.

[3.75] Fahlman, S., Lebiere, C.: The cascade-correlation learning architecture. Advances in Neural Information Processing Systems 2, pp. 524–532 (1990)

[3.76] Kaemarungsi, K.: Distribution of WLAN received signal strength indication for indoor location determination. 1st International Symposium on Wireless Pervasive Computing, 2006. pp.6 (Jan. 2006)

[3.77] Shang Y., Wah W. B.: Global Optimization for Neural Network Training, IEEE Computer Society, pp. 45-56 (March 1996)

4 WLAN Positioning Using ANNs

The goal of Indoor Positioning System (IPS) research was to develop a low-complexity, high-accuracy positioning model. The model ought to be used in environments with already deployed infrastructural WLAN network optimised for Internet access. The models herein are based on Artificial Neural Networks (ANN) which are an optimisation procedure known to yield good results with noise polluted processes [4.1]. The approach including the ANNs does not insist upon a detailed knowledge of the indoor structure, propagation characteristics, or the position of APs.

4.1 Chosen Test-bed

The performance of a positioning technique largely depends on the choice of an appropriate verification surrounding. Thus, the building which is to be used as a test-bed should be chosen with care.

Indoor WLAN positioning techniques are commonly explored in a two-dimensional test-bed. This is because in an indoor environment the altitude parameter (Z) is usually a discrete parameter depicting the floor on which the user is located, and is evaluated through the probability that the estimated floor is correct. Extending the positioning algorithm to cover multiple floors would not be complicated and it is expected that, due to the significant attenuation of the obstacles in-between the floors, the Z parameter would plainly be assessed.

The essential requirements that a test-bed had to meet are: ① the number of APs and their deployment optimized for Internet access, and not for positioning, ② dimensions large enough so that the accuracy of the positioning technique could be fully investigated, ③ a complex building structure with different room types, invoking a number of radio-propagation effects (e.g. the tunnel effect) which would increase the test-bed's complexity – positioning wise.

Since all of the aforementioned requirements were met by the ground floor of the Technical Schools' building at the University of Belgrade, this setting was used as the test-bed. The dimensions of this floor are 147.1 m x 66.1 m, with more than 80 lecture theatres, classrooms, long corridors and offices of different sizes and interiors. Extended Service Set (ESS)

comprised eight IEEE 802.11 b/g APs placed so as to provide optimal radio coverage for wireless Internet access. Fig. 4-1 depicts the layout of the chambers and APs.

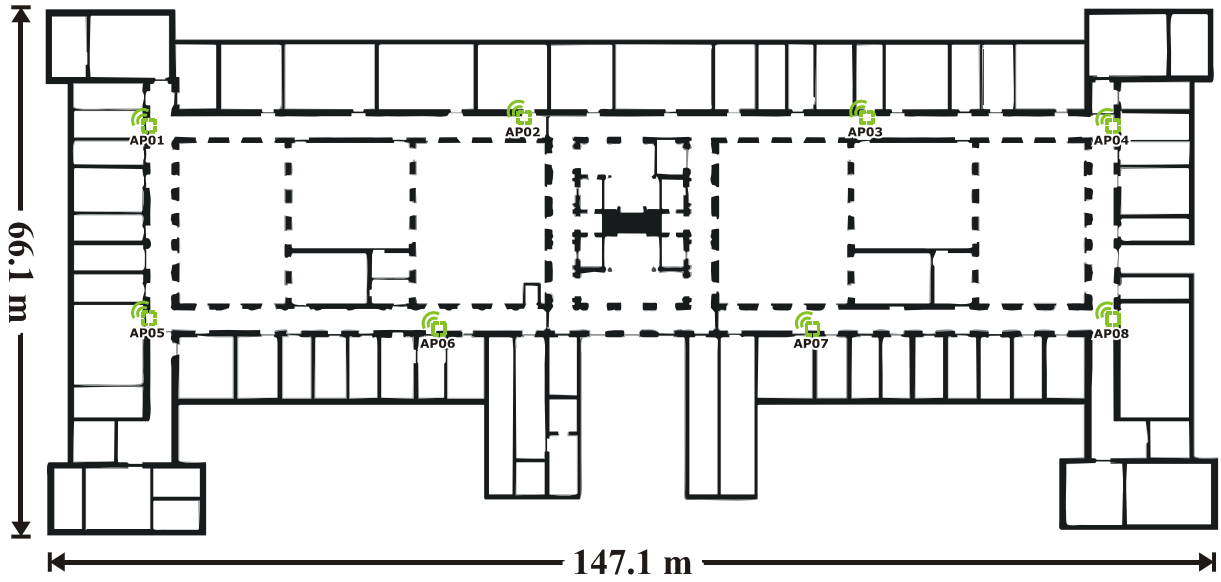

Fig. 4-1 The verification surroundings and the placement of APs

4.2 Measurement campaigns

During the course of this research, two measurement campaigns have been conducted. The principal difference between the two was the number of the measurements and the orientation of the receiver at each RP.

4.2.1 First Measurement Campaign

The First Measurement Campaign (FMC) consisted of experiments performed on a number of nearly uniformly distributed RPs. A laptop computer with Cisco Aironet 802.11a/b/g Cardbus AIR-CB21AG-E-K9 wireless card and encompassing software was used as measuring equipment. The orientation of the receiver was randomly chosen for each RP. At each RP the RSSI vector was recorded along with the position of the measurement equipment and the room number and room type the equipment was in. The elements of RSSI vector ranged from -100 dBm to -40 dBm (dynamical range of the measuring receiver). The information that an AP is not radio-visible at a RP was coded with -105 dBm. The measuring campaign comprised 433 RPs. The layout of the test-bed as well as the positions of APs and RPs are shown in Fig. 4-2.

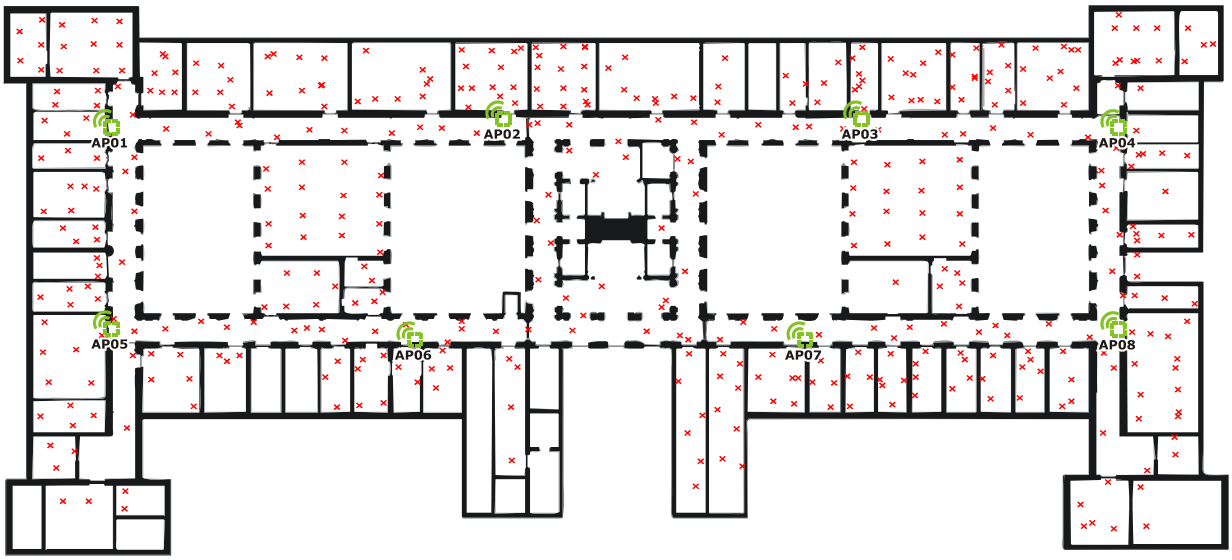

Fig. 4-2 First measurement campaign: The red "x" signs denote positions of the RPs

The measurements repeatability was also evaluated. Bearing in mind that all positioning techniques reside on the existence of correlation between the physical values repetitively measured on the same location, it can be concluded that measurement repetitiveness and positioning technique accuracy are directly related. For the purpose of quantifying measurements repeatability, the measurements on a number of RPs were repeated. Measurements repeatability was evaluated through a set of three parameters: the probability that the subset of radio-visible APs will be the same on both the first and the repeated measurement ($P_{\Omega_1=\Omega_2}$), the mean absolute difference of RSSI from the observed AP (η) and standard deviation of the mean absolute difference (σ). Obtained repeatability results are shown in Table 4-I.

Table 4-I The repeatability of the first campaign measurements

Parameter	$P_{\Omega_1=\Omega_2}$ [%]	η [dB]	σ [dB]
Value	20	5.12	4.13

From the results shown in Table 4-I, it can be seen that repeatability is extremely low which indicates limited positioning capabilities (regardless of WLAN technique used). Two main reasons can be accounted for such low repeatability: the complexity and dynamic behaviour of the test environment and the short time that receiver spends measuring on a channel (which was chosen intentionally so that the obtained results would be applicable for a broad range of wireless adapters and drivers).

Since these were the first measurement results the statistical properties of the signal were also surveyed. This was done in order to reveal the basic propagation characteristics of the environment in which the WLAN was deployed.

The entire measurement set was split into two more homogenous groups. The first group (G1) comprised of measurements collected from RPs in the corridors whereas the second group (G2) was made from the measurements conducted in closed chambers.

The performed statistical analysis consisted of determining the RSSI parameter Probability Mass Function (PMF). This was done by classifying the RSSI values received at all RPs into 5dB intervals, from -95dBm to -40dBm (boundary values included). Then, by counting the number of samples in each interval and dividing it with the overall number of samples, the PMF of a discrete random variable (each interval was regarded as a discrete value) was obtained. This process was conducted both for each AP separately and for the entire collection of the APs.

Concerning the G1 measurements, the average number of radio-visible APs was 3.54. The probability that a particular AP is radio-visible on a RP was 44%. With G2 measurements, the average number of radio-visible APs was only 1.72, whereas the probability that a particular AP is radio-visible on a RP was merely 30%. The radio-visibility parameters are summed in Table 4-II.

Table 4-II The radio-visibility parameters of the measurement from the first campaign

Measurement Group	Probability that an AP is radio-visible [%]							
	AP01	AP02	AP03	AP04	AP05	AP06	AP07	AP08
G1	46	31	36	51	56	41	47	49
G2	27	13	17	33	31	16	19	15

Bearing in mind that the space distribution of RPs is nearly uniform, the size of the covering areas for each APs can be evaluated through Table 4-II.

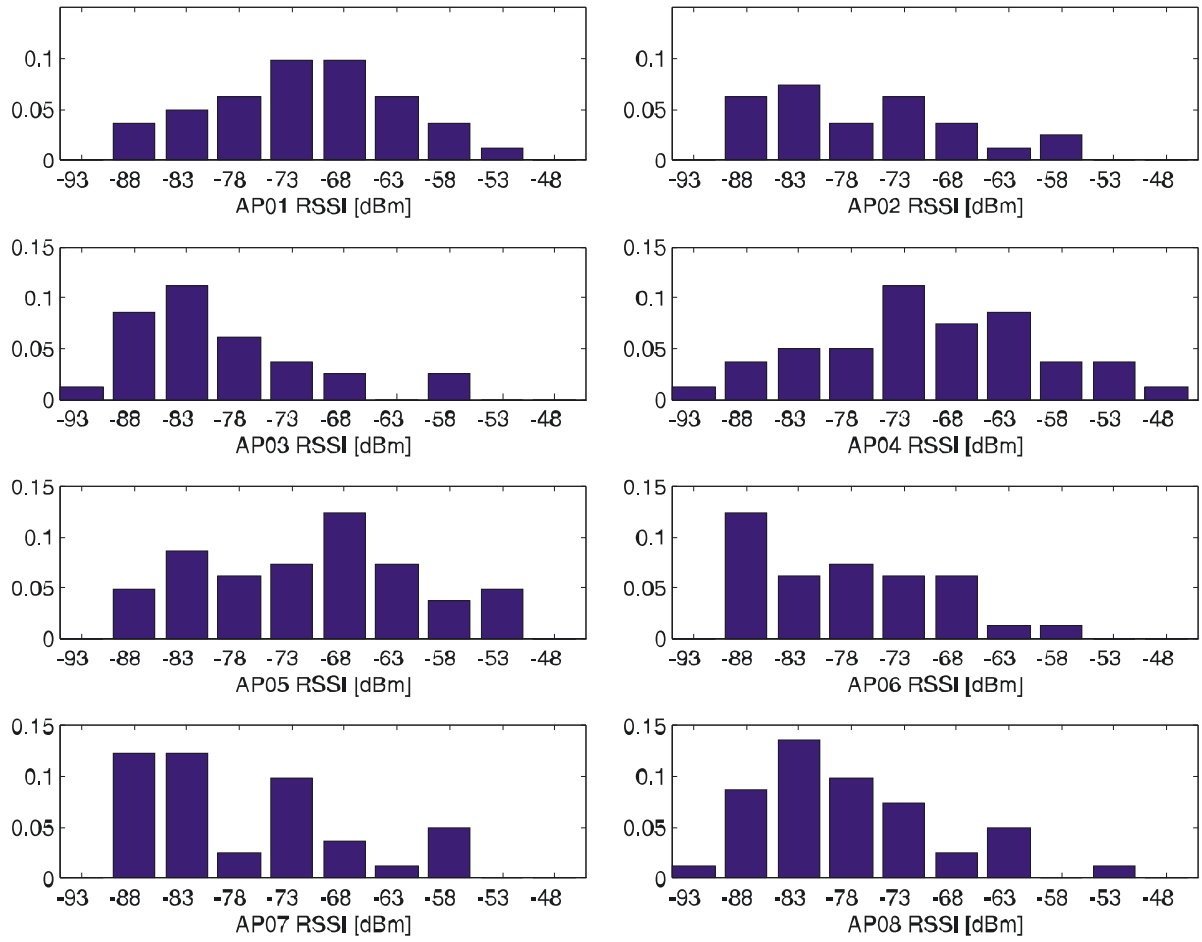

Fig. 4-3 RSSI PMFs for the individual AP and G1 measurements (FMC)

Fig. 4-3 illustrates the RSSI PMFs for each of eight APs. The results have been obtained by using the measurements from G1, and the value of PMFs are equal to zero in the omitted intervals.

Concerning the results from Table 4-II and Fig. 4-3, it can be concluded that the APs deployed around the corners of the test-bed (AP1, AP4, AP5 and AP8) have greater probability of being radio-visible than other APs. Moreover, their RSSI PMFs are translated to greater power with respect to the lateral APs (AP2, AP3, AP6 and AP7). Bearing in mind that corner APs are placed at a cross-section of two corridors and that they obtain a better radio-coverage (than the lateral APs), the aforementioned behaviour can be regarded as logical and expected.

Fig. 4-4 shows the RSSI PMF from all the APs together. The results have been obtained by using the measurements from G1, and the value of PMFs are equal to zero in the omitted intervals.

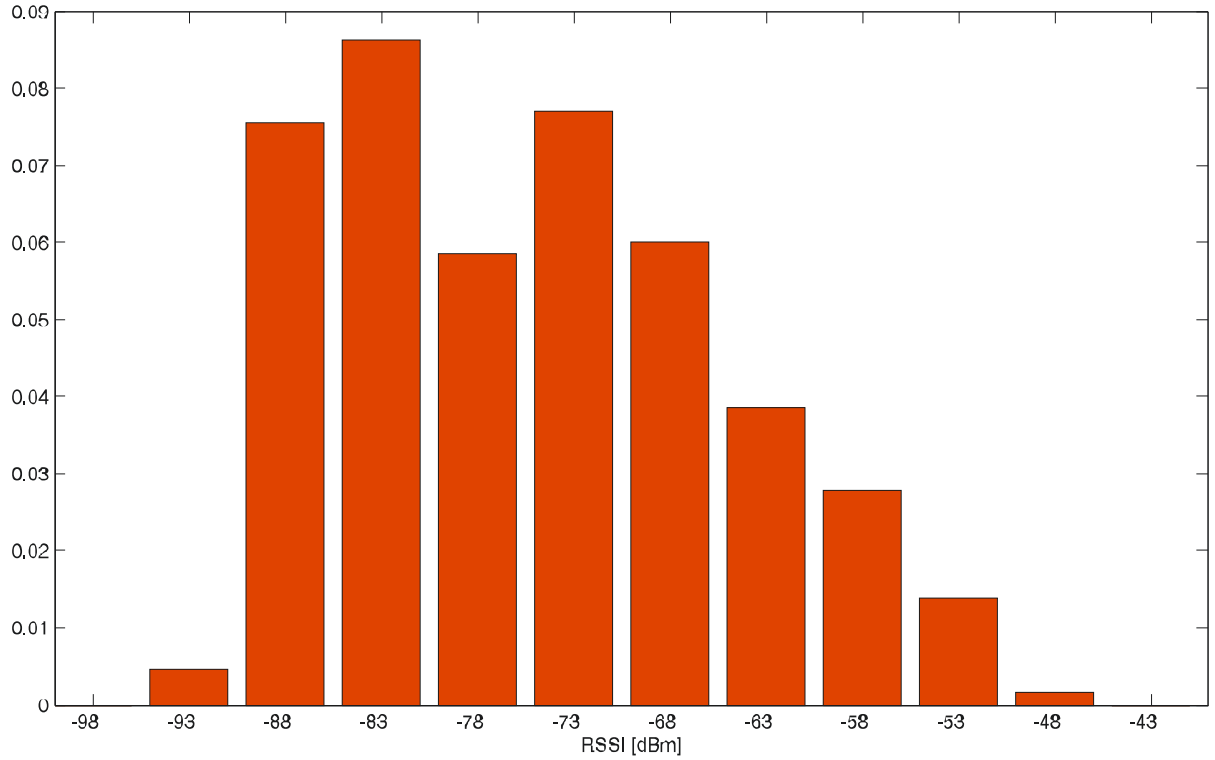

Fig. 4-4 Joined RSSI PMFs for all APs and G1 measurements (FMC)

Fig. 4-5 illustrates the separate RSSI PMFs for each of the eight APs where the results have been obtained by using the measurements from G2. Finally, the RSSI PMF from all the APs together and the results from G2 measurements are shown in Fig. 4-6.

Focusing on the measurements from G2, made in the offices, lecture theatres, laboratories, etc, the similar conclusions can be drawn from Table 4-II and Fig. 4-5 as with measurements from G1. The corner APs are more radio-visible with the exception of the AP8, whose reduced radio-visibility can be explained with the specific content of the chambers in that part of the test-bed (large machines and equipment limits the service zone of this AP). With respect to the G1, all PMFs are translated to smaller power, and there is no such distinguishable difference between the corner and the lateral APs as was the case with G1 measurements. The only noticeable difference between the RSSI PMF of the corner and the lateral APs is that the PMFs of the lateral APs are more inclining towards the uniform distribution than the corner ones.

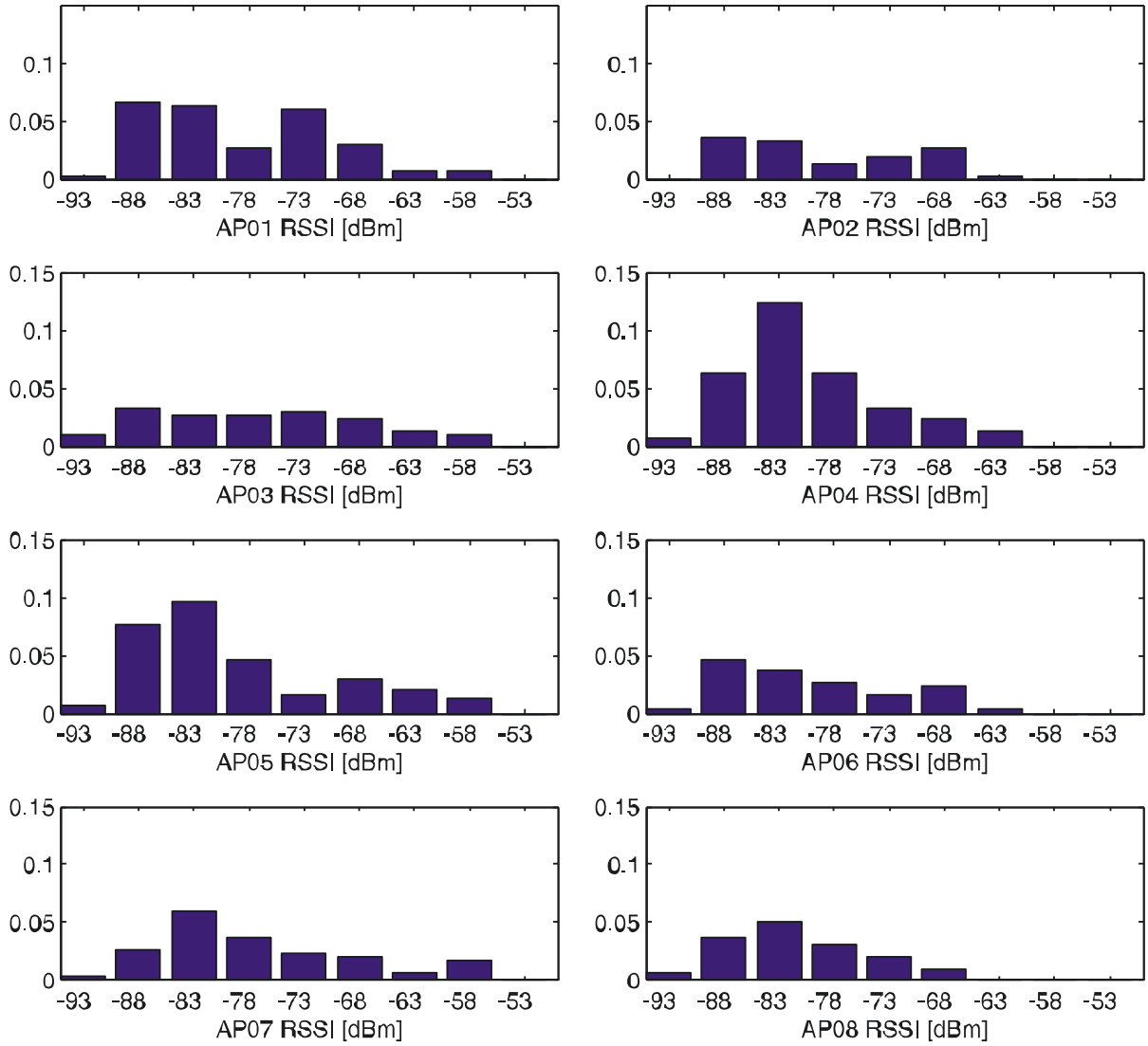

Fig. 4-5 RSSI PMFs for the individual AP and G2 measurements (FMC)

If the joined RSSI PMFs are observed, from Fig. 4-4 and Fig. 4-6, it can clearly be noticed that the power profile with G2 measurements is shifted towards smaller power. This comes as a consequence of the fact that APs are deployed in corridors and the LoS condition cannot exist with G2 measurements (at least one wall between the AP and the client) whereas the LoS condition is most often met with G1 measurements.

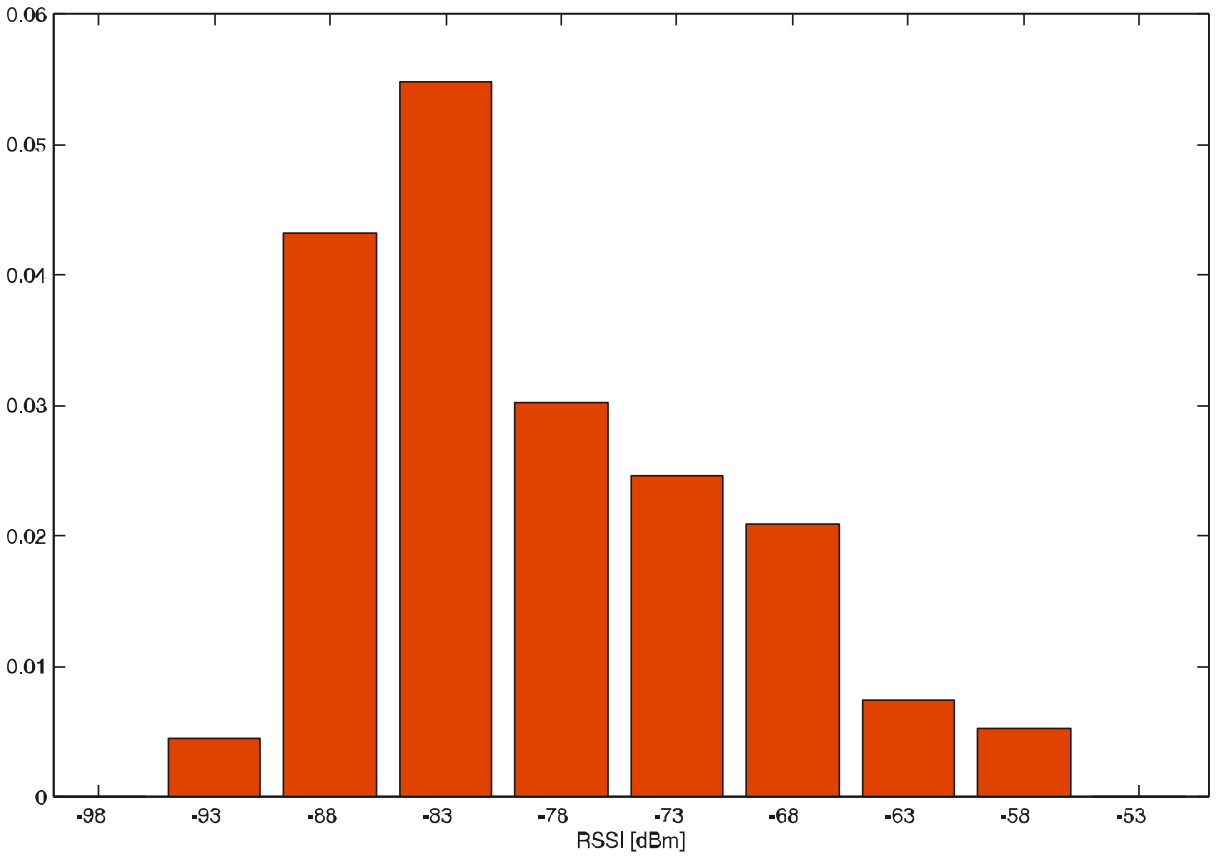

Fig. 4-6 Joined RSSI PMFs for all APs and G2 measurements (FMC)

Being that the propagation conditions are largely varied across the covering areas of some APs, the implementation of a propagation model based positioning technique with trilateration would not present a comprehensive and sound solution. This claim is supported by the average number of radio-visible APs, as well as the results from Table 4-I. All these goes to say that trilateration procedure would be feasible only on a part of corridors, but it would be practically impossible to determine the user's position in a closed chamber in this manner.

The presented statistical analysis indicates that the chosen test-bed is extremely "hostile" regarding the WLAN IPS implementation.

4.2.2 Second Measurement Campaign

As with the FMC, the Second Measurement Campaign (SMC) consisted of experiments performed on a number of nearly uniformly distributed RPs. The measurement set was the same as with the FMC. It consisted of a laptop computer with *Cisco Aironet 802.11a/b/g Cardbus AIR-CB21AG-E-K9* wireless card and *AirMagnet Laptop Analyzer* software. The principal difference in comparison to FMC was that, at each RP, RSSI, Signal to Noise (SNR) and Noise (N) samples were collected in four orthogonal receiver orientations. RSSI vectors were then stored into the database along with the corresponding position. The elements of RSSI and N values ranged from -100 dBm to -40 dBm, and the information that an AP is not

radio-visible at a RP was coded with -105 dBm. As for the SNR values, they ranged from 0 dB to 60 dB. The extensive measuring campaign comprised the total of 403 RPs. Since the concluded measurements do not require time averaging of samples, collecting a single RSSI vector sample is done almost instantaneously, whereas the measurement for one receiver orientation, inclusive of equipment rotation and/or relocation, lasted about 15 s on average. Therefore, the total effective time spent for measurement campaign was slightly over 400 minutes. The positions of APs and RPs, are shown in Fig. 4-7.

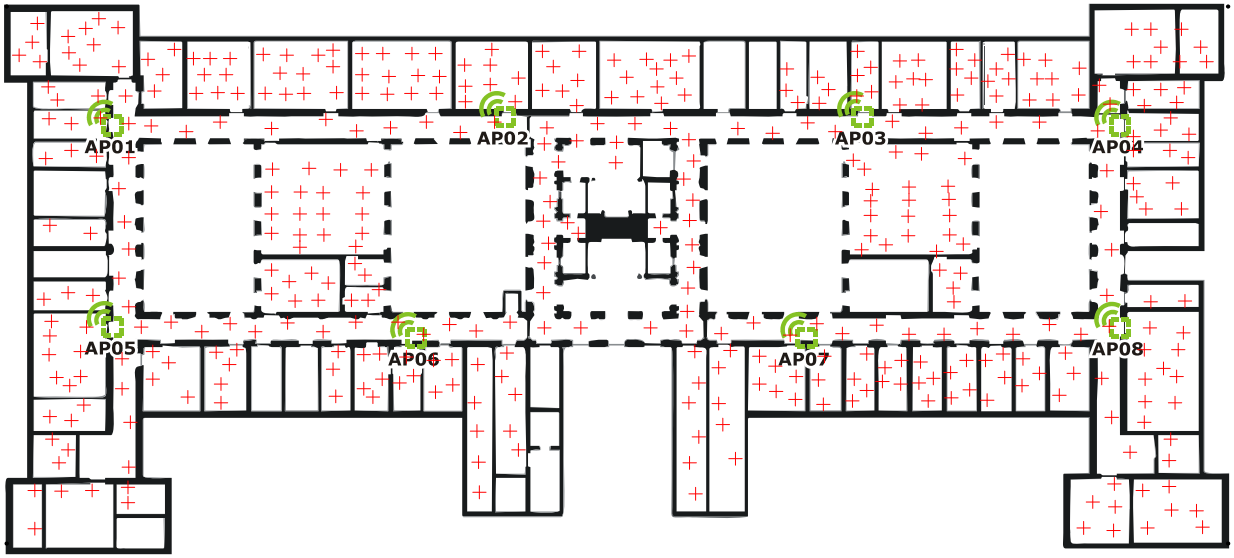

Fig. 4-7 Second measurement campaign: The red "+" signs denote positions of the RPs

As with the FMC, the measurement repeatability was evaluated through the same set of parameters: the probability that the subset of radio-visible APs will be the same in both the first and the repeated measurement ($P_{\Omega_1=\Omega_2}$), the mean absolute difference of RSSI from the observed AP (η) and standard deviation of the mean absolute difference (σ). Obtained repeatability results are shown in Table 4-III.

Table 4-III The repeatability of the second campaign measurements

Parameter	$P_{\Omega_1=\Omega_2}$ [%]	η [dB]	σ [dB]
Value	50.55	4.70	4.25

The results shown in Table 4-III indicate better repeatability of the SMC than with the FMC. However, even the SMC repeatability can be considered as low to moderate which will condition the positioning capabilities of any WLAN positioning technique implemented in this test-bed.

Following the same methodology as with FMC, the results obtained from this measurement campaign were evaluated and statistically analysed. However, on the contrary to the FMC, the herein obtained results were not separated in two, more homogenous groups (the similar effects were expected). The individual RSSI PMFs of APs are presented in Fig. 4-8, whereas the joined RSSI PMFs for all APs are shown in Fig. 4-9.

Regarding the radio-visibility, the parameters are summed in Table 4-IV.

Table 4-IV The radio-visibility parameters of the measurement from the second campaign

Probability that an AP is radio-visible [%]							
AP01	AP02	AP03	AP04	AP05	AP06	AP07	AP08
41.36	22.9	39.95	45.33	45.09	33.64	33.88	27.34

Bearing in mind that the space distribution of RPs is nearly uniform, the size of the covering areas for each APs can be evaluated through Table 4-IV.

In comparison to FMC it can be concluded that the radio-visibility has increased. Also, it can be noticed, from Fig. 4-8 and Fig. 4-9, that the RSSI distributions are now more regular and resemble slightly right-skewed distribution.

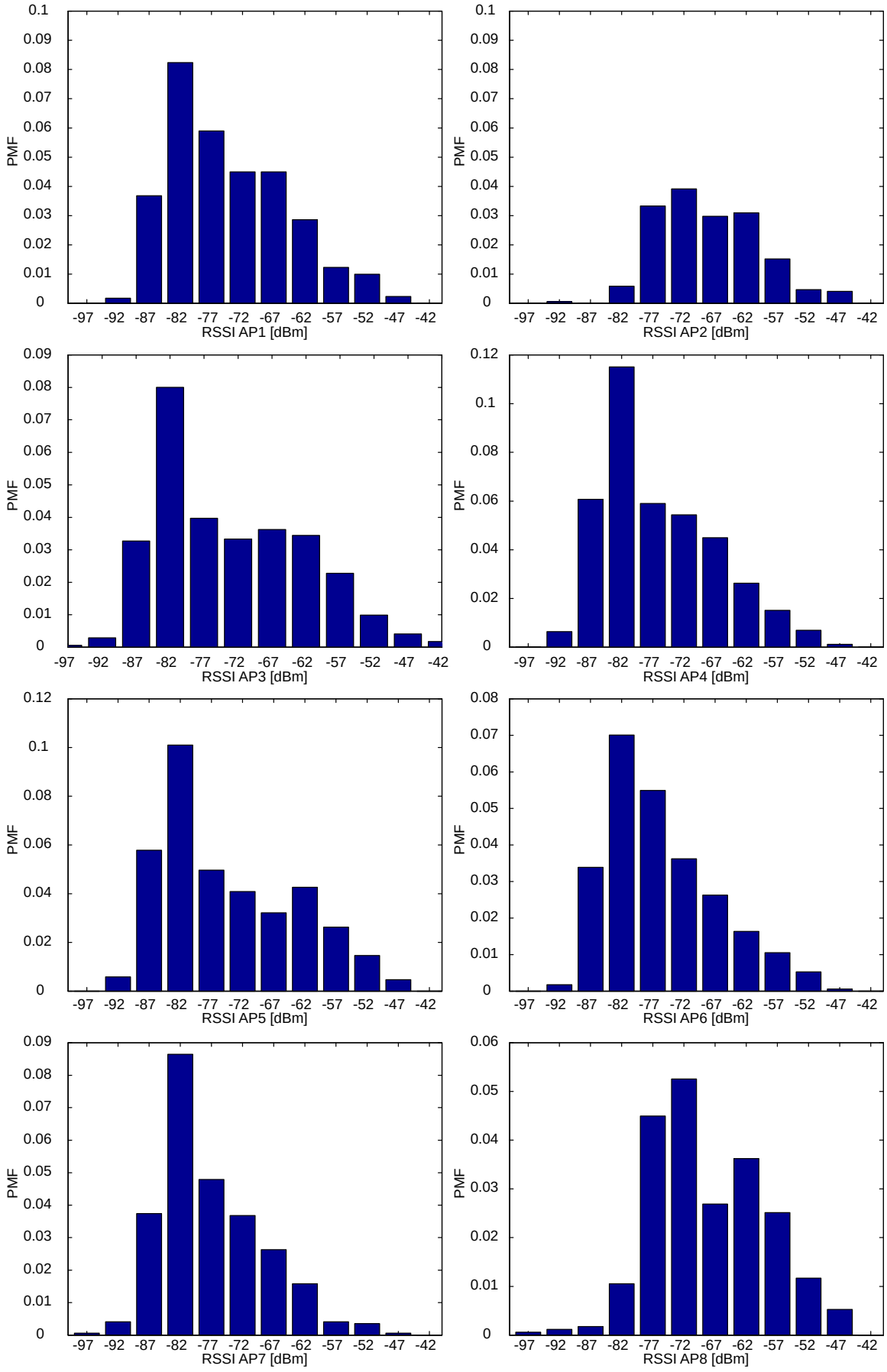

Fig. 4-8 RSSI PMFs for the individual AP (SMC)

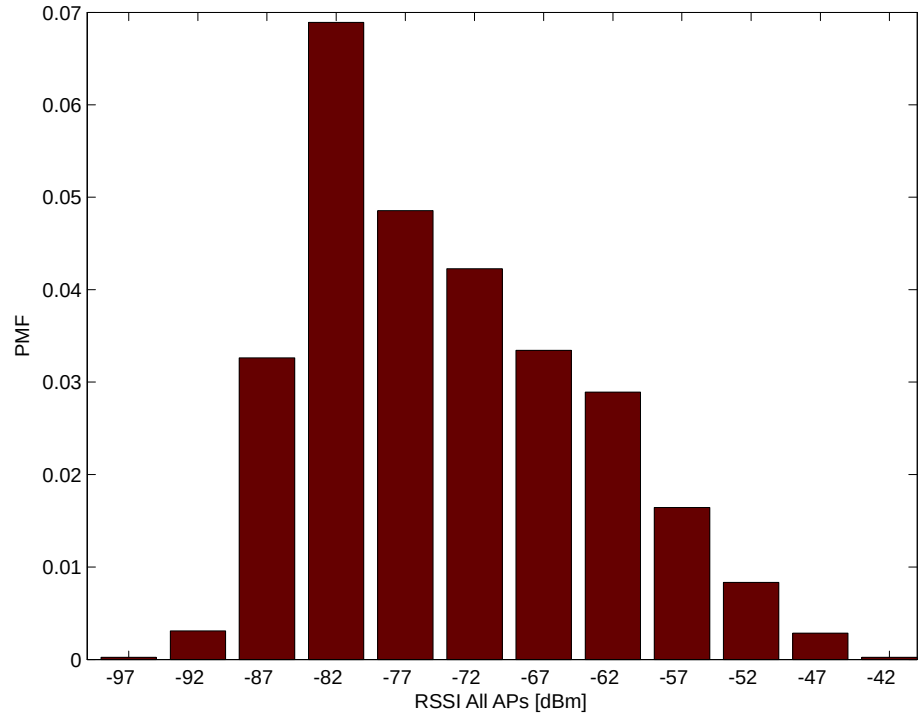

Fig. 4-9 Joined RSSI PMFs for all APs (SMC)

4.3 ANN Positioning Models

In the way the measurement campaigns were carried out, the herein presented positioning algorithms fall into client-based positioning solutions group. However, it should be stated that the derived models themselves can equally be implemented as a network-based solution with the only difference made in the measurement campaign: instead of having a client collecting RSSI samples from APs, the client's RSSI at each RP ought to be collected at various APs.

The ANNs do not fall entirely into any of the WLAN positioning system categories (propagation model based, fingerprinting or hybrid). However, the ANNs are generally classified as a fingerprinting technique. In the off-line phase, the set of collected RSSI fingerprints is used to train the network and set its inner coefficients to perform the positioning function. In the on-line phase, the trained network replaces multilateration and position determination processes. Using ANNs requires no detailed knowledge of the APs positions or the indoor environment in which the positioning technique is implemented.

4.3.1 Models Obtained from the FMC

4.3.1.1 The Single ANN Position Estimation Model

This model, comprised of a single feedforward ANN, ought to provide position estimate from the **APs RSSI** vector. The block scheme of this model is given in Fig. 4-10.

Fig. 4-10 Block scheme of a single ANN position estimation model

The outer interfaces of the ANN must be in compliance with the number of the APs, on the input side, and with the number of values that are expected as a result on the output side of the ANN. Since this model ought to provide position coordinates estimate (two coordinates, since our test-bed consisted of only one floor), the chosen ANN has eight neural units (perceptrons) on the input end and two neural units on the output end.

Given the guidelines for constructing the ANN's inner structure, presented in section 3.3, the number of perceptron units per layer is (from input to output) 8, 15, 9, 5 and 2. The inner structure of this model is illustrated in Fig. 4-11. It has been derived through the trial-and-error procedure.

For the purpose of determining the optimal training parameters as well as the optimal training length (in epochs), the complete set of measurements was split in two subsets containing 10% and 90% of the RPs. The larger subset was used to train the ANN, while the smaller was used to validate the obtained model. To verify the performance of the obtained model with higher accuracy, this process was repeated 10 times and each time different RPs were taken for validation purpose. This way, the verification set of 433 measurements was obtained. The performance of a single ANN position estimation model were evaluated for training lengths of 1000, 1500, 2000, 3000, 5000, 10000, 20000, 50000 and 100000 epochs. The results are shown in Fig. 4-12.

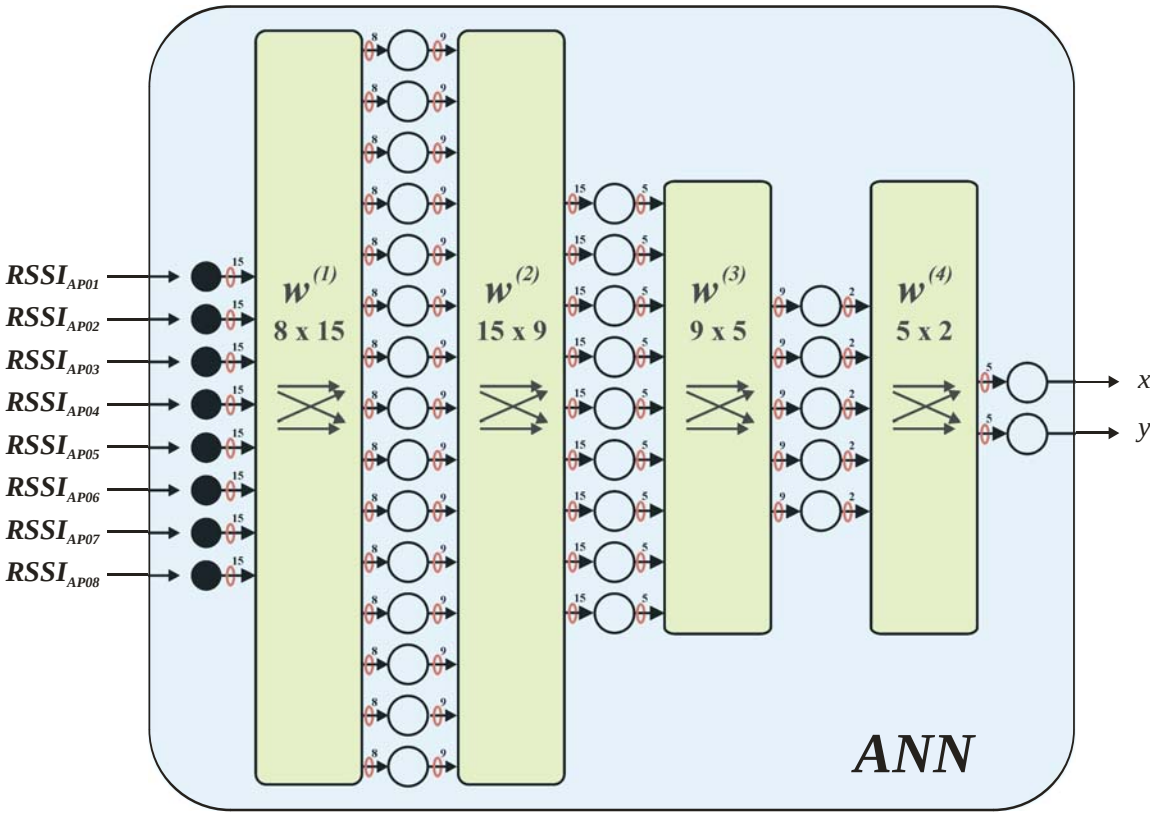

Fig. 4-11 The inner structure of a single ANN position estimation model

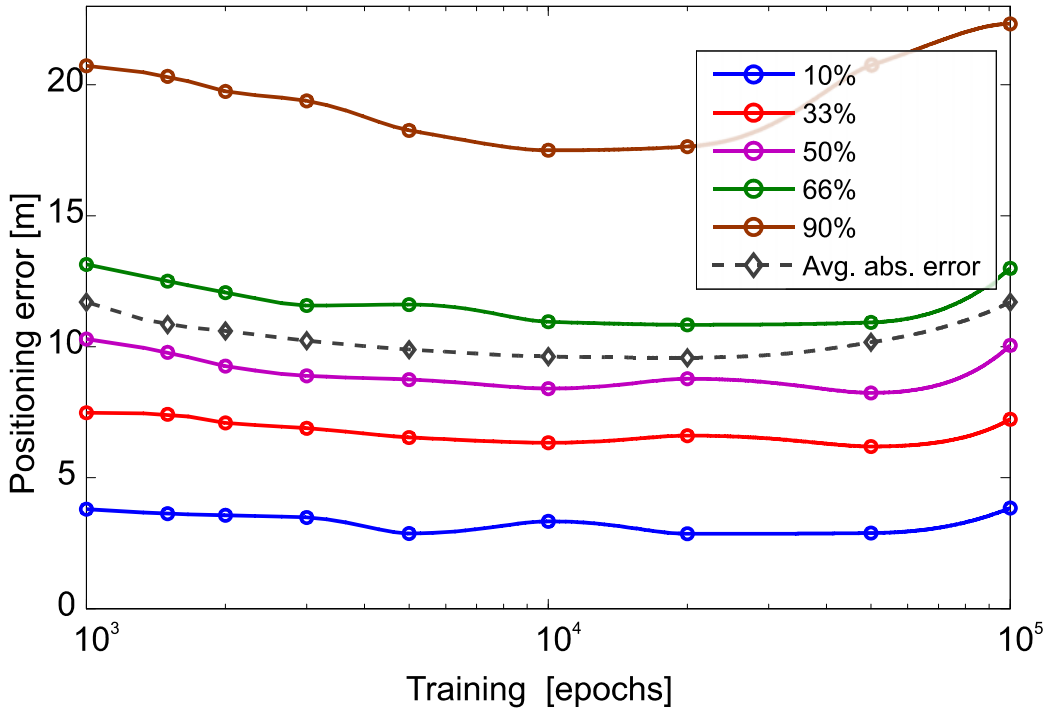

Fig. 4-12 Distance error vs. training – graph parameter are confidence percentiles (probability that a positioning error, for a given training length, is under the curve), except for the grey dotted line which represents the average absolute positioning error

Optimal training length could be defined as a "bottom" of some of the curves depicted in Fig. 4-12. Which curve's minimum should be concerned as optimal training length depends mostly on the expected set of LBS technique ought to comply with. However, for a broad range of services, it is good enough to optimize the network according to minimum of the average absolute positioning error. Fig. 4-12 shows a minimum of the average absolute positioning error at 20000 epochs of training for which this error equals 9.58 m.

Because of the disproportion between the width and length of the test-bed, the positioning error results obtained by verification were split to *X* and *Y* axes. For optimally trained network, the *X* axes median positioning error equals 5.46 m, while the *Y* axes median positioning error was only 3.75 m. This result shell be discussed later on in the document.

4.3.1.2 The Single ANN Room Type and Number Estimation Model

This model was used to provide the Room Number (RN) and Room Type (RT) estimates. The ground floor of the Technical Universities building in Belgrade has more than 80 lecture theatres, classrooms and offices of different sizes. Rooms were numbered in circular fashion and classified with respect to propagation characteristics into the following six categories: long corridors, short corridors, hall, lecture theatres, classrooms (laboratories) and offices.

Again, the outer interfaces of the ANN must be in compliance with the number of the APs, on the input side, and with the number of values that are expected as a result on the output side of the ANN. Since this model ought to supply room and room type estimates, network should provide two outputs. Therefore, the chosen ANN has the same outer and inner structure as the model previously described in section 4.3.1.1 (Fig. 4-11), but with different outputs function, as depicted in Fig. 4-13.

Fig. 4-13 Block scheme of a single ANN RN and RT estimation model (RN Est and RT Est are scalar values estimating the room number and room type the user is located in, respectively)

The same training and verification sets of measurements were used as with the single ANN model that estimates the user's position. The performances of this model were evaluated for the set of training lengths comprising 1000, 1500, 2000, 3000, 5000, 10000, 20000, 50000 and 100000 epochs. Results obtained by training and validation are summarized in Table 4-V. The accuracy of this model could not be evaluated in an ordinary fashion due to the nature of its

estimates. Therefore, this model was evaluated through the use of two parameters: probability that the room number was correctly estimated ($P_{RN=\hat{R}N}$) and probability that the room type was correctly estimated ($P_{RT=\hat{R}T}$).

Table 4-V Performance of the single ANN room type and number estimation model

Training Length [epochs]	$P_{RN=\hat{R}N}$ [%]	$P_{RT=\hat{R}T}$ [%]
1000	5.34	41.98
1500	4.58	45.40
2000	6.87	46.06
3000	7.63	48.60
5000	6.62	46.82
10000	8.40	51.66
20000	8.91	55.72
50000	11.45	62.34
100000	11.20	62.34

According to Table 4-V, this model shows its best performances for training length of 50000 epochs. For this training length, the room in which the user is located is correctly estimated in 11.45% of the cases and the user's room type is correctly estimated in 62.34% of the cases.
Since this approach yielded less promising results, and other well-known WLAN positioning techniques do not attempt room locating, this model will not be taken into further comparison with the other presented techniques.

4.3.2 Models Obtained from the SMC

4.3.2.1 The Single ANN Position Estimation Models

Four single ANN models for positioning, employing different input vectors and two different ANN structures, have been implemented and verified. The principal difference between the ANN models was in their input vector values:

- RSSI,
- SNR,
- Noise level (N), and
- RSSI & SNR.

It should be noted that the noise level value includes, not only the background noise, but also the interfering signals from other transmitters.

As mentioned above, the outer interfaces of the ANN must be in compliance with the number of the APs on the input side, and with the number of values that are expected as a result, on the output side of the ANN. The exception to this rule is the ANN model that ought to support both RSSI and SNR values from all the APs. In this case, the number of inputs to the ANN must be equal to twice the number of APs.

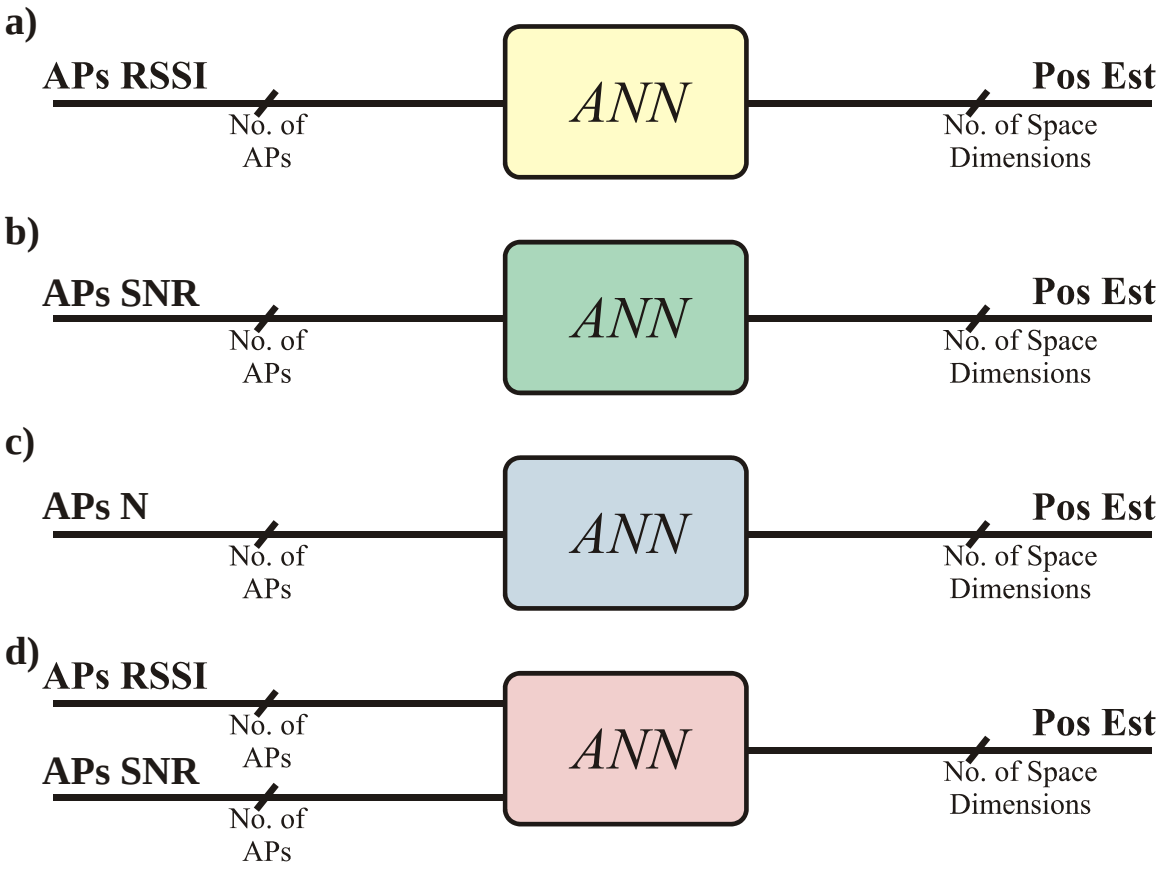

Fig. 4-14 Block scheme of a single ANN position estimation models: a) with RSSI vector as inputs, b) with SNR vector as inputs, c) with N vector as inputs, and d) with RSSI and SNR vectors as inputs

All ANN models ought to provide an estimate of relative position coordinates (two coordinates, since our test-bed consisted of only one floor and was considered as two-dimensional). Therefore, two output units are common for all ANN models. The chosen ANN models have eight neural units on the input end and two neural units on the output end in case of RSSI, SNR and Noise level values as inputs. In case of the ANN model combining both RSSI and SNR values as inputs, 16 neural units on the input end and two neural units on the output end were implemented. The block scheme of the these ANN models is illustrated in Fig. 4-14. The RSSI, SNR and N input vectors were denoted **APs RSSI**, **APs SNR**, **APs N**, respectively while the output, position estimation vector, was denoted **Pos Est**.

Conveying to the aforementioned principles, the inner structure of all ANN models consisted of the input layer, three hidden layers and the output layer. When concerning the ANN models with RSSI, SNR or noise level values as inputs, the inner structure was identical to the model described in section 4.3.1.1. Namely, the number of perceptron units per layer was (from input to output) 8, 15, 9, 5 and 2, whereas in the case of ANN model with both RSSI and SNR values as inputs the number of perceptron units per layer was (again, from input to output) 16, 24, 16, 6 and 2.

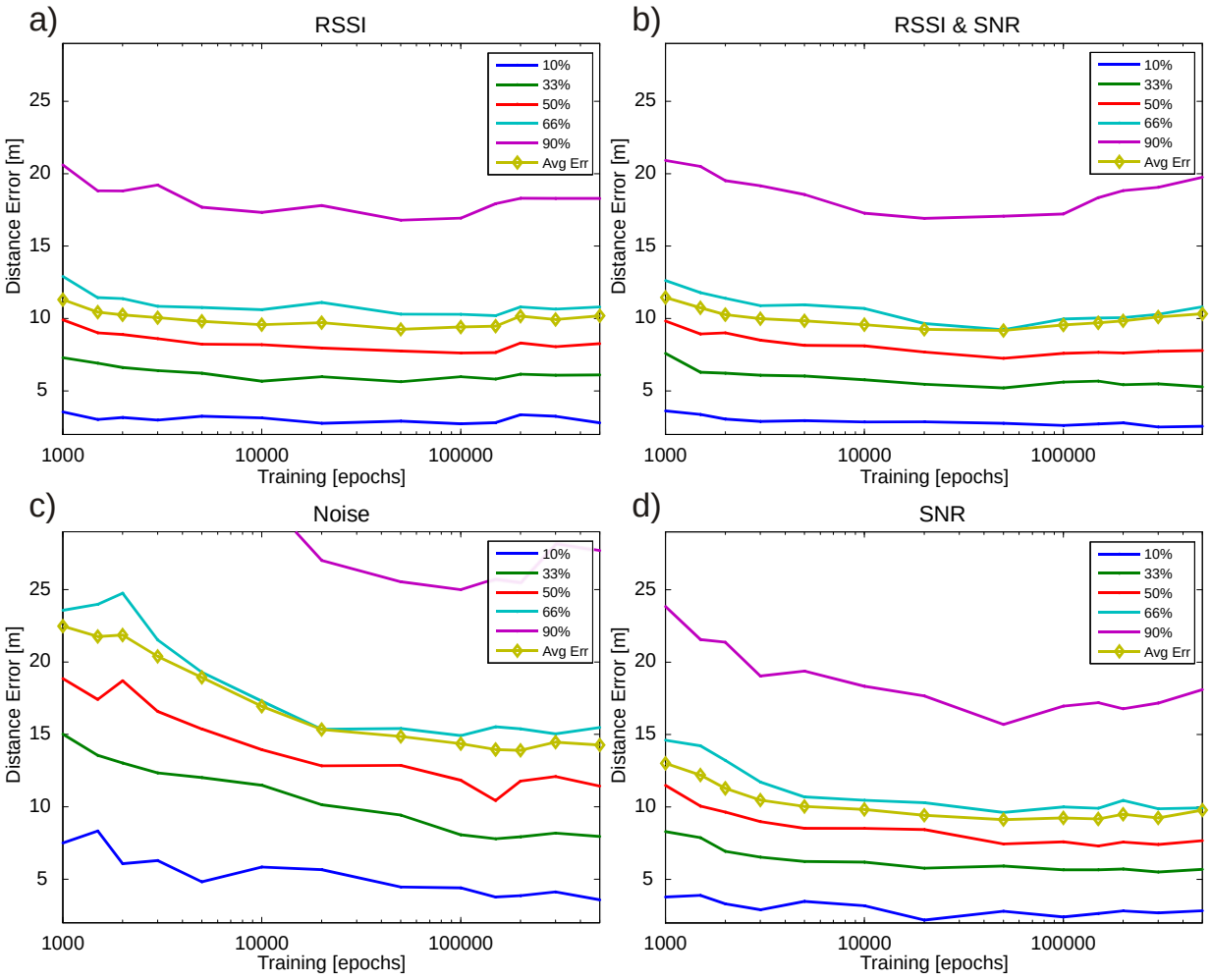

Fig. 4-15 Positioning distance error (DE) vs. training process for ANN with a) RSSI, b) SNR, c) Noise level, and d) both RSSI and SNR inputs. Graph parameters are confidence percentiles (probability that a positioning error, for a given training length, is less than the corresponding DE), except for the solid yellowish line (with markers) which represents the average absolute positioning error

For the purpose of determining the optimal training parameters, as well as the optimal training duration, the complete set of measurements was split in two subsets. The larger subset was used to train the ANNs, while the smaller, containing measurements from a 100 randomly chosen RPs, was used to validate the obtained model.

The performance of described ANN models were evaluated for training lengths ranging from 1000 to 500000 epochs. Fig. 4-15 shows the obtained results in terms of distance error for different ANN models. The performance of positioning model with RSSI values as ANN inputs is depicted in Fig. 4-15 a), with both RSSI and SNR values as ANN inputs in Fig. 4-15 b), with Noise level values as ANN inputs in Fig. 4-15 c), and with SNR values as ANN inputs in Fig. 4-15 d).

Again, the network training process was optimized according to minimum of the average absolute positioning error.

Fig. 4-15 shows a minimum of the average absolute positioning error at 50000 epochs of training for models using RSSI, SNR and both RSSI and SNR values as inputs. As for the ANN model relying on Noise level inputs, its minimum of the average absolute positioning error is reached after 200000 epochs of training. The positioning performance parameters of all ANN models (optimally trained) are shown in Table 4-VI.

Table 4-VI Positioning performance parameters of all ANN models for optimal training length

Parameter	RSSI	SNR	Noise	RSSI & SNR
Optimal Training [*k*epochs]	50	50	200	50
Average DE [m]	9.26	9.13	13.9	9.17
DE (10th percentile) [m]	2.92	2.80	3.87	2.76
DE (33th percentile) [m]	5.63	5.92	7.93	5.21
DE (median) [m]	7.75	7.44	11.8	7.24
DE (66th percentile) [m]	10.3	9.62	15.4	9.22
DE (90th percentile) [m]	16.8	15.7	25.5	17.1

From Table 4-VI, as expected, it can be seen that by far the worst positioning performances are achieved by Noise level based ANN model shown in Fig. 4-15 c). In comparison to other models shown in Fig. 4-15 a), b) and d), Noise level based model attains its best performances for greater training durations. Bearing in mind that, for a chosen test-bed, a positioning system that has no location dependant information as its inputs, would have the average positioning error equal to 53.76m (see section 4.4) it can be concluded that Noise level vectors indeed contain location dependant information. On the other hand, worse accuracy of Noise level based model (in comparison to other model) suggests that Noise level parameter is less location dependant information than RSSI or SNR parameter.

Regarding the RSSI and SNR models, from Fig. 4-15 a) and b), it can be seen that for under-trained ANN, RSSI model performs slightly better. This result might indicate that SNR is more influenced by the noise process than RSSI values. However, when optimally trained, both RSSI and SNR models achieve similar performances as shown in Table 4-VI. As for the model that uses both RSSI and SNR values as ANN inputs, from Fig. 4-15 it can be noticed that it has almost the same performances, when regarding the training duration, as RSSI based model. This implies that the noise process information is included in both RSSI and SNR values. To further clarify this, the reverse case might be observed. If the noise process was to contain location information independent to those of RSSI or SNR processes, the RSSI&SNR model would achieve superior positioning performances (because it contains separate information about RSSI and noise processes). Since, that is not the case, it can be concluded that the aforementioned hypothesis, that the noise process location dependent information is included in both RSSI and SNR values, is valid. In other words, this validates that the noise measurement process includes, not only the background noise, but also the part of the signal from some other access points. This is perhaps most obviously visible in Fig. 4-16 which depicts the cumulative distribution function (CDF) of the distance error for optimally trained ANN models. Certainly, to obtain a full scrutiny of a positioning technique one should not disregard technique's latency, scalability or implementation costs. However, when concerning solely the positioning capabilities of a technique, they are most comprehensively described with distance error's CDF. In those terms, as shown in Fig. 4-16, the positioning performances of the three models using RSSI, SNR and both RSSI and SNR as ANN inputs, are virtually the same whereas the Noise level based model underperforms.

The obtained results show that, contrary to the common knowledge, SNR parameter is equally suitable for WLAN positioning purposes as RSSI parameter. Furthermore, positioning in WLAN environments can be achieved relying solely on Noise level information. However, noise level distribution is shown to be less location dependent than RSSI or SNR distributions and, therefore, yields worse positioning capabilities. Finally, the model with RSSI & SNR inputs performs slightly better that the model with RSSI inputs. Nevertheless, the increase in model's complexity (due to the greater number of inputs) can hardly be justified with the minor improvement in performances.

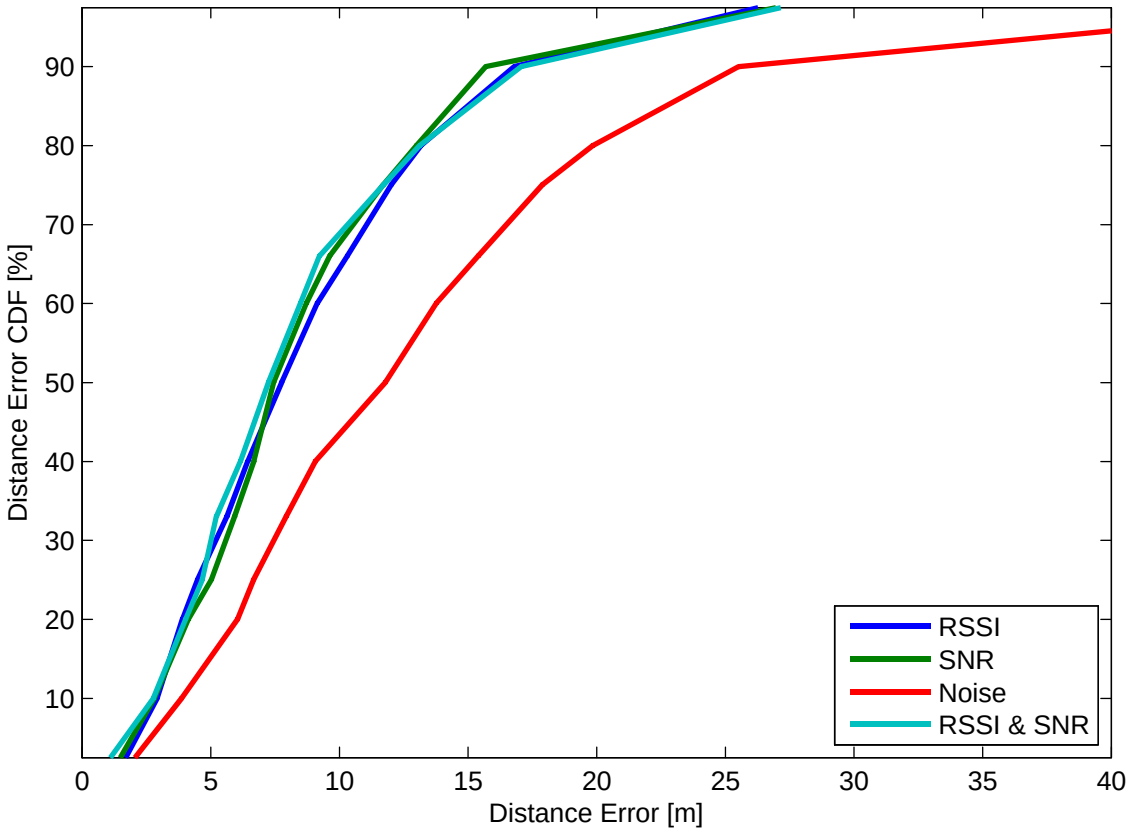

Fig. 4-16 Cumulative distribution function (CDF) of the distance error for optimally trained ANN models

4.3.2.2 The Cascade-Connected ANN Position Estimation Models

When testing the single ANN models, due to the disproportion between the width and the length of the test-bed, the obtained positioning error results (DEs) were split into *X* and *Y* axes. For the optimally trained single RSSI ANN model discussed within section 4.3.2.1, the *X* axis median positioning error equals 5.43 m, while the *Y* axis median positioning error was only 3.01 m. As the accuracy along the *X* axis is worse than along the *Y* axis, it was worth considering that, given the constant AP density, the performance of the positioning technique degrades with the increase in the dimensions of the test-bed. Hence, we decided to evaluate the performances as a function of a test-bed size.

To further verify the impact of test-bed size on accuracy, the same positioning technique was applied on a smaller part of the original test-bed. The single RSSI ANN structure discussed in section 4.3.2.1 was used and trained with measurements collected at 60 RPs. The absolute average distance (positioning) error obtained in this small-scale test-bed, which consisted of two offices and a classroom with overall dimensions of 18 m x 12 m, was 1.82 m, while the median error was only 1.67 m. It should be noted that, in the case of a smaller test-bed, the estimated position is always forced to be inside that test-bed, which may decrease the positioning error given that the AP density remains the same.

Bearing in mind the aforementioned, the idea of a positioning process where the environment is being partitioned in subspaces has risen. The positioning would then be, according to this paradigm, segmented into a two-stage process. The first stage has the classification task, i.e. to estimate the subspace in which the user resides. The second stage has the task of estimating the position of a user within the particular subspace (which is identical to the single ANN model, only in a smaller part of the environment). The benefits of using this approach should come as a consequence of the positioning process splitting in two phases where each phase can be solved independently with the most adequate model.

In this work, the space-partitioning process is utilizing cascade-connected (C-C) ANNs. The block structure of this system is depicted in Fig. 4-17. The input of this structure is the observed RSSI signal vector, **APs RSSI**, and the position estimate vector, **Pos Est**, is its output.

In the first stage, an ANN (type 2) is used to determine the likeliness of a measured RSSI vector belonging to one of the subspaces. This ANN (type 2) also has 8 inputs and the number of outputs is equal to the number of subspaces the environment is partitioned to. Each output corresponds to the likeliness that a received RSSI vector originates from a particular subspace. The outputs of the type 2 ANN, **SubSp Ln**, are connected to the Forwarding block which, depending on the inputs, employs only one of the second stage networks by forwarding the **APs RSSI** vector.

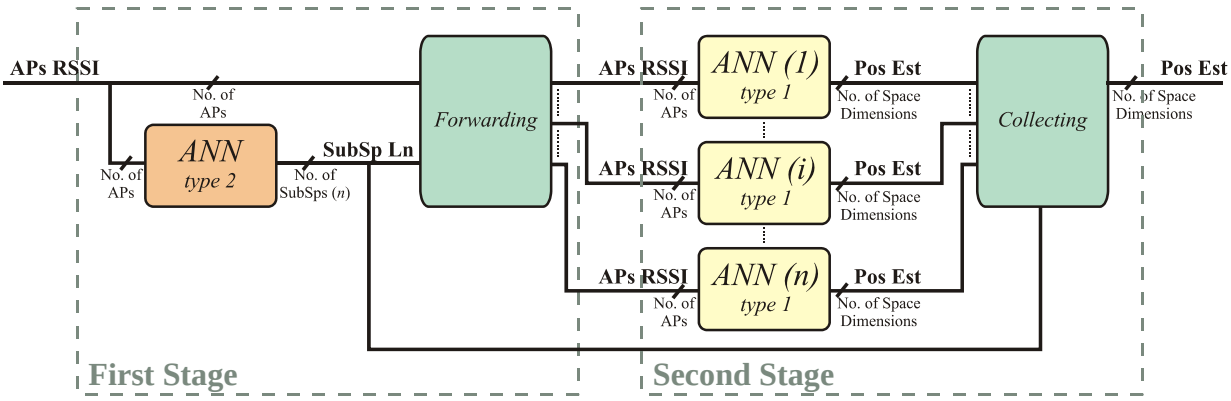

Fig. 4-17 Cascade-connected system structure with space-partitioning

The inner structure of ANN (type 2) was designed using the same guidelines as with other models. Therefore, it also has three hidden layers and the number of perceptron units in those layers is varied, according to the previously stated principles, to fit the different number of subspaces. The second stage ANNs are type 1 networks with structure identical to the previously described ANN used with single ANN approach. The second stage may be

considered as a collection of single ANN models for smaller parts of the environment, employed when a client is presumed (by the first stage ANN) to be in a particular subspace.

In the off-line phase, type 2 ANN is trained with the fingerprinting database that originates from the whole environment. The targeted output vector has only one non-zero element (equal to 1). The index of that element corresponds to the number of the subspace from which the RSSI vector originates. Type 1 networks are trained following the training methodology from the single ANN approach with the only difference being that each type 1 ANN is trained with only the part of the fingerprinting database which originates from a particular subspace.

In the on-line phase, the appropriate subspace, from which the measured RSSI vector is most likely to originate, is chosen by the first stage ANN (type 2) and a proper second stage ANN (type 1) is employed using the Forwarding block. In order to make use of the best fitting second stage network, the Forwarding block searches for the maximum value in the output vector from the ANN (type 2). The appropriate second stage ANN then determines the estimated position of the user and a collecting block forwards that estimate to the structure output.

Several space separation patterns were conducted yielding a different number of subspaces ranging from 4 to 44. The space-partitioning patterns that have been engaged are shown in Fig. 4-18.

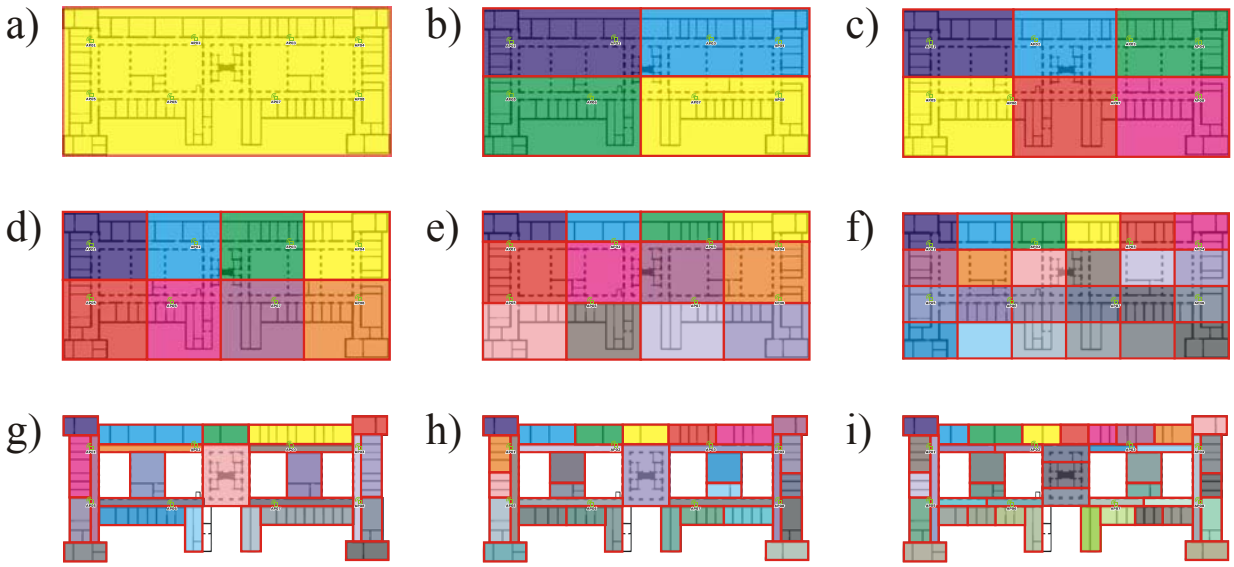

Fig. 4-18 Space-partitioning patterns: a) no space-partitioning (1x1), b) 2x2, c) 2x3, d) 2x4, e) 3x4, f) 4x6, g) x24, h) x32, and i) x44

The partitions with a smaller number of subspaces were made strictly on geometrical bases. However, with the increase in the number of subspaces, the subspace size decreased so, eventually, the subspace size has come to a room size level. It was then worth to consider

partitioning space in another manner. Starting with 24 subspaces (which was also portioned on geometrical bases), the partitions were made on "logical" bases (i.e. x24, x32 and x44). This logical separation opted for subspaces to be as homogeneous as possible in the propagation manner. For future comparison, the single ANN model is herein referred to as 1x1 partitioning. The results obtained for different space partition patterns, for optimally trained ANNs, are presented in Table 4-VII.

Table 4-VII Performance overview for different partitioning patterns

Pattern	1x1	2x2	2x3	2x4	3x4	4x6	x24	x32	x44
Overall Average DE [m]	9.26	9.00	8.97	8.91	8.54	8.28	8.14	8.58	9.11
Overall Median DE [m]	7.75	7.49	6.87	5.86	5.59	5.10	4.57	4.70	4.44
Average DE in Incorrect Subspace [m]	-	21.35	22.66	21.22	18.99	18.04	18.37	19.53	19.22
Median DE in Incorrect Subspace [m]	-	15.41	17.41	15.30	16.34	14.72	17.50	15.81	16.11
Average DE in Correct Subspace [m]	9.26	8.35	6.99	6.96	5.76	4.20	4.07	3.78	3.72
Median DE in Correct Subspace [m]	7.75	7.33	6.13	5.52	4.40	3.87	3.56	3.39	3.32
Probability of Correct Subspace Estimation	1.00	0.95	0.87	0.86	0.79	0.71	0.72	0.69	0.65
Probability of Correct Room Estimation	0.26	0.42	0.48	0.52	0.58	0.62	0.66	0.62	0.61

From Table 4-VII, it can be seen that, with geometrical partitioning, the overall median and average distance errors decrease with the increase in the number of subspaces. This behaviour is even more emphasized with the distance errors in the correctly chosen subspace which confirms the influence of environment size on positioning accuracy. When concerning the logical partitioning, it obtains slightly better results for 24 subspaces (4x6 vs. x24) but, with the further increase in the number of subspaces, their average distance error is starting to rise again. Also, with the increase in the number of subspaces the probability of correct subspace being chosen declines as expected while the probability of correct room estimation rises from 26% for a 1x1 positioning to as much as 66% for a x24 configuration after which it starts declining slightly. This behaviour is illustrated in Fig. 4-19.

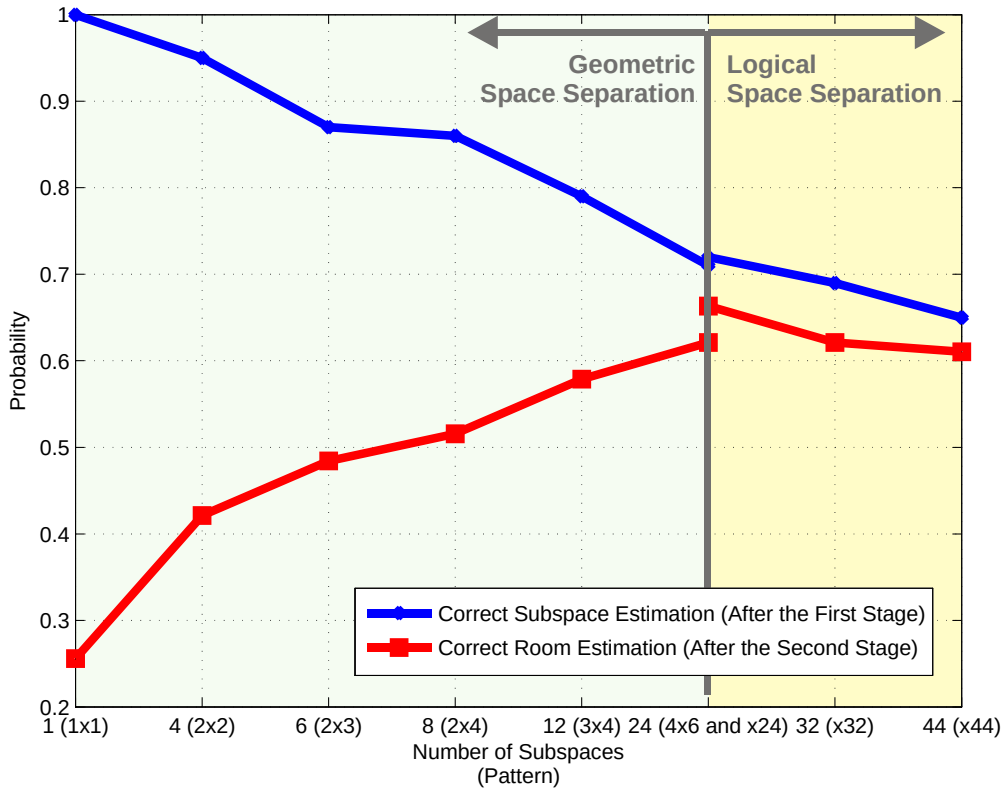

Fig. 4-19 Probabilities of correct subspace and room estimation

As for the distance errors in incorrectly chosen subspaces, they are influenced by the two colliding factors. Firstly, the subspaces are decreasing in average size inducing the positioning error of the adjacently chosen subspace to decline. On the other hand, as the probability of correctly chosen subspace decreases, the chances of incorrectly chosen subspace not being adjacent to the correct one are rising.

The distance errors presented in Table 4-VII are depicted in Fig. 4-20.

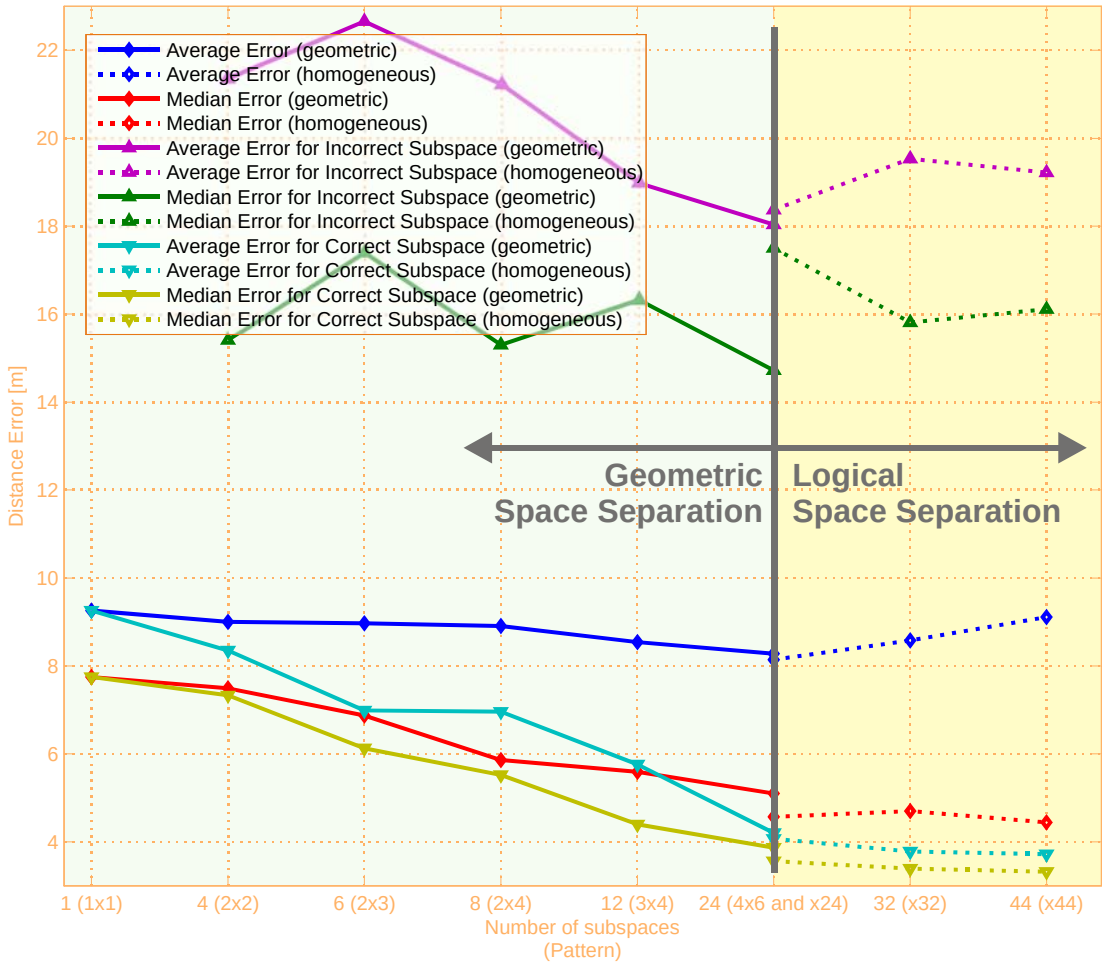

Fig. 4-20 Distance Error vs. Space Partition Pattern

To further evaluate the performances of C-C ANNs with space-partitioning, we observed and compared the distance error's Cumulative Distribution Function (CDF) of a single ANN approach with the C-C ANNs. The obtained CDFs are presented in Fig. 4-21.

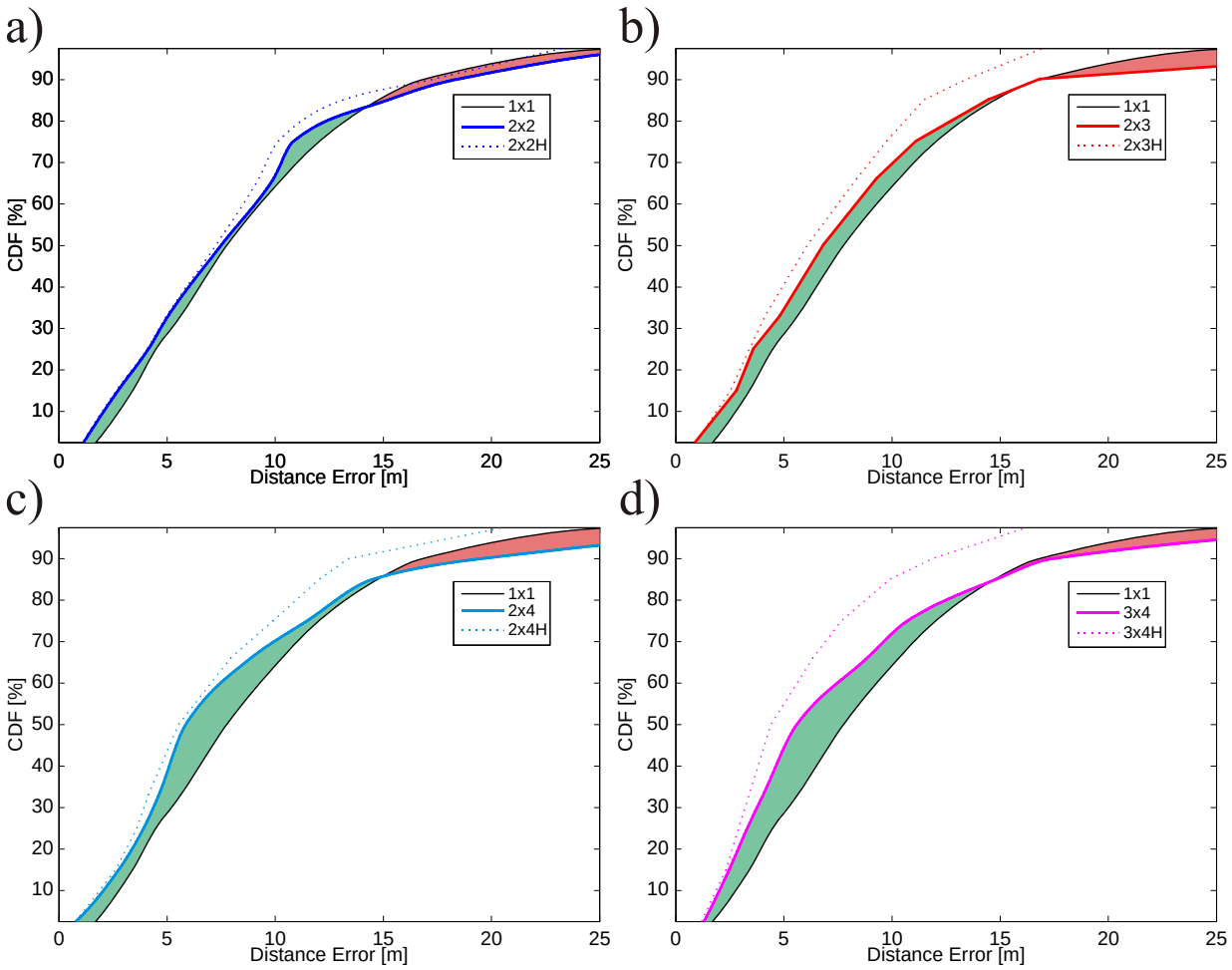
a)
b)
c)
d)
CDF [%]
Distance Error [m]
1x1
2x2
2x2H
2x3
2x3H
2x4
2x4H
3x4
3x4H

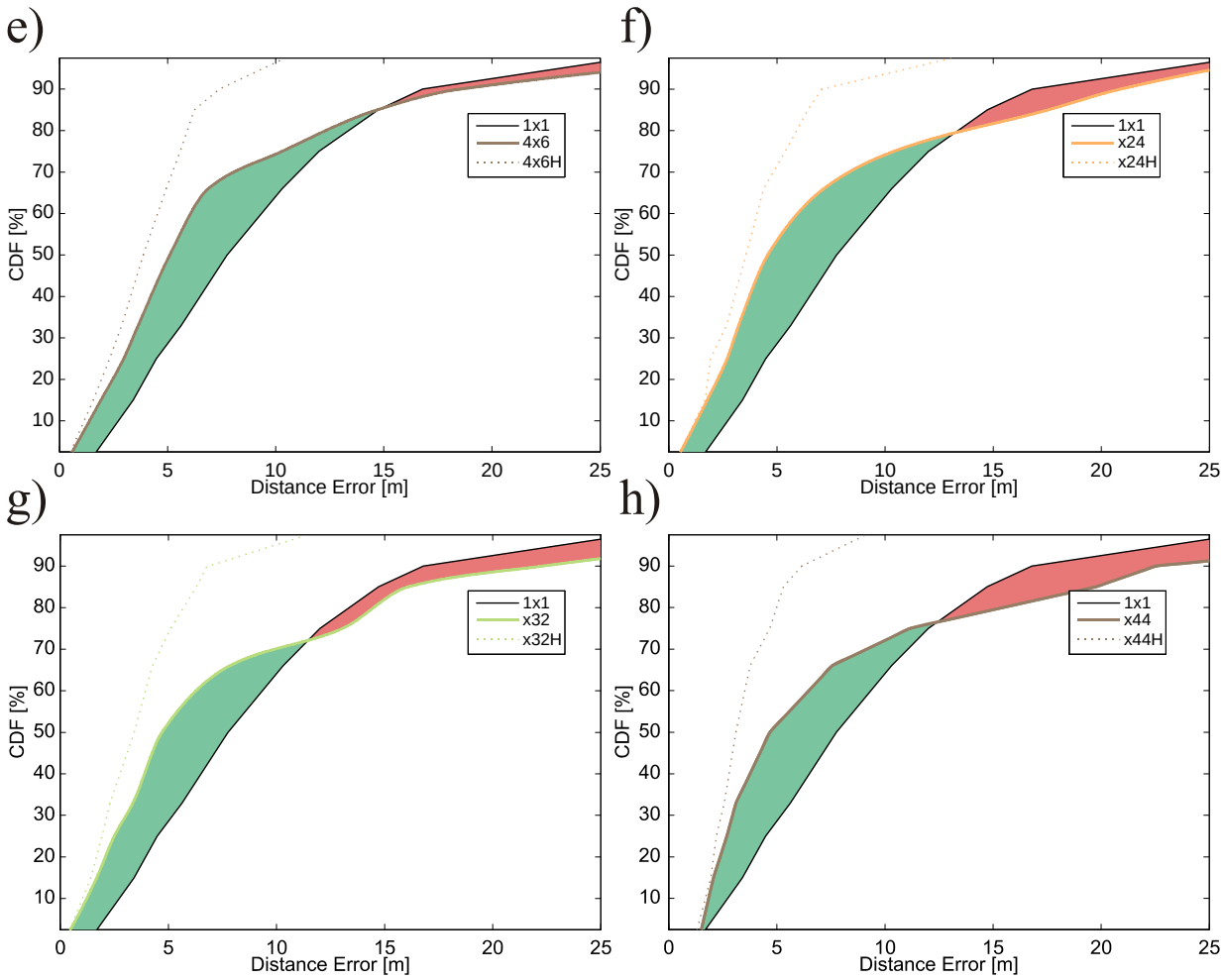

Fig. 4-21 Cumulative Distribution Function of distance error: a) 1x1and 2x2 partitioning and correct subspace estimation – 2x2 H; b) 1x1and 2x3 partitioning and correct subspace estimation – 2x3 H; c) 1x1and 2x4 partitioning and correct subspace estimation – 2x4 H; d) 1x1and 3x4 partitioning and correct subspace estimation – 3x4 H; e) 1x1and 4x6 partitioning and correct subspace estimation – 4x6 H; f) 1x1and x24 partitioning and correct subspace estimation – x24 H; g) 1x1and x32 partitioning and correct subspace estimation – x32 H; h) 1x1and x44 partitioning and correct subspace estimation – x44 H

The green filled areas in Fig. 4-21 could be considered as a partitioning gain in comparison to 1x1 positioning, while the red filled areas could be considered as partitioning loss. It can be seen that, with geometrical partitioning, the gain areas are increasing with the increase in the number of subspaces and the crossing point between the geometric space-partitioning and 1x1 positioning is always in-between 80 and 90%. This value is also affected by two conflicting factors. The rising of the probability of incorrect subspace detection ought to be pushing this crossing point towards the lower percentages. Still, it appears that, with the increase of the number of subspaces, there is a growth in the number of errors in the incorrectly chosen subspaces that are smaller than in 1x1 positioning case. This tends to drive the crossing point towards higher percentages. When concerning logical space-partitioning Fig. 4-21 f) – h), it can be noticed that the best performances are obtained with x24 pattern – average distance

error 8.14m, median error 4.57m. With the further increase in the number of subspaces, the benefit of decreasing the median error has faded, even though the median error in correct subspace continues to decrease, whereas the average distance error is starting to rise again. In other words, with the further increase in the number of subspaces, the partitioning gain surfaces are still expanding however, the partitioning loss surfaces are rising as well. Furthermore, it should be noticed that with the increase in the number of subspaces, the CDF is starting to create a knee roughly around 60^{th} percentile. This has two effects: the green surfaces are getting larger as discussed and the crossing angle between the space-partitioning model and 1x1 positioning is increasing while the crossing point between the two is being pushed towards lower percentiles. The latter of the two effects has a negative impact on positioning performances (especially when bearing in mind that the upper limit on the Fig. 4-21 is 97.5^{th} percentile so the entire partitioning loss is greater in this case).

The increase in the number of subspaces causes a larger training time for the first ANN cascade (due to the larger number of perceptron units). Although an individual second stage ANN is trained slightly faster when it covers smaller area (more subspaces – fewer RPs), the overall training time somewhat increases with the increase in the number of subspaces. For the given subspace divisions, the computational times for training the C-C ANNs were never more than 15% greater than those in the single ANN approach.

Fig. 4-22 shows the DE's PDF functions for the bordering cases – 1x1 and x44 models. The transformation of PDF function with space-partitioning can be observed. Clearly, the variance of PDF (σ) is decreasing with the use of space-partitioning. Moreover, the PDF of x44 is again greater than the one of 1x1 with high DEs (over 20m). This confirms the separation effect the space-partitioning has on the DE. Namely, the errors, with the increase in the number of subspaces are divided into two subsets: one containing small DEs (less than 5m) and the other one containing large DEs (more than 20m). In other words, with space-partitioning, the probability of obtaining a position estimate with a medium sized error (in this case 5 to 20m) is decreasing. This might even be useful. If the overlaying mechanism for detecting such large DEs could be devised then the additional increase in the number of subspaces might be exploited to further benefit the positioning performances. For instance, the system that could recognize potentially large DEs, could opt to reassess the position in such cases.

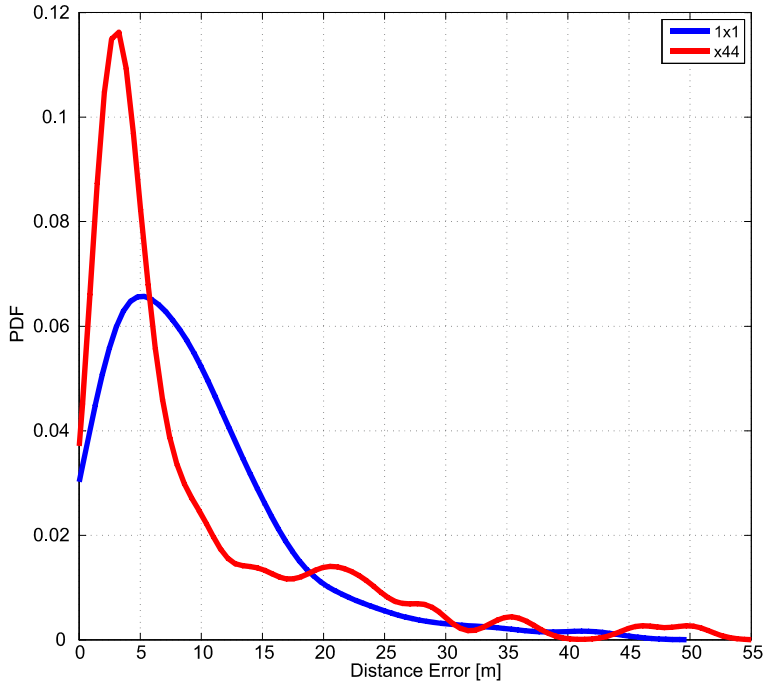

Fig. 4-22 Transformation of the DE's PDF with space-partitioning in WLAN environment

As for the latency of this technique, once the ANN cascade structure is trained, its increase, which is caused by the increased number of subspaces, is negligible, as it takes nothing more than a series of multiplications and additions to provide positioning information. The real-time positioning is not perceivably affected by the number of subspaces, once the training is performed.

Scalability wise, the expansion of network infrastructure would impact the first stage (type 2) network and some second stage (type 1) networks. The second stage networks that would be affected are the ones covering the subspaces bordering with the new part of the environment. As a result, there is no need for recollecting the complete fingerprinting database, rather supplementing it with measurements from the expanded areas.

4.3.2.3 The Cascade-Connected ANN SOFT Position Estimation Model

This model has an identical block scheme to the C-C ANN models illustrated in Fig. 4-17. The only difference to those models is that with SOFT model, the forwarding and collecting block have somewhat different function.

The Forwarding block does not send **APs RSSI** vector to only one second stage ANN (type 1). It forwards the **APs RSSI** to all of the second stage networks regardless of the **SubSp Ln** vector. On the other hand, the function of the Collecting block with the soft model is to normalize the **SubSp Ln** vector so that its values $p_1, p_2, \ldots, p_i, \ldots, p_n$ (where n is the

number of subspaces) resemble the probabilities of a user being detected in a certain subspace, i.e. $\sum_{i=1}^{n} p_i = 1$. Then the position estimate can be obtained with:

$$\mathbf{Pos\ Est} = \sum_{i=1}^{n} p_i \mathbf{Pos\ Est}_i \tag{4.1}$$

In Eq. (4.1), $\mathbf{Pos\ Est}_i$ is the output of the *i*-th second stage ANN and **Pos Est** is the overall position estimate. As a result, this model supports soft decision making, being that the overall user's location is not only dependent on one second stage ANN estimate, but all of them. The leverage of individual outputs of the second stage ANNs is proportional to the probability that a user is presumed in a given subspace.

Following the training and verification methodology from the previously described models, the soft C-C model was implemented on 4x6 space-partitioning pattern and the obtained CDF in comparison to 1x1 positioning is given in Fig. 4-23.

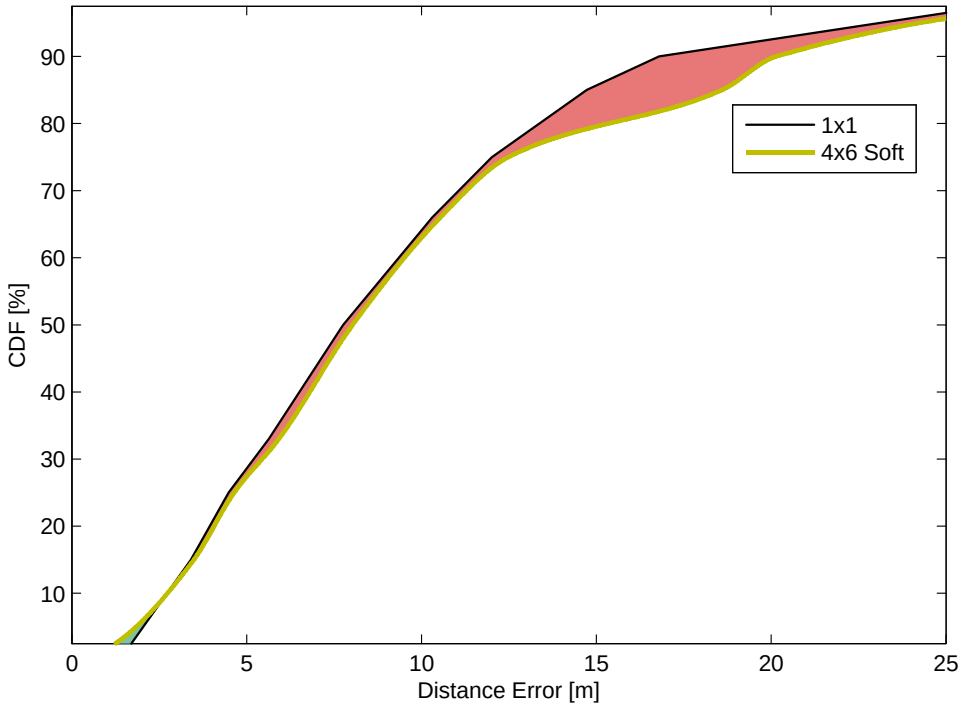

Fig. 4-23 Cumulative Distribution Function of distance error for 1x1and 4x6 soft space-partitioning

It can be seen from Fig. 4-23, that soft C-C model underperforms in comparison to single ANN model (red coloured surface) with the exception of the extremely low percentiles region where it's slightly more accurate (green surface).

Bearing in mind that this model is more complex than regular C-C ANNs model and that it gives unpromising results, it will not be taken into further comparison.

4.4 Comparison

First, let us consider the effect of the test-bed size on accuracy. If the overall DEs in correct subspace for geometrical partitioning strategy (from Table 4-VII) are compared with the average subspace area (the total environment size divided by the number of subspaces), it can be seen that with the increase in the size of the subspaces (for this purpose regarded as separate test-beds) the increase in DEs is getting saturated. This behaviour is illustrated in Fig. 4-24. The obtained values have been connected with the shape-preserving interpolant curves. So, given the constant APs and RPs density, it can be concluded that the further increase in the size of the test-bed should induce only the minor rise of the DE. This also goes to say that the chosen verification environment was large enough to adequately include the influence of the test-bed size on positioning performances.

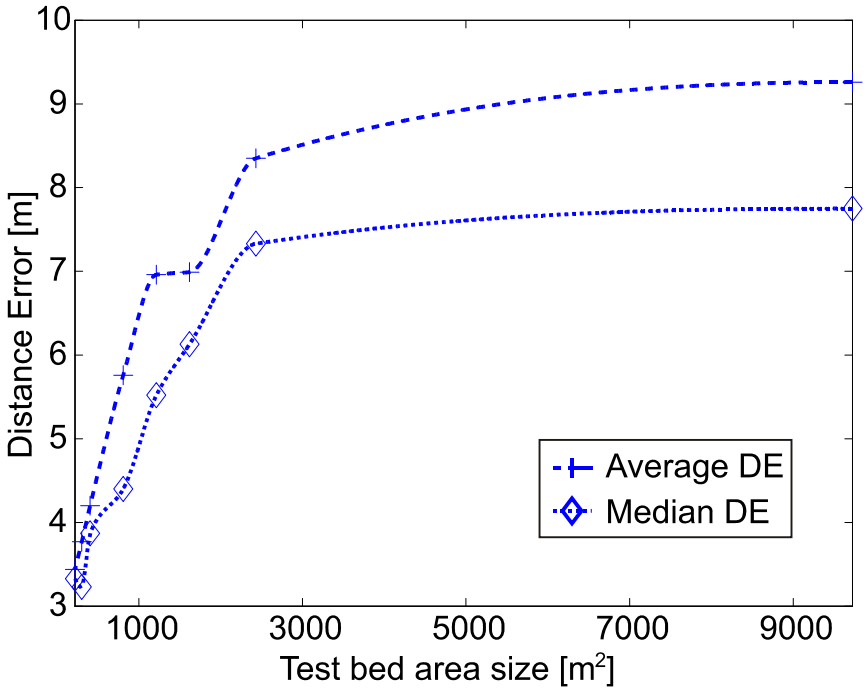

Fig. 4-24 Distance error vs. the test-bed area size

To account for the influence of the environment size on positioning accuracy a new comparison parameter, is introduced. This parameter, referred to as the *environment positioning error*, is solely a function of the environment and is not technique dependent. This parameter would be equal to the mean positioning error, given that a positioning technique has no input information other than the size of the test-bed. In other words, if a two-dimensional rectangular environment and a two-dimensional, uniformly distributed random variable as a position of the user are assumed, this parameter can be calculated as the mean absolute

difference of two uniformly distributed random variables (user's position and user's position estimate). It can be easily shown that the mean absolute difference of two uniformly distributed random variables on [0,1] interval is equal to 1/3 [4.2]. Therefore, if we denote the dimensions of test environment as *a* and *b*, *environment positioning error*, $\varepsilon_{env}(a,b)$, is given as:

$$\varepsilon_{env}(a,b) = \frac{1}{3}\sqrt{a^2 + b^2} \tag{4.2}$$

This error could be considered as the maximal positioning error of the environment and is similar to the random error used in Table 2-I.

To normalize the positioning errors regarding the size of the test-beds we used the ratio between the *environment positioning error* and the median error for a particular test environment where specific techniques were implemented. This parameter is intended to show the level of relative accuracy the specific technique achieved in a given environment.

Table 4-VIII Comparative analysis of WLAN positioning systems

Technique / Parameter	RADAR	Bayesian	Horus	Battiti ANN	Single ANN (FMC)	Single ANN (SMC)	C-C ANNs (x24)
Test-bed size – *a* x *b* [m] x [m]	43 x 22	25 x 15	59 x 19	20 x 15	144 x 66	144 x 66	144 x 66
Covering area – *S* [m^2]	946	375	1121	300	9504	9504	9504
Number of APs – N_{AP}	3	5	12	3	8	8	8
m^2 per AP – ρ_{AP}^{-1}	315	75	93	100	1188	1188	1188
Required APs number to cover chosen test-bed area size with same density	30	127	102	95	8	8	8
RPs	70	132	110	56	433	403	403
Rx orientation at each RP	4	4	1	1	1	4	4
No. of samples for avg.	20	20	300	100	1	1	1
Average covering area of a RP [m^2]	13.51	2.84	10.19	5.35	21.95	23.58	23.58
Total no. of samples / m^2	5.92	28.2	120	18.7	0.04	0.17	0.17
Median error – $\varepsilon_{50\%}$ [m]	3 / 4.3[a]	2	2	1.69	8.4	7.75	4.57
Env. error – ε_{env} [m]	16.1	9.72	35.8	8.33	52.8	52.8	52.8
$\varepsilon_{env} / \varepsilon_{50\%}$	5.36 / 3.74[a]	4.86	17.9	4.93	6.24	6.81	11.55

[a] fingerprinting approach /propagation model approach

From Table 4-VIII, it can be seen that the best performance[3], regarding exclusively accuracy, is achieved by Battiti *et al.* ANN technique (excluding herein presented single ANN approach on a small-scale test-bed which has a median positioning error of 1.67 m). On the other hand, the accuracy of techniques implemented in the full-size test-bed (Fig. 4-1) is somewhat worse than other presented techniques. However, herein presented approaches can be successfully applied in widespread WLAN networks implemented above all for Internet access. In particular, all other techniques require a minimum of three radio-visible APs (more often, that number is significantly higher), while with our test-bed (which is also the case with most other WLAN networks), the average number of radio-visible access points was only 2.38. Furthermore, in 61% of the RPs less than three APs were "visible" (for SMC, while for FMC this difference is even more emphasized). Hence, the derived parameters, which are used to give the insight into the technique's ability to be used in a real WLAN network, should be granted considerable attention.

The most significant comparison can be made concerning the ratio between the environment and median positioning error. Regarding this ratio, the C-C ANNs and single ANN approaches (FMC & SMC) fall to the second, third and fourth place, respectively, while the Horus technique is unjustifiably favoured. Namely, in this case (Horus) the measurements were made solely in corridors with outer dimensions 59 m x 19 m while the offices surrounded by the corridors and outside of the corridors were not taken into account for positioning. In this way, the actually covered surface was significantly smaller than the one used for this comparison. So, the test-bed that was used for the Horus positioning technique would make an excellent example for space-partitioning approach. Moreover, the accuracy of the Horus technique benefits from time correlation of the samples, but there is another end to such approach. Taking more time samples in the on-line phase increases the latency of the technique and narrows the potential range of the LBSs it can be used for.

The density of APs should not be neglected, either. Frequency spectrum is a scarce resource in WLAN networks (the 2.4 GHz band has a total of 14 channels of which only 3 can be non-overlapping). If we were to implement the existing WLAN positioning techniques in even remotely larger areas, such as the environment in which the herein presented techniques were implemented, the increased interference due to a number of APs working on the same channel would induce a major setback regarding the packet data services. This would have the highest impact on the ANN (Battiti *et al.*), Horus and Bayesian approaches because the density of

[3] The accuracy performances of techniques other than the single ANN and C-C ANN models were copied from the respective publications.

deployed APs, within these approaches, is primarily optimized towards the use of the LBS and practically hinders any efforts on frequency planning. Certainly, the increase in price of the network (network devices, cabling, etc.) should be considered as well.

Finally, the effort put into the collection of off-line measurements should be stated too. The total number of measurements made per square meter is by far the smallest with our approach (0.04 measurements per m^2 – for SMC). All other techniques have a significantly greater measurement density, the worst case being the Horus technique (120 measurements per m^2). The implementation of Horus technique in our test-bed would require 90 APs and more than 1,000,000 measurements which is, of course, very impractical.

As we noted before, a single ANN approach can obtain superb accuracy when applied to a small-scale test-bed. The same approach, applied on the full-scale test-bed, has somewhat worse accuracy than other well-known techniques. It is shown that such accuracy degradation comes as a result of increase in environment induced error. When regarding the C-C ANNs approach, it has been shown that it yields better accuracy than the single ANN approach. At first, the partition benefit augments with the number of subspaces. But there is a limit to such behaviour. Nevertheless, the optimal number and size of subspaces as a function of the size and type of the environment, number and density of RPs, is to be the object of upcoming research.

Bearing in mind that ANNs have superior latency compared to other commonly used positioning methods [4.3], once the training is performed, proposed C-C ANNs positioning is performed in real-time regardless of the number of subspaces. As for the scalability of C-C ANNs, it can be considered comparable with other well-known WLAN positioning techniques.

4.5 References

[4.1] Hasoun H. M., „Fundamentals of Artificial Neural Networks", Massachusetts Institute of Technology, 1995.

[4.2] Weisstein, Eric W: Uniform Difference Distribution. From MathWorld--A Wolfram Web Resource.

[4.3] Lin, T-N., Lin, P-C.: Performance comparison of indoor positioning techniques based on location fingerprinting in wireless networks. International Conference on Wireless Networks, Communications and Mobile Computing, Volume 2, pp.1569 - 1574 (June 2005)

5 Positioning in PLMN Using ANNs

The number of PLMN subscribers has been growing significantly for years. Increased user mobility and ubiquitous coverage are some of the key reasons for the great efforts applied to finding appropriate positioning techniques in this environment.

The most commonly implemented second generation PLMN technologies comprise GSM and DCS. DCS is technically very similar to GSM but translated to the higher frequency band (1800MHz instead of 900MHz for GSM). As for the third generation of PLMN systems, the UMTS is mostly represented. The research on positioning in these three systems is the object this chapter.

The research on the topic of positioning in PLMN can be divided into two major categories. The first one includes empirically modelled behaviour of the timing advance parameter (GSM/DCS) and a specific mathematical algorithm for estimating the MS position. The second, more broad, group continues the efforts from the previous chapter – RSS parameters, gathered from GSM, DCS and UMTS systems, were measured and single and C-C ANN models have been implemented and verified.

5.1 Measurement Campaigns

5.1.1 TA Measurement Campaign (GSM, DCS)

The Cell-ID method estimates the position of the MS as the location of the BTS (Base Transceiver Station), which the MS is served by. Cell-ID+TA, however, uses Timing Advance (TA) parameter to decrease the positioning error. Namely, GSM uses multicarrier TDMA (Time Division Multiple Access) at its air interface [5.1]. Due to the variable distances between BTS and MSs the synchronization of bursts arriving to a BTS is required. TA parameter, assigned to each MS by the serving BTS, is proportional to the propagation delay of the round trip from BTS to MS. Timing advance parameter is coded with 6 bits. TA takes value from the interval [0,63], where one increment of TA corresponds to approximately 550m. Therefore, by using TA parameter the distance between the MS and the BTS (d) can be described as [5.2]:

$$550m \cdot \left(TA - \frac{1}{2} \right) \le d \le 550m \cdot \left(TA + \frac{1}{2} \right), 0 < TA < 64$$
$$0 \le d \le 225m, TA = 0 \tag{5.1}$$

Thus, this method locates the MS in annuli (rings) defined by the eq. (5.1). Cell-ID+TA can be upgraded using triangulation. However, the techniques [5.3], [5.4] made using this upgrade show limited improvement due to a significant number of situations where TA circles, defined by eq. (5.1) do not overlap. In such cases the position of MS cannot be determined.

Measurements [5.2], [5.3] show that in different propagation environments TA can differ from the expected values given in eq. (5.1). This is because the eq. (5.1) corresponds to ideal conditions (line of sight, maximum propagation speed, etc.). Phenomena like multipath propagation (reflections, diffractions, scattering) produce further jitter and delay, therefore affecting the assigned TA value.

To solve this inadequacy, the TA parameter was modelled [5.2]. The distance between MS and BTS (d) can take values from the interval [0, 35km] (GSM has a maximum cell radius of 35km). The model for each TA value (i) is described by a probability function f_i:

$$\Pr\{TA = i, d\} = f_i(d) \quad i = \overline{0,63} \quad d \in [0, 35km] \tag{5.2}$$

The sum of all probability functions satisfies the following condition:

$$\left(\forall d \in [0, 35km] \right) \left(\sum_{i=0}^{63} f_i(d) = 1 \right) \tag{5.3}$$

In order to determine three different sets of probability functions f_i, for urban, suburban and rural propagation environments, over 1800 measurements have been made. Each measurement included recording the distance between the MS and the BTS (using a GPS receiver), and the TA value assigned by that BTS. The results were classified as (d, TA, environment) triplets, and processed using SQL (Structured Query Language) queries.

5.1.2 RSSI Measurement Campaign (GSM, DCS, UMTS)

For the purpose of exploring RSSI based positioning in PLMN, a new, massive measurement campaign was qualitatively designed and implemented. The campaign covered the urban area of the capital of Serbia – Belgrade. For this campaign, the specialized measurement system – TSMQ & ROMES (Rohde&Schwarz), shown in Fig. 5-1, was mounted in a specially adopted vehicle [5.5]. TSMQ Radio Network Analyzer is the fundamental element of this system. This, state of the art measurement system is able to measure and record many physical layer parameters of GSM, DCS and UMTS systems. Up-to-date BTS/Node-B databases, along with their coordinates, from both "Telekom Serbia" and "VIP Mobile" network operators were obtained. At the time, the first network operator (MTS) had roughly 200 GSM BTSs, 130 DCS

BTSs and 120 UMTS Nodes B across the city area. The second operator - VIP, due to allocated frequency bands, had just a few GSM BTSs for macro-coverage, around 170 DCS BTSs and more or less 70 active UMTS Nodes B.

In addition, measuring system has a differential GPS receiver attached, and all measurements made are georeferenced. This system can usually achieve under 5m median error [5.6] which is by order of a magnitude better than the accuracy expected from PLMN positioning system. Therefore, it can be used for reference localization. The measurement and GPS location data was acquired by using a laptop computer equipped with "R&S Romes v4" software. This software can load the BTS/Node B database and directly produce distances from measured sites along with measured parameters.

Fig. 5-1 Specialized Measurement System – TMSQ & ROMES (Rohde&Schwarz)

The measurement campaign was carried out during the first quarter of the 2009. It comprised about 50 hours of measurement. During this period, a distance of more than 600 km was covered and measurements on more than 1,000,000 locations were performed. Almost every single street in Belgrade was covered with this measurement campaign and a total of more than 10GB data was collected. Among other, the received signal strength of every radio-visible base

station (often more than 20) was recorded along with the power delay profile of the serving Node B.

With this campaign, a set of measurements of truly respectable proportions and quality was obtained. Future research work should immensely benefit from this measurement campaign.

5.2 TA Based Positioning Model (GSM/DCS)

5.2.1 TA Model

The TA model was obtained from the TA measurement campaign depicted in section 5.1.1. Positioning based on TA values has two main entities: the statistical TA model (different for each environment and for each TA value), and the core positioning algorithm that relies on modelled TA behaviour to estimate the user's position. This algorithm is also referred to as Enhanced Cell-ID + TA or E-CIDTA.

The database of TA values obtained by measurements was used to derive a statistical TA model. The process of deriving TA probability functions was divided into the following steps:

1) Initially determine the type and parameters of the distribution functions from the collected data for representative TA values in different environments (one TA value for each environment).
2) Interpolate the probability functions for other TA values for respective environments.
3) Correct/validate the model based on a test series of location estimation measurements.

The analysis was performed using a simple Matlab program. The obtained model gives a probability that a TA parameter will take a certain value at distance d, in a predefined environment.

Since the algorithm that was eventually going to use the TA models was implemented and run on the computer, the domain of probability functions (d) was chosen to be discrete. In favour of minimizing the additional error, the probability functions were sampled on every 5m. The quantifying step presents a trade-off between execution time of the algorithm and the error that model itself brings into computation. Using Matlab, the model for each environment was created and stored into an ASCII file. ASCII files are divided into sections corresponding to different TA values for which the probability is greater than zero. These files are further used by the algorithm.

To determine the type and parameters of the distribution function $f_1(d)$ (probability function for TA=1) approximately 700 measurements, made in a suburban environment, were used. The observed interval of distances from the measurement location to BTS was [200m, 1300m], which, according to eq. (5.1), should be wide enough to record $f_1(d)$.

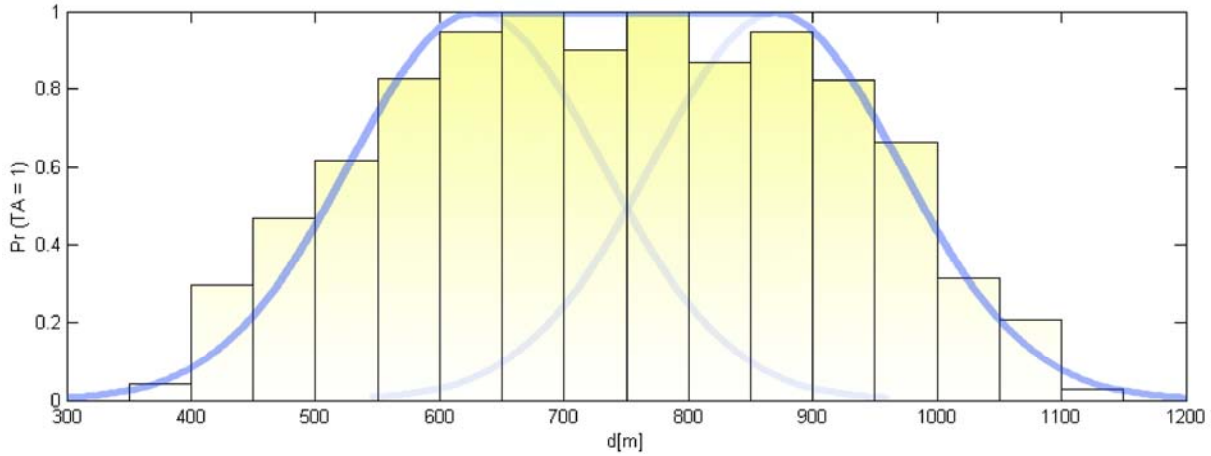

Fig. 5-2. Measurement results (bar graph) and the model of the probability function f_1(d)

Fig. 5-2 shows the results obtained by TA parameter modelling process, where the values of $f_1(d)$ for the omitted distances are very close to zero.

Graph bar in Fig. 5-2 denotes the measured $f_1(d)$ averaged on 50m intervals. It can be shown that for a certain value d no more than two adjacent TA values are likely to be assigned. Furthermore, in-between the ascending and descending edges of an $f_1(d)$ exists a region where $\Pr\{TA=1\}\approx 1$. The domain of the probability function can therefore be contained within the finite distance interval and divided into three regions: the ascending edge (with the width[4] w_a), the central region (where the $f_1(d)$ is nearly constant), and the descending edge (with the width w_d). The Gaussian distribution functions are also given in Fig. 5-2, and represented with thick blue lines. The parameters of these distribution functions (mean value and variance) can be determined from the Fig. 5-2 as well, to obtain the best-fit.

Based on the full set of measurements the following conclusions can be made:

1) The ascending and descending edges are symmetrical in respect to central distance d_c and have the same width $w_a = w_d = w$
2) The widths of the edges, for a specified environment, are the same for all TA values
3) When crossing from rural to urban environment the widths of edges increase, while the central region narrows. Also, all probability functions translate to smaller distances.

Obtained values of the width of edges and central distances for different types of environments and several most commonly assigned TA values are given in Table 5-I. The models of other TA values can be deduced using the Table 5-I and the aforementioned conclusions.

[4] The edges were defined as areas where $f_1(d)\in(0.05,0.95)$.

Table 5-I The width of edges and central distances of TA regions

TA	*RURAL*		*SUBURBAN*		*URBAN*	
	d_c [m]	w [m]	d_c [m]	w [m]	d_c [m]	w [m]
0	–	260	–	300	–	380
1	827,5	260	787,5	300	767,5	380
2	1382,5	260	1342,5	300	1322,5	380
3	1937,5	260	1897,5	300	1877,5	380

5.2.2 E-CIDTA Positioning Algorithm

The input data for the E-CIDTA algorithm are the triplets that correspond to: geographic position of the BTS, TA value assigned by the BTS and the TA model for the appropriate propagation environment. The number of input entries is equal to the number of assigned TA values (radio-visible BTSs).

The algorithm uses "a map" as an abstraction that represents real space in which BTSs and MSs reside. The map is a two-dimensional array of points. Each point, apart from its coordinates, contains a list of values k_m which represent the probabilities obtained from TA models for that point. Main operations on the map are "the population" and computing the estimated location.

The first stage of the position estimation is the map population. This process is done for each pair of (BTS, point) separately. First, the distance between the observed point and the BTS is calculated (to the multiple of 5m). Then, section of the ASCII file containing the recorded TA value and propagation environment (specific to the BTS) is observed. If the coefficient that matches the calculated distance exists (i.e. differs from zero), it is copied from the ASCII file section into the point's list of values. After the map is populated, the number of elements in the point's list is named the *level* of that point (n) and the maximum level of all the points in the map (n_{max}) is also referred to as the *level of the map*. The process of map population is illustrated in Fig. 5-3.

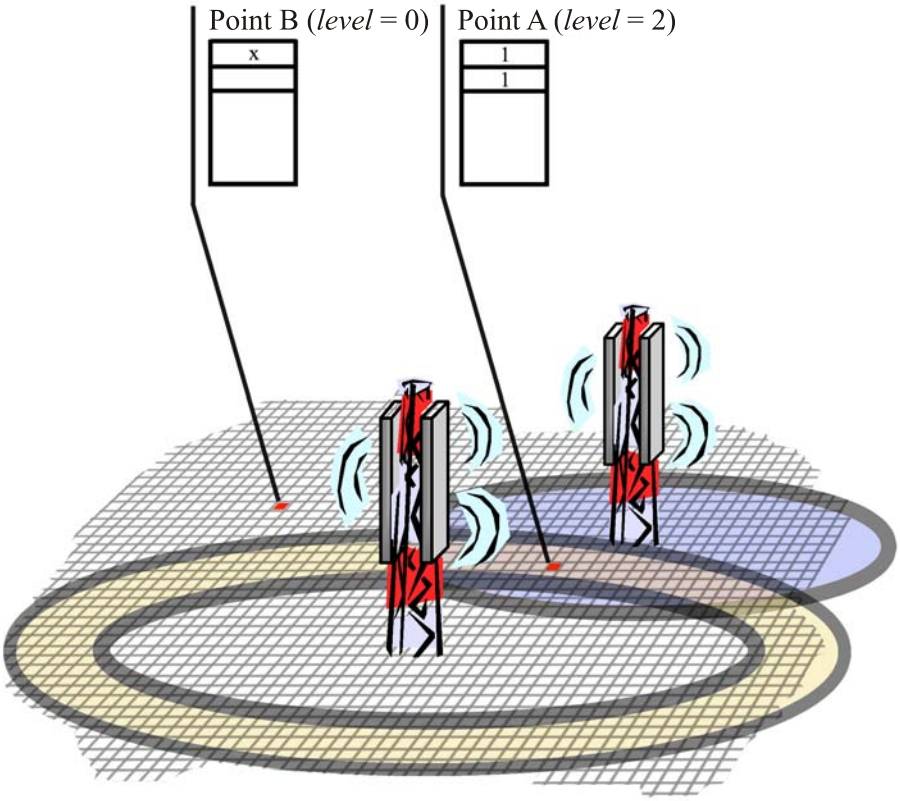

Fig. 5-3 The map population process

Further computing of the estimated location can be divided into three steps:

1) Derive the equivalent coefficient

The function that computes the point's equivalent coefficient ($k_{ekv}^{(1)}$) from the list of values must fulfil the following: the result must reside in [0,1] interval and the function must be additive. The simple function that meets these requirements is the average of the list values (k_m):

$$k_{ekv}^{(1)} = f\left(k_1, k_2, \ldots, k_n\right) = \begin{cases} \dfrac{k_1 + k_2 + \cdots + k_n}{n}, n \geq 1 \\ 0, n = 0 \end{cases} \tag{5.4}$$

2) Multiply the equivalent coefficient with "scaling factors" – $F(n, n_{\max})$

The role of the scaling factors is to decrease the density of points with relatively low level, thus emphasizing the points with level close to the level of the map. The exponential characteristics of the scaling factors, given in eq. (5.5), have been proposed. Based on a series of test measurements, it was determined that these scaling factors give good performance results for urban environment.

$$F(n,n_{\max})=\begin{cases}1, n_{\max}=1, n=1\\ \dfrac{e^{-2\cdot(n_{\max}-n)}}{n_{\max}-n+1}, n_{\max}>5, n>1\\ \dfrac{e^{-(n_{\max}-n)}}{n_{\max}-n+1}, 5\geq n_{\max}>1, n>1\\ 0, n_{\max}>1, n=1\end{cases} \tag{5.5}$$

Each point's density can now be defined by the $k_{ekv}{}^{(2)}$ as:

$$k_{ekv}^{(2)}=F(n,n_{\max})\cdot k_{ekv}^{(1)} \tag{5.6}$$

3) Estimate location

The location estimate is equal to the weight centre of the map where density of each point is equal to $k_{ekv}^{(2)}$ of that point.

The first two operations are done for each point separately, for as many times as there are points in the map, while the third operation treats all the points in the map and is performed only once. The E-CIDTA algorithm was implemented using Microsoft Visual C++.

The described algorithm was tested in an urban environment. A complete new set of measurements was performed for the purpose of evaluating the performances of E-CIDTA. TA values were collected from all "visible" BTSs, and processed using the E-CIDTA algorithm. Fig. 5-4 shows the map after the population process. Each point on the map is presented with its equivalent coefficient $k_{ekv}^{(1)}$. Darker points on the map have greater $k_{ekv}^{(1)}$ value. Fig. 5-5 shows the map after multiplication of $k_{ekv}^{(1)}$ with the scaling factors. Each point on the map is presented with its $k_{ekv}^{(2)}$. Darker points on the map have greater $k_{ekv}^{(2)}$ value.

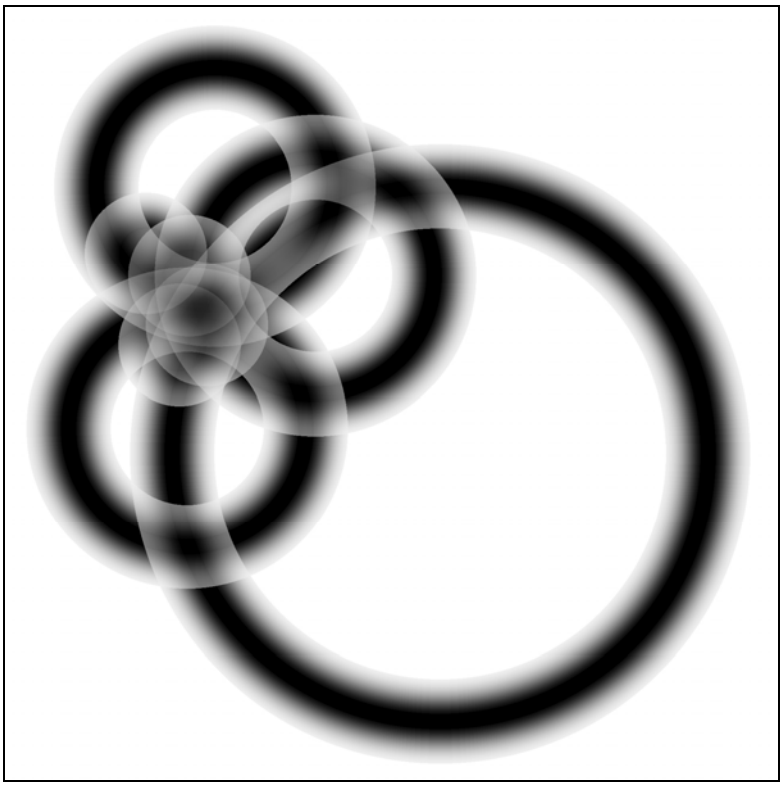

Fig. 5-4 The map after the population process – expressed via $k_{ekv}^{(1)}$

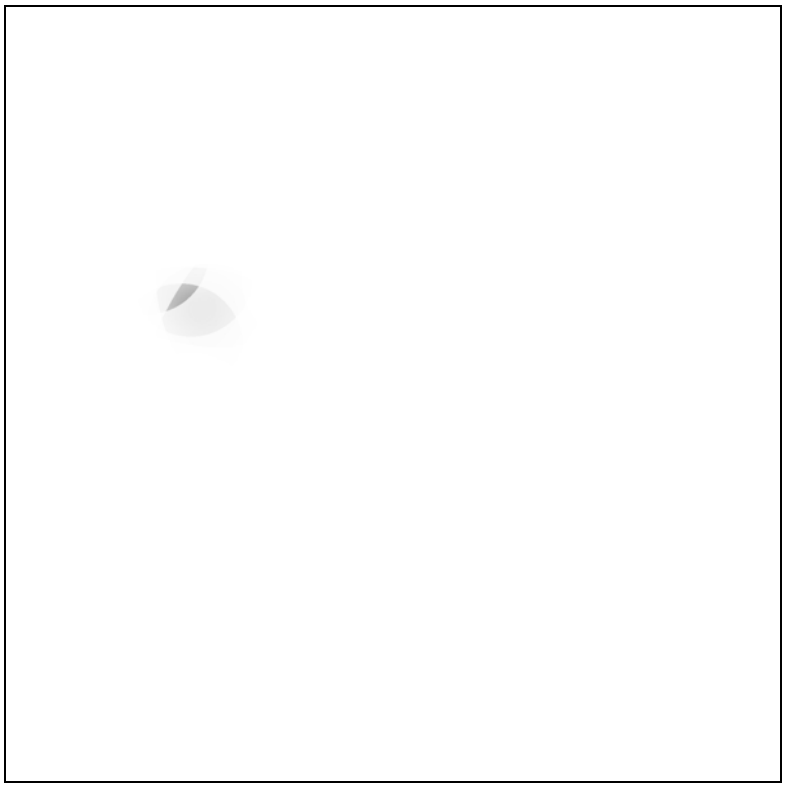

Fig. 5-5 The map after multiplication of the equivalent coefficients with scaling factors – expressed via $k_{ekv}^{(2)}$

Cell-ID+TA defines the user location in the annulus (ring). The accurate position largely depends on the assigned TA value, since the area in which the user is located increases with the TA value. Measurements show [5.7] that in an urban environment the error of Cell-ID+TA is 283m with 67% accuracy. Generally, E-CIDTA has better performance over Cell-ID and Cell-ID+TA, and somewhat worse performance than TOA, E-OTD, and A-GPS (all of these require additional hardware components installed either in the network and/or in the handset). The location error, in urban environment, with E-CIDTA is 135m with 67% accuracy, and 245m with 95% accuracy.

The availability of E-CIDTA is very high, since in the case of only one available BTS, this technique degrades to Cell-ID (or Cell-ID+TA in the case of sectored cells). The other location techniques have less or equal availability. The accuracy of E-CIDTA increases with the number of BTSs the MS is receiving TA value from, as shown in Table 5-II.

Table 5-II The influence of the number of BTSs to E-CIDTA accuracy

Number of BTSs	Accuracy [m] (67%)
2 – 3	595
4 – 5	425
6 – 7	200
8 – 9	105

Fig. 5-6 illustrates the dependence of technique's performances on the number of radio-visible BTSs.

The latency of this technique could not be determined precisely, since the TA measurement process itself increased the time to obtain the position, and this additional latency could not have been adequately measured. The estimate should increase depending on the number of BTSs from which the TA value is taken. However, the time to obtain the position should be less than 10s, which is comparable to other available techniques.

The presented technique overcomes some of the major flaws inherent in Cell-ID+TA with triangulation, and gives better performance than two basic techniques Cell-ID and Cell-ID+TA. The presented algorithm can be further improved using additional data like Rx level (RSSI) to improve precision in suburban and rural environments.

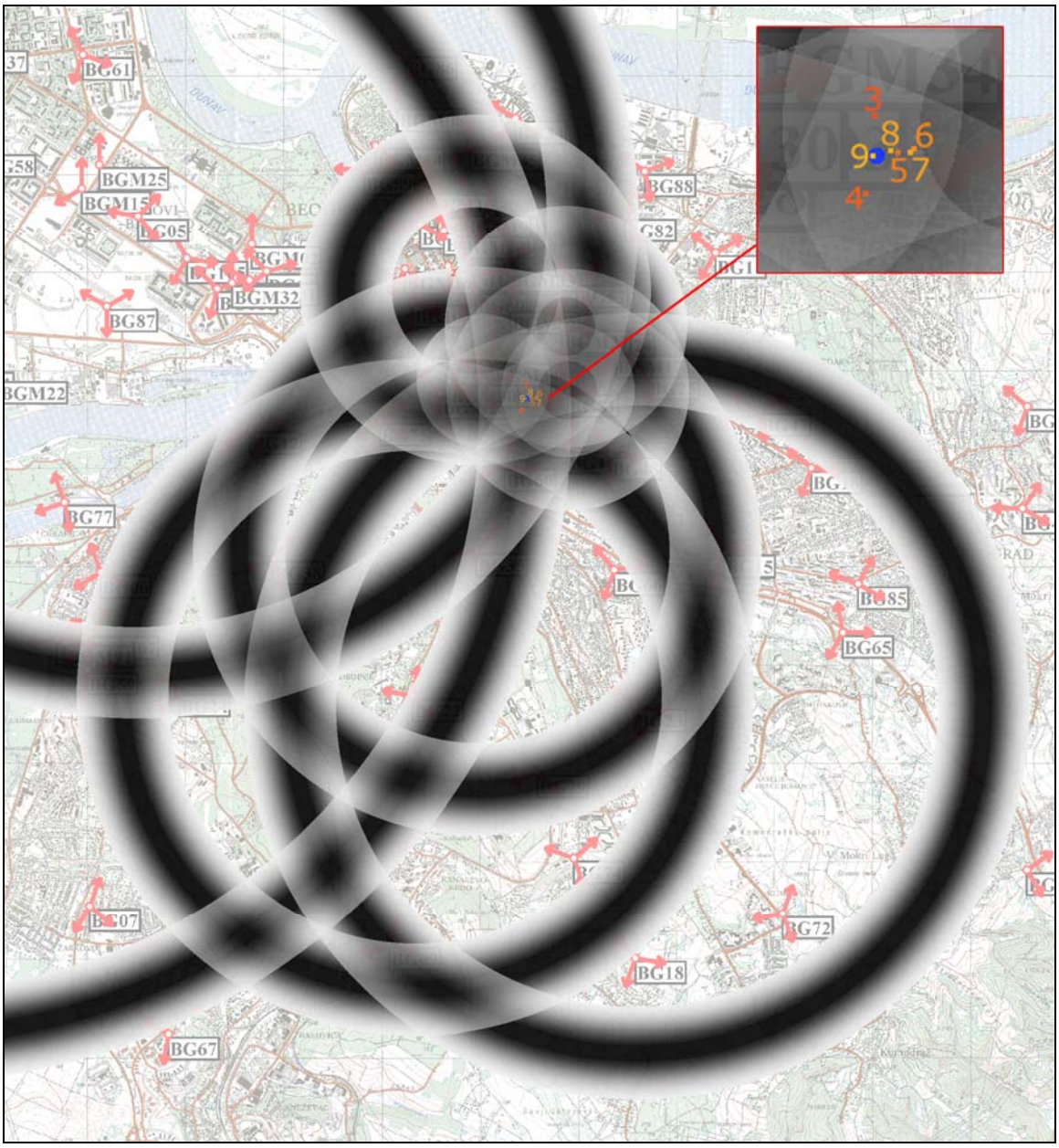

Fig. 5-6 The illustration of technique's accuracy vs. the number of BTSs in calculation (digits indicate the amount of BTSs involved in position estimation whereas the associated dots indicate corresponding estimated position; user's position is denoted with thick blue dot)

Additionally, the algorithm can be enhanced by selecting optimal coefficients for the scaling factors. The algorithm can easily be adapted for UMTS, due to similarity between RTT (round trip time) and TA, which should probably decrease the positioning error [5.7].

However, for implementation, E-CIDTA requires additional signalling to be conducted in the GSM network.

5.3 ANN RSSI Positioning Models

5.3.1 Single ANN Positioning Models

5.3.1.1 Positioning Method

New implementations of GSM/DCS signalization allow for up to 32 neighbouring cells to be included in the BA list (Broadcast Control Channel Allocation List) [5.8]. The RSS levels (RxLev parameters) from these cells are measured periodically at the MS in idle mode and could be transferred back to the network in the form of standardized report. The cells in the BA list are defined by the network operator. However, the network operator can include, besides its own cells, cells from other operators into its cell's BA list. This opens the door for the use of RSS values from other network operators for positioning the mobile station. In addition, UMTS capable MSs can measure a number of Received Signal Code Power (RSCP) parameters (CPICH_RSCP_LEV [5.9]) belonging to serving and other networks. Reports containing these values are also sent to the network. The set of RSS values, including both RxLev and CPICH_RSCP_LEV parameters obtained at MS, will be referred to as the Reference Inputs (RIs).

Ideally, the MS should be served by the closest node of the network. That would invoke the highest probability that an MS is served by the cell with the strongest signal. However, due to the other system limitations (ping-pong handover effect, load balancing, etc.) the criterion for serving BTS is somewhat more complicated. Being that these system limitations do not affect the positioning algorithm, in the proposed algorithm, the cell with the highest RSS value was used instead of the serving cell as a model selection criterion. When regarding the general operation of the algorithm, once the positioning request is received, the Serving Location Mobile Centre (SLMC), based on the Cell-ID of the highest reported RSS value, employs a matching model for the particular site (i.e. for each site a specific positioning model is applied). The Model Inputs (MIs) are RSS values of a particular set of BTSs (significant RSS inputs). The number of these inputs can vary and different MI selection criteria can be applied. The RI list is then, in SLMC, matched with the MIs, specific for the area of the particular model. The RI values that do not have corresponding MIs are discarded whereas the missing MIs are entered with the threshold value (-130dBm for CPICH_RSCP_LEV and -110dBm for RxLev). The overall functioning of the proposed positioning algorithm is illustrated in Fig. 5-7 a) whereas the major phases in providing the location estimate are given in Fig. 5-7 b).

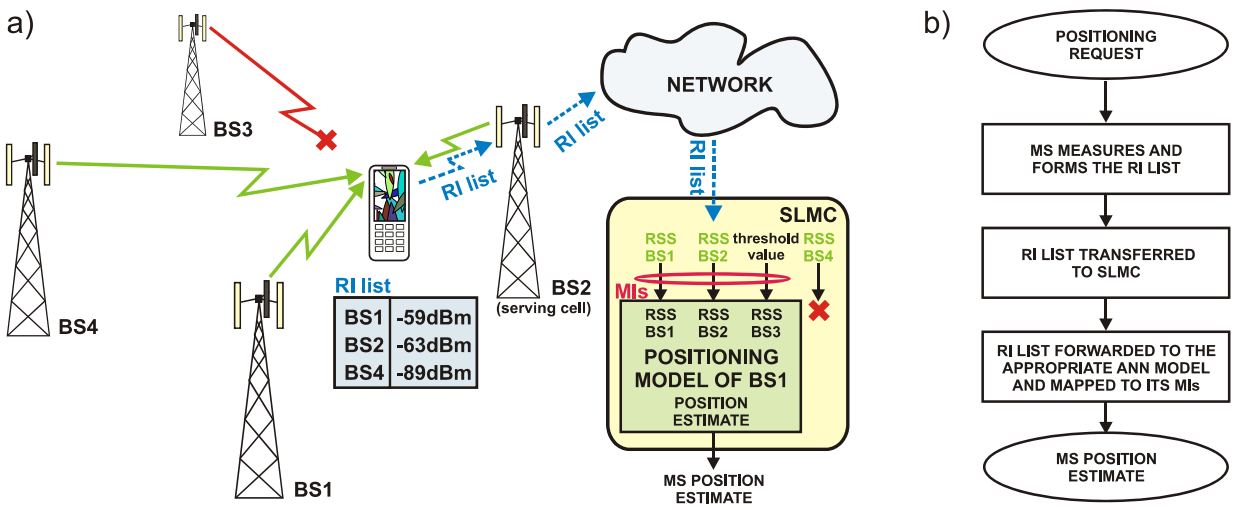

Fig. 5-7 The functioning of the positioning algorithm: a) illustration and b) phases diagram

The models used for positioning were based on ANNs. The multilayer perceptron feedforward network, depicted in section 3.2.5, with a varying number of perceptron units formed the structure of every positioning model. The guidelines followed for the inner network structure are the same given in section 3.3.

5.3.1.2 Model Generation

To train, validate and verify the proposed models, the data from the measurement campaign given in 5.1.2 was used.

Being that each model corresponds to an individual site, at first, the MTS site in a light urban environment was selected for the purpose of examining the proposed models. This site shall hereon be referred to as S1. The geographic area from which the measurements are used to train the model and, moreover, the area in which the model can estimate the user position is referred to as the model area. The shape of this area was chosen to be circular, centred to the position of the BS. To determine the radii of the model area, the measured locations where the highest measured RSS was received from the chosen cell were observed first. Next, the radii were chosen (in 100m steps) so that more than 99.9% of the observed locations were inside this area. A limitation of this kind had to be induced in order to minimize the model area size. The model area determination procedure is illustrated in Fig. 5-8. Regarding the S1, the aforementioned procedure resulted in a database of measurements performed on 31,391 locations inside 1km radius from the BS.

The models that were tested on S1 can be split into the following categories: group 1 (G1) – models using several significant RSS inputs from one or more systems belonging to one operator, group 2 (G2) – models using several significant RSS inputs from multiple systems

belonging to multiple operators, and group 3 (G3) – models using all available inputs from multiple systems belonging to multiple operators. It should be noted that the G3 models have a much greater number of MIs than G1 and G2 models (one of the G3 models has as much as 163 MIs). G1 – G3 models and their descriptions are presented in Table 5-III.

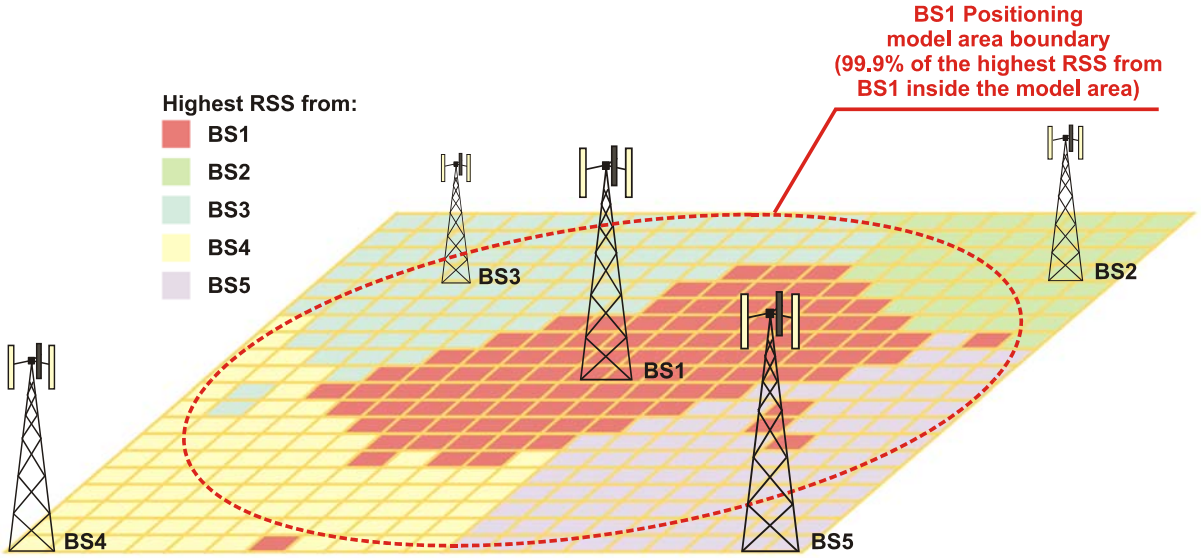

Fig. 5-8 Model area radius determination criterion

Table 5-III Positioning models for S1

Group	Model	Label	Model Inputs
G1	M1	7G(MTS)	7 GSM RSS (MTS)
	M2	7D(MTS)	7 DCS RSS (MTS)
	M3	3U(MTS)	3 UMTS RSS (MTS)
	M4	7G7D(MTS)	7 GSM and 7 DCS RSS (MTS)
	M5	7G7D3U(MTS)	7 GSM, 7 DCS and 3 UMTS RSS (MTS)
G2	M6	7G(MTS)&7D(VIP)	7 GSM RSS (MTS) and 7 DCS RSS (VIP)
	M7	7G7D3U(MTS)&7D3U(VIP)	7 GSM, 7 DCS, 3 UMTS RSS (MTS) and 7 DCS, 3 UMTS RSS (VIP)
G3	M8	G(MTS)&G(VIP)	All available GSM RSS from both operators
	M9	D(MTS)&D(VIP)	All available DCS RSS from both operators
	M10	U(MTS)&U(VIP)	All available UMTS RSS from both operators
	M11	GD(MTS)&GD(VIP)	All available GSM and DCS RSS from both operators
	M12	GDU(MTS)&GDU(VIP)	All available GSM, DCS and UMTS RSS from both operators

For models using only significant RSS inputs (groups G1 and G2), it should be pointed out that the MIs were chosen based on the probability of their radio-visibility throughout the model area. This parameter was calculated as the ratio between the number of locations in which the particular cell's RSS was recorded (as RI) against the overall number of locations across the model area. The top seven RSS were selected (due to the typical cell structure comprising the serving cell and six neighbouring cells) except in the case of UMTS where, due to the worse

coverage and less Nodes B in the area, this number was reduced to only three (the remaining UMTS RSS had radio-visibility of less than 10%).

The current signalling schemes cannot support the transfer of all available RSS signals measured by the MS to the network. On the other hand, MS has the hardware capability and could easily be adapted to measure and monitor a great number of RSSs (e.g. by using "R&S Romes to go" software [5.10]). Then, additional signalling would be required to send the measured values back to the network. To perform this, first the BA list should be expanded (this has already been done in some proprietary solutions). Then, the measuring report ought to be changed to support transferring more RSS values. This should not have a high impact on the network capacity. However, the standardized signalling cannot carry this extra data and would, therefore, have to be altered. Overall, making use of all available RSSs could be performed requiring only software changes and maintaining the existing hardware infrastructure intact. Hence, the impact, on both the network and the handset side, would be limited.

5.3.1.3 Performance Assessment

a) S1 models' performances

The training of models was performed by using only 10% of the model measurement data set due to its immense size. The validation of models was performed using 40% and the final verification of the models' performances was done with the remaining 50% of the data set (verification subset). The database was divided into the aforementioned subsets randomly, with a uniform distribution. The subsets were filtered and only the measurements where the strongest RSS belonged to the modelled site were actually used (other measurements would be, according to the algorithm, dispatched to their corresponding models). To validate the performances, the models were trained with different training lengths ranging from 100 to 500,000 epochs. The obtained validation performances are shown in Tables 5-IV – 5-VI for model groups G1 – G3, respectively.

Table 5-IV Validation Distance Error – DE for G1 models

Group	Model	Average DE [m]	Median DE [m]	67% DE [m]	95%DE [m]	Optimal training length [epochs]
G1	M1	157	126	173	389	150k
	M2	217	168	229	604	50k
	M3	447	398	601	888	300k
	M4	113	91	124	281	150k
	M5	110	88	119	276	150k

Table 5-V Validation Distance Error – DE for G2 models

Group	Model	Average DE [m]	Median DE [m]	67% DE [m]	95%DE [m]	Optimal training length [epochs]
G2	M6	108	87	118	262	200k
	M7	88	70	97	223	200k

Table 5-VI Validation Distance Error – DE for G3 models

Group	Model	Average DE [m]	Median DE [m]	67% DE [m]	95%DE [m]	Optimal training length [epochs]
G3	M8	92	65	100	260	500k
	M9	76	57	80	223	500k
	M10	127	101	141	324	200k
	M11	59	48	68	146	500k
	M12	60	51	69	139	500k

The performances of G1 models, in terms of absolute average and various percentile (50%, 67% and 95%) Distance Errors (DEs), first improved with the increase in training length. After roughly 50k epochs of training, the improvement in performances enters saturation or even starts decreasing slightly. The criterion used in the selection of the optimal training length for all models was the minimal sum of average and median DE. Being that some LBSs are limited by the average and some by the median DE, this criterion was chosen to equally account for the influence of both DEs. The obtained validation performances for G1 models are shown in Table 5-IV.

Concerning the G2 models and Table 5-V, the optimal training length, according to the aforementioned criterion, has moved towards a longer training duration (200k epochs). As for the G3 models, as can be seen from Table 5-VI, the optimal duration of training is further moved to greater number of epochs. Such results indicate that the increase in the number of MIs (i.e. more complex ANN structure) invokes a higher optimal training duration. Although most of the G3 models achieve their best performances for 500k epochs, the difference in performances for 300k and 500k epochs are usually minor. Bearing in mind the time needed to perform the training, the models were not trained for more than 500k epochs.

The performances of the optimally trained models have been verified with the measurement verification subset for the selected site S1. The obtained DE's Cumulative Distribution Functions (CDFs) for models 1-5 are shown in Fig. 5-9. CDFs for models 6-7 are shown in Fig. 5-10, whereas the CDFs for models 8-12 are presented in Fig. 5-11. The regions below 2.5% and above 97.5% have been omitted due to the relatively small number of samples therein.

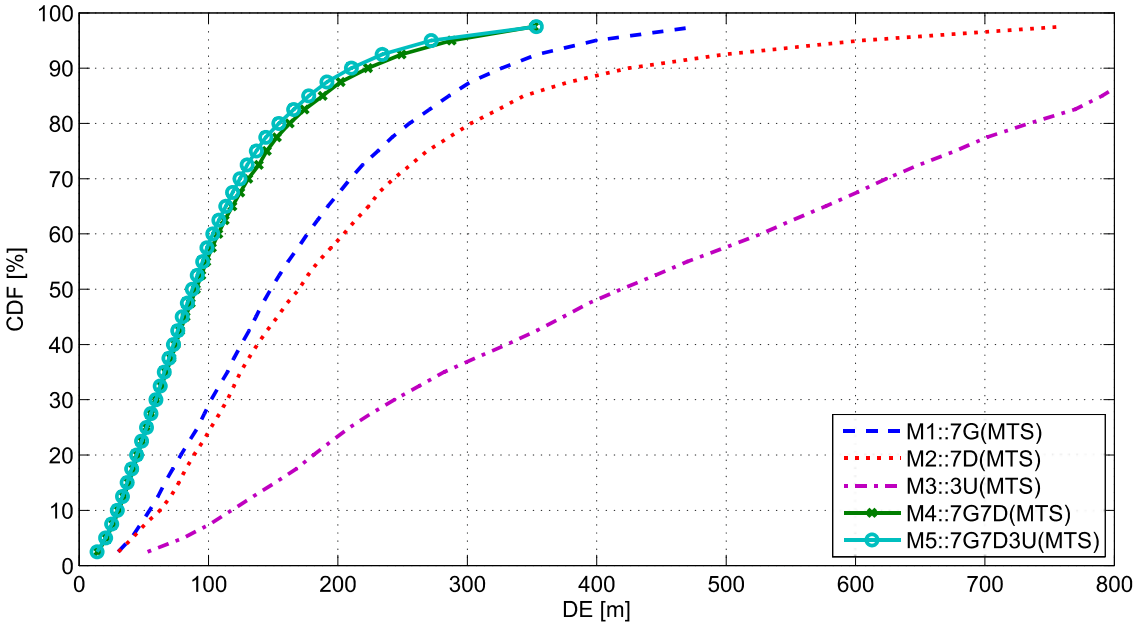

Fig. 5-9 DE's CDF for G1 models

From Fig. 5-9, it can be seen that the models employing signals from individual systems (M1 to M3) have performances generally proportional to the number of MIs. The exceptionally poor performances that the 3U(MTS) model demonstrates could be explained by significant areas inside the model area with no UMTS coverage (from the three selected UMTS cells). In this case all MIs are equal to the threshold value and the model estimates all such locations into a single point producing almost uniformly distributed distance errors over the model area. On the other hand, even though the UMTS had the worst radio-visibility, this system still adds a bit to the overall performance of 7G7D3U(MTS) model. Another interesting point is that although the DCS and GSM antennas are usually collocated (often enough deployed as single multi-band antenna), the 7G7D(MTS) significantly improves in performance when comparing to either of the two models employing RSS from individual systems.

Fig. 5-10 shows the performances of two models employing a limited number of RSS values from both network operators. Being that they have the same number of inputs from the corresponding systems, it might be interesting to discuss and compare the performances of M4::7G7D(MTS) and M6::7G(MTS)&7D(VIP) models. As can be seen, the M6 model slightly outperforms the M4 model. Being that the 7G(MTS) and 7D(VIP) signals have similar visibilities, the difference in performance can be explained as a result of the additional transmitter locations in case of the M6::7G(MTS)&7D(VIP) model. In other words, this result indicates that the additional transmitter carries more location dependent information if it is on a different location than previously used RSS sources – which is logical.

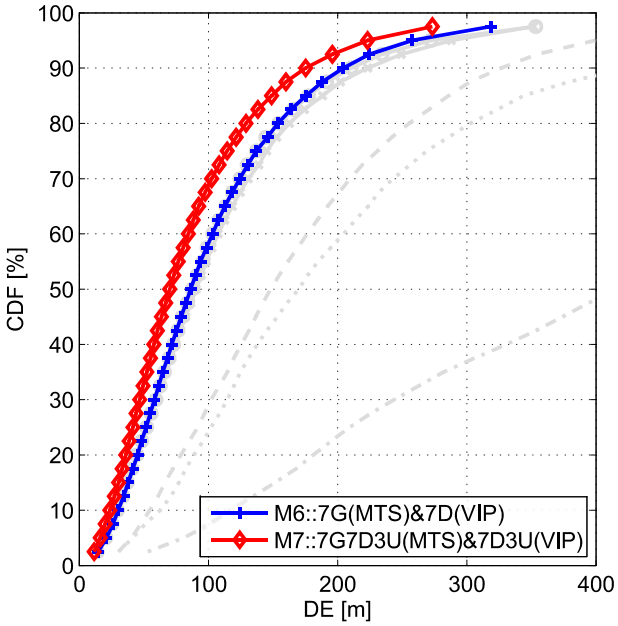

Fig. 5-10 DE's CDF for G2 models (Models 1-5 are also shown in faded gray, with the markers and a line-style consistent to those shown in Fig. 5-9)

Positioning models employing all the available RSS inputs are presented in Fig. 5-11. If the models employing different numbers of RSSs only from a single system are mutually compared, it can be seen that all models have vastly improved in terms of their accuracy with the increase in the number of RSS inputs. Models employing UMTS – 3U(MTS) and U(MTS)&U(VIP) still have the worst positioning performances. Yet, contrary to the 7G(MTS) model outperforming the 7D(MTS) model, the D(MTS)&D(VIP) performs better than G(MTS)&G(VIP). This again confirms the influence of the number of RSS inputs to the model accuracy since the VIP network operator has very limited GSM coverage. The GD(MTS)&GD(VIP) and GDU(MTS)&GDU(VIP) models further excel in their performances. These two models have basically the same accuracy performances which goes to show that at a certain point the additional RSSs cease to benefit the overall positioning performances. This might be induced by poor radio-visibility of the UMTS system. On the other hand, difference in the high percentiles (above 90%), which these two models experience indicates that the increase in the number of MIs, even if they belong to a system with poor radio-visibility, limits the maximal positioning error.

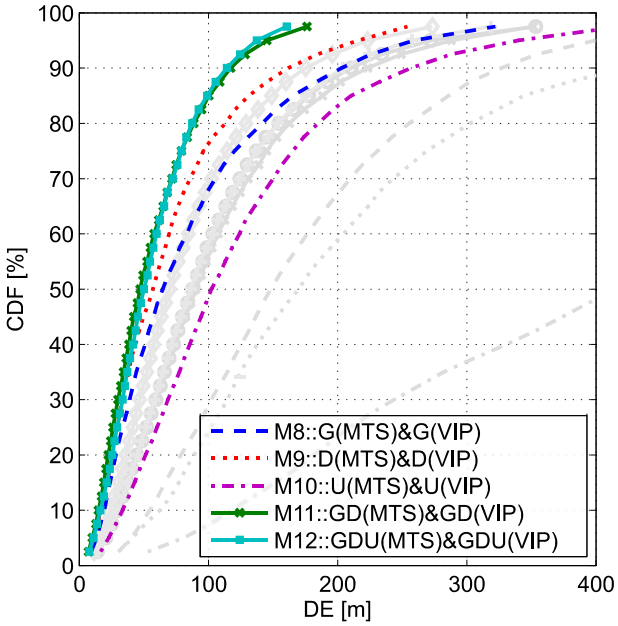

Fig. 5-11 DE's CDF for G3 models (Models 1-7 are also shown in faded gray, with the markers and a line-style consistent to those shown in Figures 5-9 and 5-10)

Table 5-VII G1 – G3 Models Accuracy Performance Summary

Group	Model	Label	Avg. DE [m]	50% DE [m]	67% DE [m]	95% DE[m]	σ DE [m]
G1	M1	7G(MTS)	175	148	199	399	118
	M2	7D(MTS)	218	170	230	604	179
	M3	3U(MTS)	450	419	598	883	266
	M4	7G7D(MTS)	114	90	123	288	96
	M5	7G7D3U(MTS)	110	88	118	272	93
G2	M6	7G(MTS)&7D(VIP)	106	86	117	258	83
	M7	7G7D3U(MTS)&7D3U(VIP)	88	70	96	223	69
G3	M8	G(MTS)&G(VIP)	92	65	100	260	85
	M9	D(MTS)&D(VIP)	75	57	79	215	65
	M10	U(MTS)&U(VIP)	129	102	141	340	101
	M11	GD(MTS)&GD(VIP)	59	47	68	145	44
	M12	GDU(MTS)&GDU(VIP)	59	50	68	137	41

The models' accuracy overview, obtained by using a verification subset and optimally trained models, are presented in Table 5-VII.

b) Performance verification on different cell sites

In order to verify and confirm the previously obtained positioning performances, two additional sites were selected and models with inputs corresponding to G3 models (M8 – M12) have been created. Site two (S2) is in an urban surrounding. The aforementioned selection criterion for a model area resulted in a database of measurements comprising 22,221 locations inside an 800m radius from the BS. The same criterion applied to site three (S3) that is located

in a light urban area with tall buildings rendered 33,140 locations inside 1100m radius from the BS. The S3 area is specific regarding the signal propagation. Due to the somewhat sporadically positioned high buildings, the situations where for proximate locations propagation paths have significantly different length (direct path vs. one or more reflections) frequently occur. This behaviour impairs the performances of the positioning model.

As stated, the overall aim of verification on additional cell sites was to show general consistency of the previously obtained performances. Besides that, the comparison with S2 ought to demonstrate the transformation of positioning performances with the urbanisation of the environment. S3 ought to illustrate the behaviour of the models in an environment which is considered to be even more challenging in terms of the received signal power estimation.

Group four (G4) models M13 to M17 (S2), and group five (G5) models M18 to M22 (S3) correspond to G3 models M8 to M12, respectively. As with G3 models, M13 and M18 use all the available GSM signals, M14 and M19 use all the available DCS signals, M15 and M20 use all the available UMTS signals, and M16 and M21 use all the available GSM and DCS signals. Finally, M17 and M22 make use of all the available signals within their respective model areas. Description of G4 and G5 models is given in Table 5-VIII.

Table 5-VIII Positioning models for G4 (S2) and G5 (S3)

Group	Model	Label	Model Inputs
G4	M13	G(MTS)&G(VIP)	All available GSM RSS from both operators
	M14	D(MTS)&D(VIP)	All available DCS RSS from both operators
	M15	U(MTS)&U(VIP)	All available UMTS RSS from both operators
	M16	GD(MTS)&GD(VIP)	All available GSM and DCS RSS from both operators
	M17	GDU(MTS)&GDU(VIP)	All available GSM, DCS and UMTS RSS from both operators
G5	M18	G(MTS)&G(VIP)	All available GSM RSS from both operators
	M19	D(MTS)&D(VIP)	All available DCS RSS from both operators
	M20	U(MTS)&U(VIP)	All available UMTS RSS from both operators
	M21	GD(MTS)&GD(VIP)	All available GSM and DCS RSS from both operators
	M22	GDU(MTS)&GDU(VIP)	All available GSM, DCS and UMTS RSS from both operators

Group four (G4) models M13 to M17 (S2), and group five (G5) models M18 to M22 (S3) correspond to G3 models M8 to M12, respectively. As with G3 models, M13 and M18 use all the available GSM signals, M14 and M19 use all the available DCS signals, M15 and M20 use all the available UMTS signals, and M16 and M21 use all the available GSM and DCS signals. Finally, M17 and M22 make use of all the available signals within their respective model areas. Description of G4 and G5 models is given in Table 5-VIII.

Tables 5-IX and 5-X show the validation performances of G4 and G5 models, respectively.

Table 5-IX Validation Distance Error – DE for G4 (S2) Models

Group	Model	Average DE [m]	Median DE [m]	67% DE [m]	95%DE [m]	Optimal training length [epochs]
G4	M13	67	48	71	190	500k
	M14	69	57	77	174	500k
	M15	118	92	119	239	500k
	M16	53	43	59	134	500k
	M17	53	45	61	124	500k

Table 5-X Validation Distance Error – DE for G5 (S3) Models

Group	Model	Average DE [m]	Median DE [m]	67% DE [m]	95%DE [m]	Optimal training length [epochs]
G5	M18	49	37	50	136	300k
	M19	79	61	87	206	500k
	M20	92	75	105	218	500k
	M21	46	36	50	119	500k
	M22	46	37	52	113	500k

Fig. 5-12 illustrates the DE's cumulative distribution function of S2 models M13 – M17.

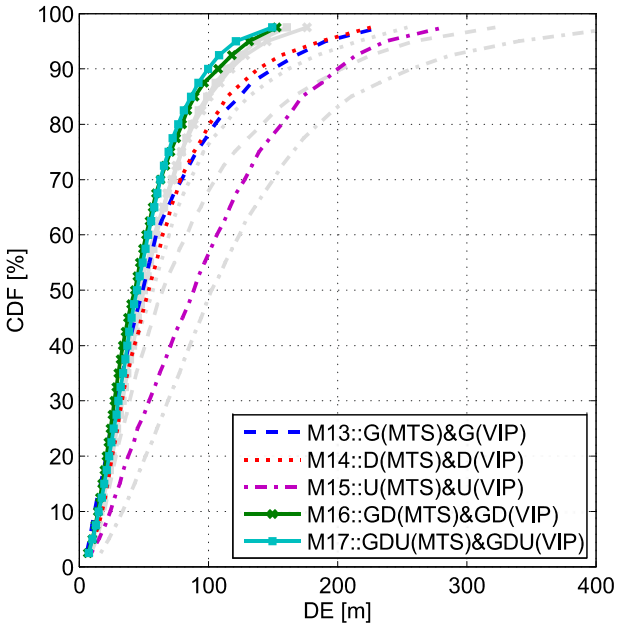

Fig. 5-12 DE's CDF for G4 models (Models M8 – M12 are displayed in faded gray, with markers and a line-style consistent to those shown in Fig. 5-11)

The more urban environment (higher density of BSs) of S2 has rendered a smaller model area (800m radius) and yet a larger number of available BSs (maximal available number of MIs). Also, respective to the number of MIs, positioning performances have generally improved. The

most significant improvement is noticeable with the M13::G(MTS)&G(VIP) model compared to the M8::G(MTS)&G(VIP). This can be explained as a result of the most noticeable increase in the number of GSM BTSs. Regarding the S2, the number of GSM and DCS BTSs is almost the same (whereas with S1 there were significantly more DCS BTSs), which then translates into significant improvement in positioning performances.

Fig. 5-13 depicts the DE's cumulative distribution function of G5 models M18 – M22. G5 models achieve superior performances with M21 and M22 reaching under 40m median errors. This result ought to be even more emphasized in light of the challenging propagation environment in which the G5 models operate. This radio-environment rendered the model area radius of 1100m which then invoked an even higher number of MIs (total of 262).

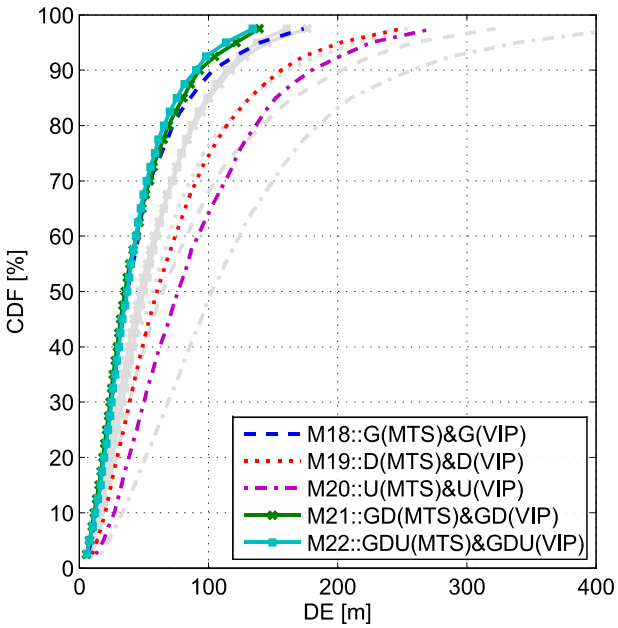

Fig. 5-13 DE's CDF for G5 models (Models M8 – M12 are displayed in faded gray, with markers and line-styles consistent to those shown in Fig. 5-11)

Table 5-XI shows a summary of the accuracy performances of G4 and G5 models. Bearing in mind Figures 5-125-12 and 5-13, as well as Table 5-XI, it can be concluded that, generally, the improvement in the models' positioning accuracy is proportional to the number of MIs, i.e. to the density of the visible BTSs. Nonetheless, there is a limit to such behaviour. The best example for that is the M18 which has almost identical performances to those of the M21 and M22 models. Conversely, as indicated earlier, it seems that the higher number of model's inputs still helps limit the maximal positioning error (lowering the DE with high percentiles).

Table 5-XI Models Accuracy Performance Summary for G4 – G5

Group	Model	Label	Avg. DE [m]	50% DE [m]	67% DE [m]	95% DE[m]	σ DE [m]

G4	M13	G(MTS)&G(VIP)	67	49	72	191	62
	M14	D(MTS)&D(VIP)	68	54	75	187	56
	M15	U(MTS)&U(VIP)	103	89	120	237	79
	M16	GD(MTS)&GD(VIP)	53	43	59	132	39
	M17	GDU(MTS)&GDU(VIP)	52	45	60	121	36
G5	M18	G(MTS)&G(VIP)	51	37	51	140	45
	M19	D(MTS)&D(VIP)	80	62	87	206	66
	M20	U(MTS)&U(VIP)	95	77	106	226	76
	M21	GD(MTS)&GD(VIP)	46	35	50	121	37
	M22	GDU(MTS)&GDU(VIP)	45	37	48	114	33

Fig. 5-14 illustrates the positioning capabilities of the M22 model. From Fig. 5-14 it can clearly be seen that the areas in which the signal from the modelled BS is the strongest (blue circles) are only a subset of the model area. As a result, the model areas of different cells overlap. The errors are evenly distributed across both sides of the streets. Therefore, it can be assumed that, with a proper map matching and/or overloaded tracking algorithm, this model's accuracy would be sufficient so that it could be used for vehicle navigation LBS.

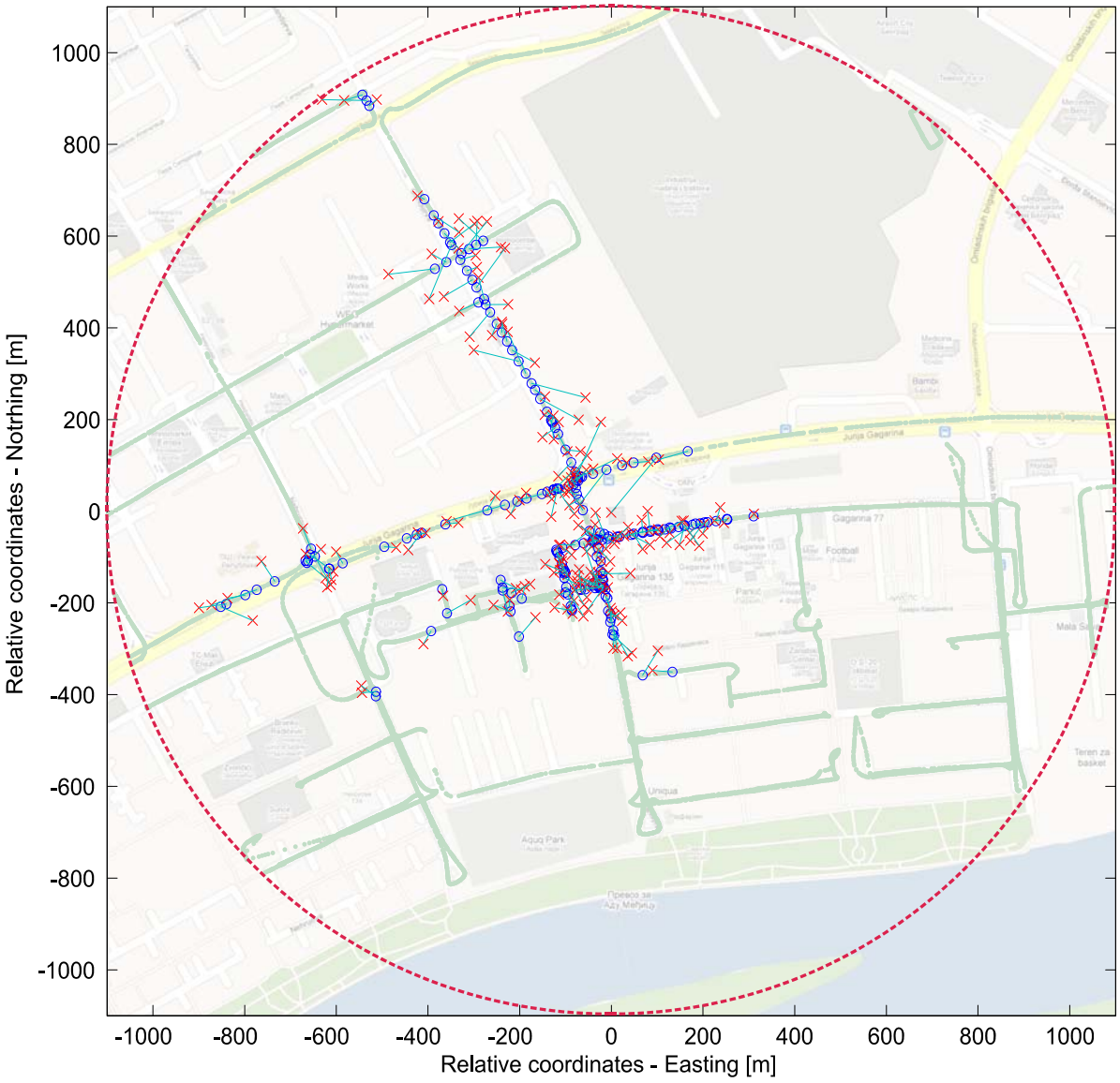

Fig. 5-14 Positioning with M22 model (the red dashed circle represents the boundaries of the model area, the green dots represent locations at which the measurements were conducted, the blue circles are the actual user positions whereas the red "x" signs stand for the estimated positions)

c) Indoor performances

Most studies exploring PLMN based positioning are based on simulation results only. Even those research efforts based on actual measurements do not tend to investigate the degradation of performances if the positioning is applied in an environment the model was not primarily made for (e.g. positioning in an indoor environment when the model was optimised for an outdoor environment). This can be very important if the positioning service aims to provide seamless cross-environment positioning capabilities. For this purpose additional measurements on a number of indoor locations throughout the S1 model area have been made. Being that these measurements have been made with a cell phone equipped with Ericsson's pocket TEMS [5.11] with no logging capabilities and that the access to personal households was limited, the

number of measurements was restricted to only 30 measurements. Hence, the indoor positioning performances have been explored less thoroughly than it was the case with outdoor performances. On the other hand, it might be good enough to give an insight into how to optimise the positioning model for the indoor environment.

The G3 models, verified for the previously stated range of training lengths, were validated using the measurement set obtained in an indoor environment.

Table 5-XII Distance Error – DE for G3 Models in Indoor Environment

Group	Model	Average DE [m]	Median DE [m]	67% DE [m]	95%DE [m]	Optimal training length [epochs]
G3	M8	180	138	176	369	2k
	M9	110	82	144	241	5k
	M10	179	166	190	340	20k
	M11	121	95	172	236	10k
	M12	105	101	107	158	5k

The results given in Table 5-XII may be interpreted as significantly worse than those presented in Table 5-VI. Another noticeable point is that the optimal training lengths are shifted towards the lower number of epochs. The fact that the optimal training length for indoor positioning is achieved with lesser training lengths shows that more noisy processes with worse overall performances (i.e. indoor positioning) invoke lesser optimal training lengths. This behaviour is illustrated in Fig. 5-15 through the average DE for the M12 positioning model. However, there might be another angle to it. When the results from Tables 5-VI and 5-XII at optimal training lengths for indoor positioning are compared, the differences between the two become slighter. Table 5-XIII provides an insight into the extent of performance degradation due to cross-environment model use. From Table 5-XIII, it can be seen that the positioning errors significantly rise for models that are not optimally trained for a particular environment.

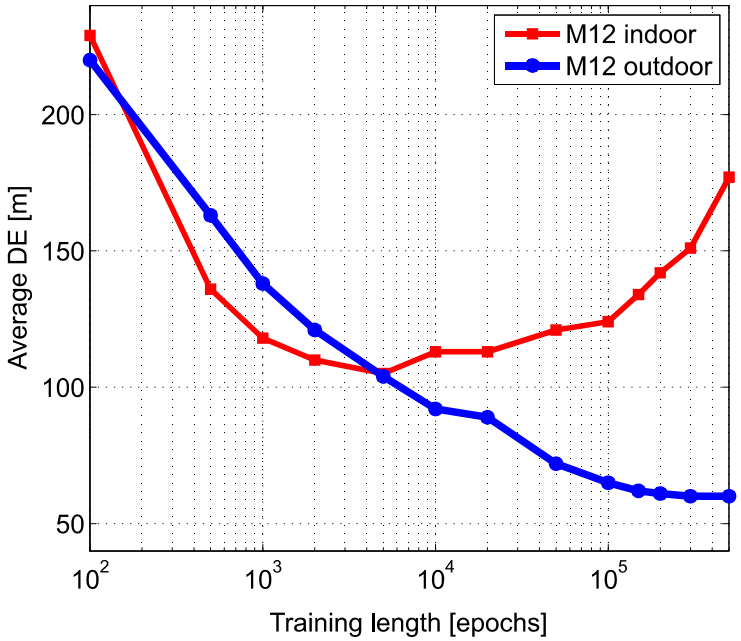

Fig. 5-15 Average DE of M12 model for the indoor and outdoor environment

Table 5-XIII Comparison of G3 Models' Positioning Performances for Indoor-Outdoor Optimal Training

Group	Model	DE type	I/IO [m]	O/IO [m]	I/OO [m]	O/OO [m]	I – O loss (IO) [%]	I – O loss (OO) [%]
G3	M8	Average DE	180	154	350	92	17	280
		Median DE	138	141	358	65	-2	451
		67% DE	176	180	383	100	-2	283
		95% DE	369	315	617	260	17	137
	M9	Average DE	110	108	175	76	2	130
		Median DE	82	99	144	57	-17	153
		67% DE	144	129	259	80	12	224
		95% DE	241	219	333	223	10	49
	M10	Average DE	179	162	348	127	10	174
		Median DE	166	140	341	101	19	238
		67% DE	190	182	435	141	4	209
		95% DE	340	370	588	324	-8	81
	M11	Average DE	121	93	176	59	30	198
		Median DE	95	83	177	48	14	269
		67% DE	172	110	219	68	56	222
		95% DE	236	202	311	146	17	113
	M12	Average DE	105	104	177	60	1	195
		Median DE	101	97	149	51	4	192
		67% DE	107	123	202	69	-13	193
		95% DE	158	206	395	139	-23	184

I – indoor, O – outdoor, IO – model training length optimised for indoor environment, OO – model training length optimised for outdoor environment

d) Models' complexity and latency

In order to fully explore the herein presented models, their complexity and latency have also been analysed.

There are many definitions for complexity depending on the domain of application. In terms of positioning systems, complexity is most often referred to as the difficulty of setting up the positioning system. Regarding the neural networks models, besides the time needed to collect the measurement database, the complexity mostly relates to the time needed to optimally train the network for positioning purposes. This property has been investigated through the time needed to train the particular model depending on the length of training and the size of the neural network structure. The processor time consumption is given to illustrate the relative energy needed to perform the training operation. Table 5-XIV shows the complexity parameters for all presented models.

Bearing in mind the size of one operator's network (in terms of the number of nodes), the training of models for the complete network might present a time consuming task. However, it should be stated that models in the suburban and rural environment have far less inputs and their training is much more prompt. Fewer inputs might indicate worse positioning capabilities in these environments. On the other hand, the propagation in these environments is considered "cleaner" (i.e. fewer reflected components) which could act to improve the positioning performances.

Location information makes sense only if it is obtained within a timeframe which remains acceptable for the provision of the LBSs. Latency represents the period of time between the position request and the provision of the location estimate. The total latency consists of propagation delays and the time the model uses to provide the positioning information. When considering PLMN the propagation delay can usually be contained within a few seconds. On the other hand, the mere process of obtaining a position estimate, in case of the models presented herein, takes nothing more than a series of multiplications and additions which consume a negligible amount of time. This is considered a rather good attribute of ANNs [5.12].

Table 5-XIV Models' Complexity

Model	Site	No. of inputs	Total no. of perceptron units	Training time per epoch [ms]	Training time for optimally trained model [hours] [a]
M1	S1	7	38	29	1.2
M2	S1	7	38	33	0.5
M3	S1	3	18	31	2.6
M4	S1	14	68	101	4.2
M5	S1	17	77	55	2.3
M6	S1	14	68	99	5.5
M7	S1	27	114	85	4.7
M8	S1	53	220	183	25.4 [b]
M9	S1	68	275	237	32.9 [b]
M10	S1	42	179	140	7.8 [b]
M11	S1	121	438	416	57.8 [b]
M12	S1	163	479	454	63.1 [b]
M13	S2	85	301	180	25.0
M14	S2	89	305	182	25.3
M15	S2	54	225	120	16.7
M16	S2	174	486	306	42.5
M17	S2	228	592	592	82.2
M18	S3	102	334	313	26.1
M19	S3	98	309	279	38.8
M20	S3	62	259	232	32.2
M21	S3	200	522	493	68.5
M22	S3	262	648	679	94.3

[a]Models were trained on a single core of the Pentium Dual Core CPU E5200@2.5GHz (60W) with 2GB of RAM, [b]For the outdoor environment

5.3.2 Cascade-connected ANN Structures

Following the same basic idea from section 4.3.2.2, we were tempted to test the use of space-partitioning process with cascade-connected (C-C) ANN structures for outdoor/PLMN positioning. This two-step process estimates the subspace in which the user resides, in the first phase, and resolves the location estimate within the subspace, using the specially adopted model for each subspace, in the second phase. Being that the areas covered by a single ANN model, in case of PLMN positioning, are much larger than the ones at which the WLAN systems are usually deployed on one side, and knowing that the use of C-C structures was initiated by the influence of test-bed size on positioning on the other, investigating the use of C-C ANN structures made even more sense.

The implementation of the most inclusive (best performing) single ANN models for PLMN positioning, discussed in previous sections, required slight changes in system signalling schemes. Besides, UMTS system occasionally has limited or no coverage, especially in rural

areas. On the other hand, one of the main goals with the C-C ANN (Fig. 4-17) models in WLAN environment was to show the performance benefit (not so much the performances *per se*) in comparison to the single ANN models. Bearing in mind the aforesaid, for the C-C ANN models, we opted to simplify and use only widely available 2G signals (GSM and DCS) and reduce the number of inputs so that the presented models would be entirely applicable in the existing GSM networks. To achieve this, the positioning algorithm shown in Fig. 5-7, with the only difference being the positioning model which is now implemented in form of a C-C ANN structure, was employed. The RI list was restricted to 7 entries so that the complete RI list could be carried in the form of standardized report. Also, the number of MIs was limited to 32 to follow the maximal number of entries in the BA list.

The S1 model area was selected for the C-C ANN models verification. As indicated earlier, it is a MTS network operator site in light urban environment. The base stations that were on the MI list were selected based on their radio-visibility inside the model area. RSS from the top 32 radio-visible base stations belonging to one of the two measured network operators (MTS and VIP) assembled the **MIs** vector.

Fig. 5-16 The S1 model area (red dashed line), locations of the measurements (blue "x" symbols) and location of the BTS (green "+" symbol)

The database for the S1 area consists of measurements performed on 31,391 locations. This area and the locations within, where the measurements were taken, are shown in Fig. 5-16.
Taking into account only the locations where the strongest received signal originated from this site, the database was filtered and narrowed to 7,331 locations.
The block structure of this system is virtually the same as one depicted in Fig. 4-17. There is a slight difference in the number of inputs, though. The structure inputs (the type 2 network inputs) should now accommodate the **MIs** vector which has 32 elements (instead of **APs RSSI** which had 8). Being that this vector is also the input of the second stage networks (type 1), their number of inputs must be expanded to 32 as well. Likewise, the number of outputs of the first stage ANN is equal to the number of subspaces the environment is partitioned to – **SubSp Ln** , and the number of outputs of the type 1 networks (also the output of the structure, **Pos Est**) is two – Northing and Easting.
The inner structure of both the type 1 and 2 ANNs was designed using the same guidelines as with previously described models. The network had three hidden layers. The number of perceptron units in those layers was varied so that the structure could accommodate for the different number of subspaces.
To thoroughly explore the use of space-partitioning for PLMN positioning a series of models with a different number of subspaces, ranging from 4 to 400, was constructed and analysed. All partitions were made strictly on geometrical bases (i.e. straight lines separating the model area into rectangles). For future comparison, the single ANN model with the same model database, RIs and MIs, is herein referred to as 1x1 partitioning.
The training of models was performed in a similar manner to the training of the single ANN models. Only the measurements where the strongest RSS belonged to the modelled site were actually used (other measurements would be, according to the algorithm, dispatched to their corresponding models). The filtered set was further divided into three subsets, for training, validation, and verification, containing 10%, 40% and 50% of the measurements, respectively. The database for a particular site was divided into the aforementioned subsets randomly. Next, the training of the type 1 networks was performed with the same 10% as for the first stage network (type 2). Of course, each second stage network was trained only with a subset of the training set containing the measurements from its corresponding subspace. The validation and verification of the second stage networks was done with the same validation and verification sets (containing 40% and 50% of the total filtered data set, respectively). Only, this time, the measurements from these sets were dispatched to the second stage networks according to the validation and verification outputs of the first stage network.

To analyse the performances, the models were trained with different training lengths ranging from 100 to 500,000 epochs. The results obtained for different space partition patterns, for optimally trained ANNs, are presented in Table 5-XV.

From Table 5-XV, it can be seen that the overall average, median and 67th percentile DEs are decreasing with the increase in the number of subspaces. Slight exception to this behaviour can be noticed with 5x5 pattern. As for the behaviour of 95th percentile DE, it is not clearly distinguishable: its large variation could be partially explained by relatively small number of samples (position estimates) within 5% of the total set. Also, this DE is dominantly influenced by the cases where the subspace was incorrectly selected by the first stage network. The variance of error in these cases can be significant. For instance, if the first stage network selected the adjacent subspace to the actual one, DE may not be large. On the other hand, if the selected subspace is not adjacent to the correct one, the DE is, in all likeliness, very large. Likewise, there is no apparent rule for the behaviour of the DEs in the incorrect subspaces. Although, the average DE in incorrect subspaces appears to be decreasing with the final increase in the number of subspaces.

Table 5-XV Performance overview for different partitioning patterns

Pattern	1x1	2x2	3x3	4x4	5x5	10x10	20x20
Overall Average Distance Error [m]	81.8	43.9	40.5	31.3	34.0	27.0	25.7
Overall Median (50p) Distance Error [m]	72.4	20.5	12.9	10.2	10.8	3.3	1.8
Overall 67p Distance Error [m]	90.2	32.7	22.5	18.8	20.8	7.4	4.0
Overall 95p Distance Error [m]	176.7	160.1	176.8	139.2	141.5	131.8	167.8
Average Distance Error in Correct Subspace [m]	81.8	37.3	30.4	22.8	23.7	10.9	5.3
Median Distance Error in Correct Subspace [m]	72.4	19.8	11.6	9.6	10.0	2.8	1.5
Average Distance Error in Incorrect Subspace [m]	-	250.3	203.9	223.2	231.3	194.7	176.3
Median Distance Error in Incorrect Subspace [m]	-	138.8	113.0	167.5	201.6	138.9	135.4
Probability of Correct Subspace Estimation	1.00	0.98	0.93	0.96	0.96	0.91	0.89

The behaviour of overall average and median DEs, as well as average and median DEs in correct subspaces are illustrated in Fig. 5-17.

Several moments can be noticed from Fig. 5-17. First, if the two sets, the overall median DE and its subset, the median DE in correctly chosen subspaces, are observed, it can be seen that they are hardly differentiable. The reason for such behaviour should be looked in high probability of correct subspace estimation as can be seen in Table 5-XV. In other words, being

that in only 2 – 11% of the cases the subspace is incorrectly estimated, the difference between the two sets originates from the samples with high DE. The lower percentile DEs are virtually the same for both sets. On the other hand, due to the same explanation – spread of the higher DEs in the overall DE, the overall average DE and the average DE in correctly chosen subspaces are parting with the decrease in the correct subspace estimation (i.e. with the increase in the number of subspaces).

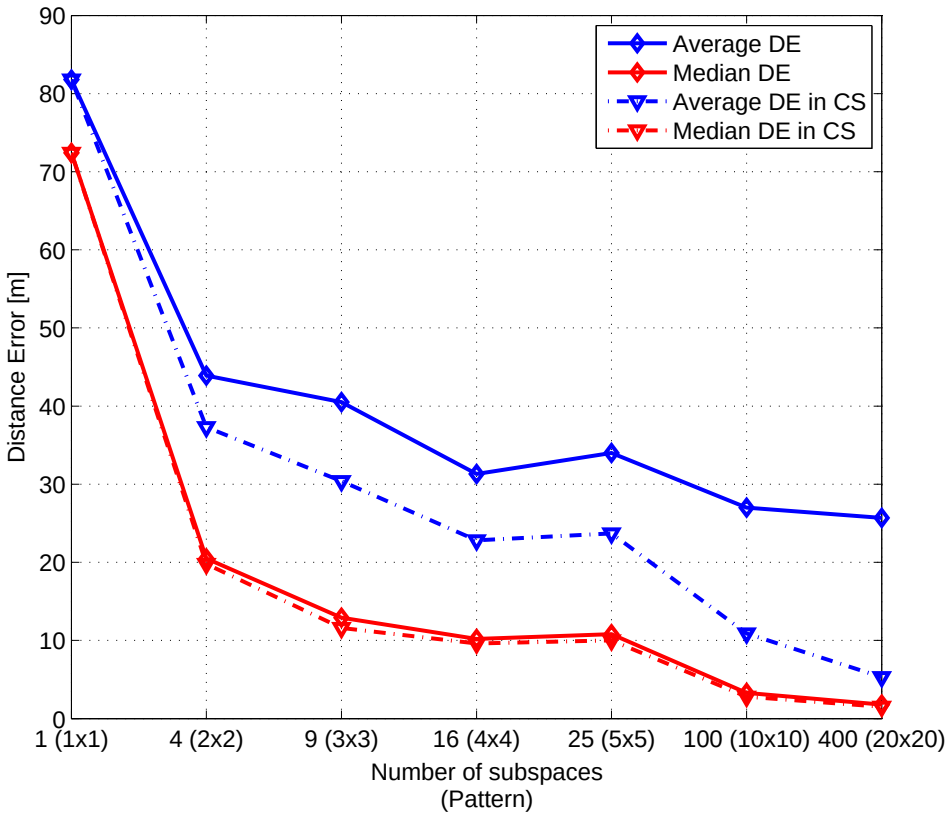

Fig. 5-17 Overall average and median DEs, average and median DEs in correct subspaces

Also, from Fig. 5-17, one can notice that the curves are likely to have entered saturation and that further increase in the number of subspaces would not induce significant decrease of the DEs. Therefore, the "range" of selected space-partitioning patterns are sufficient to thoroughly explore the positioning performances.

To illustrate the abovementioned behaviour, the distance error's Cumulative Distribution Function (CDF) of a single ANN approach (1x1) is compared with other applied partitioning patterns. The obtained CDFs are presented in Fig. 5-18.

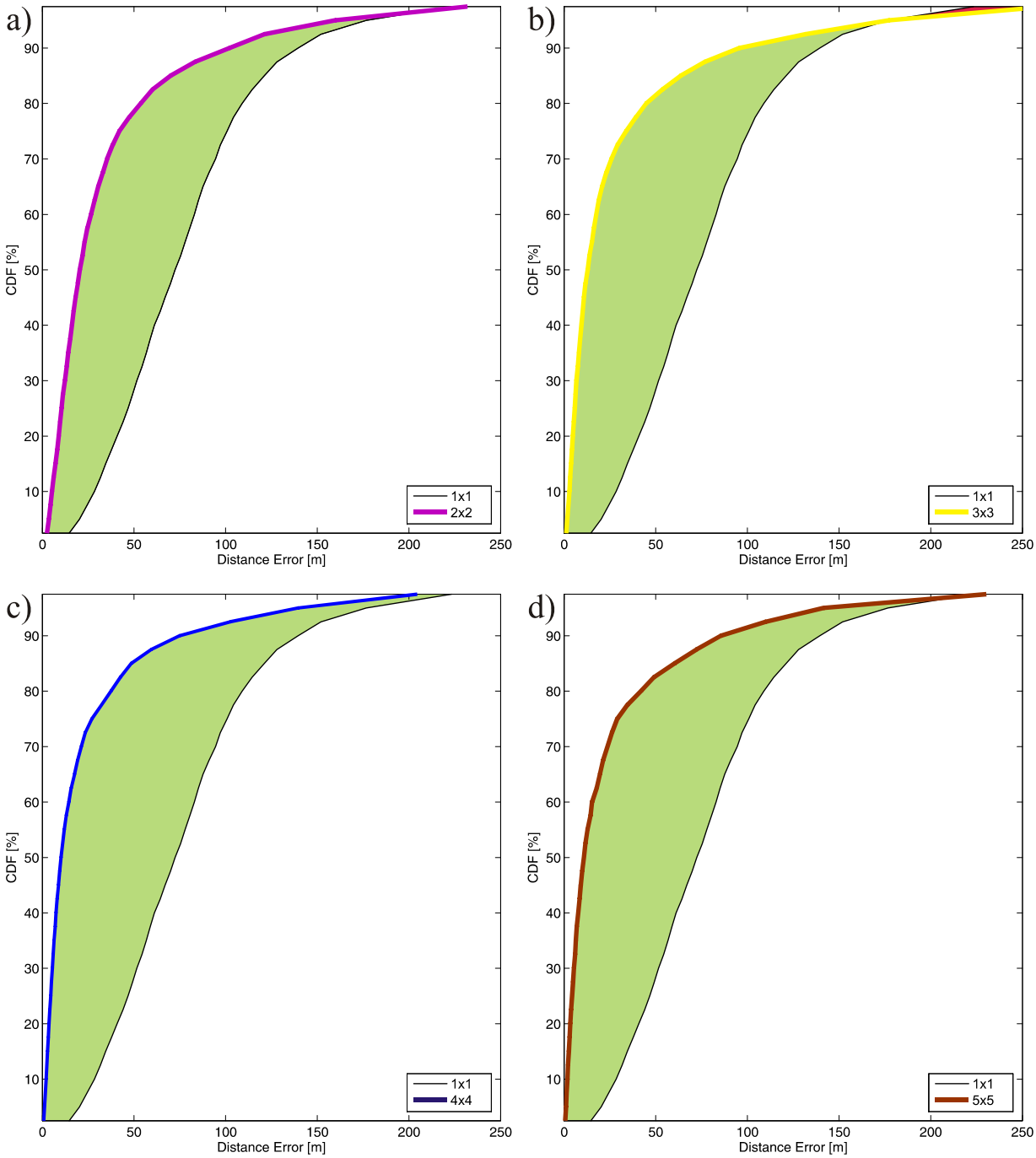
a)
b)
c)
d)
CDF [%]
Distance Error [m]
1x1
2x2
3x3
4x4
5x5

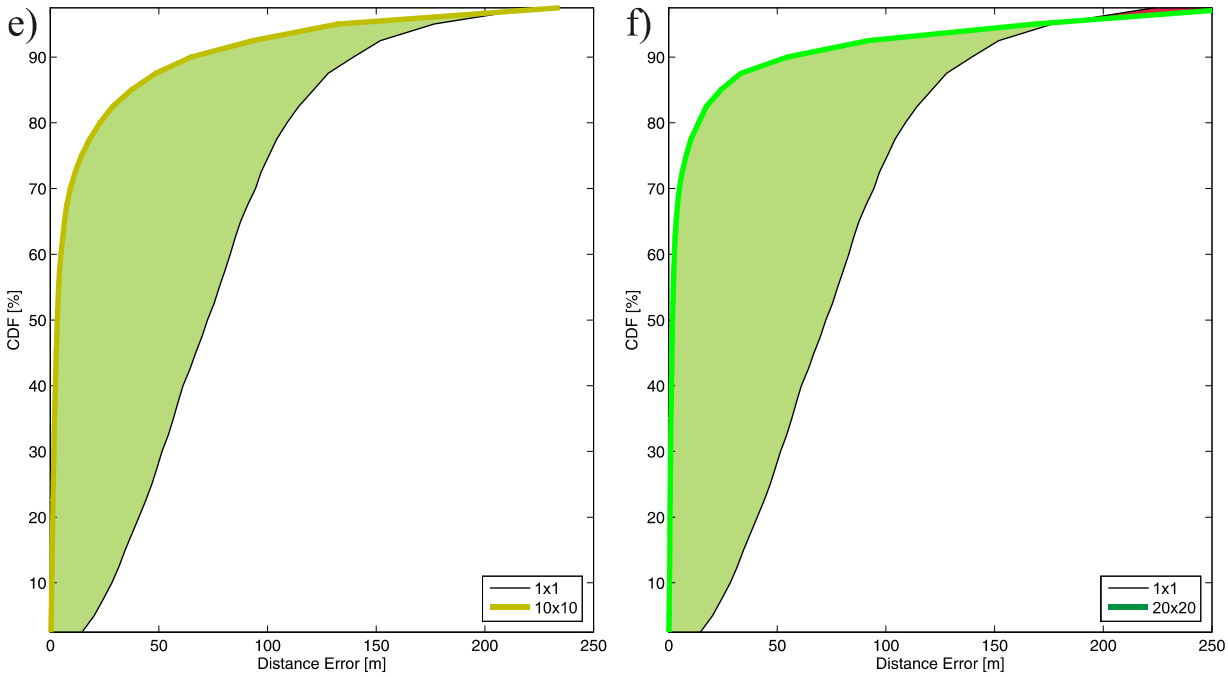

Fig. 5-18 Cumulative Distribution Function of distance error:
a) 1x1and 2x2; b) 1x1 and 3x3; c) 1x1and 4x4; d) 1x1and 5x5; e) 1x1and 10x10; and f) 1x1and 20x20;

In Fig. 5-18, the areas below 2.5% and above 97.5% have been omitted due to the insufficient number of samples in those regions. Let the green surfaces in Fig. 5-18 be regarded as partitioning gain and the red surfaces, visible only in Fig. 5-18 b) and f), as partitioning loss. The balance between the two areas translate to equal average DE. Green areas larger than red areas mean lower average DE and *vice versa*. From Fig. 5-18 a), it can be noticed that the crossing point of the 1x1 and 2x2 partitioning is in-between 95% and 97.5%. Therefore, there is almost no partitioning loss for this case and the positioning performances of 2x2 positioning are superb for all but the highest percentile errors. The similar behaviour can be observed for all other partitioning patterns except partially for 3x3 and 20x20 patterns which produce somewhat lower crossing points with 1x1 and, hence, somewhat larger loss areas. Bearing in mind the absolute size of the loss areas, it can be concluded that they hardly affect the positioning performances apart from the slight increase in the spread of high DEs. Nonetheless, the dominant effect is the growth of the gain areas with the increase in the number of subspaces. To better illustrate this effect, the CDFs for 1x1, 2x2, 4x4, 10x10 and 20x20 have been overlapped in Fig. 5-19. To avoid impairing the readability of the figure, 3x3 and 5x5 patterns have been omitted.

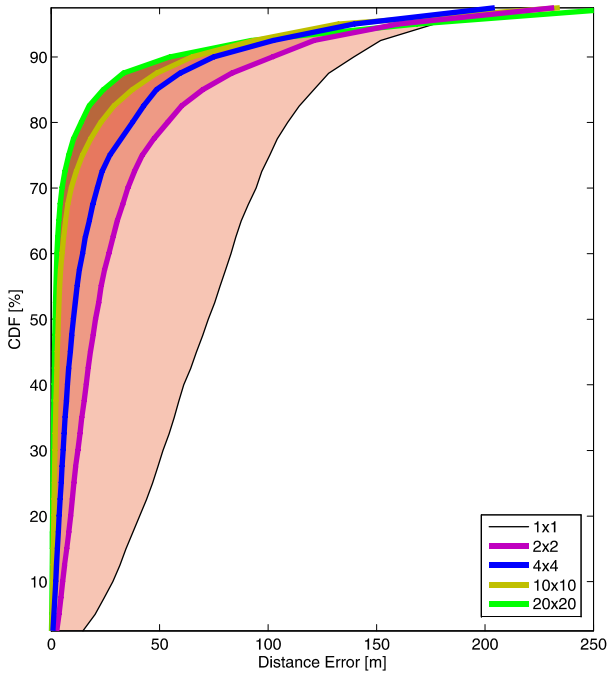

Fig. 5-19 Partitioning gain with the increase in the number of subspaces

The most substantial gain, from Fig. 5-19, is observed between 1x1 and 2x2 patterns. In other words, this presents the greatest absolute difference in overall average DEs (which concurs with the data shown in Table 5-XV). Also, further increase in the number of subspaces, induces additional enhancement in the positioning performances.

To better visualize the obtained positioning performances, the actual map with user locations and estimated locations, for 1x1, 2x2, 4x4, 10x10 and 20x20 patterns, have been shown in Figures 5-20 through 5-24, respectively. The red dashed circle represents the boundaries of the model area, the blue circles are the actual user positions whereas the red "x" signs stand for the estimated positions. Green lines connecting the actual and estimated user position correspond to the positioning DE. To maintain the readability of the figures, only 10% of the total verification set was uniformly selected and shown.

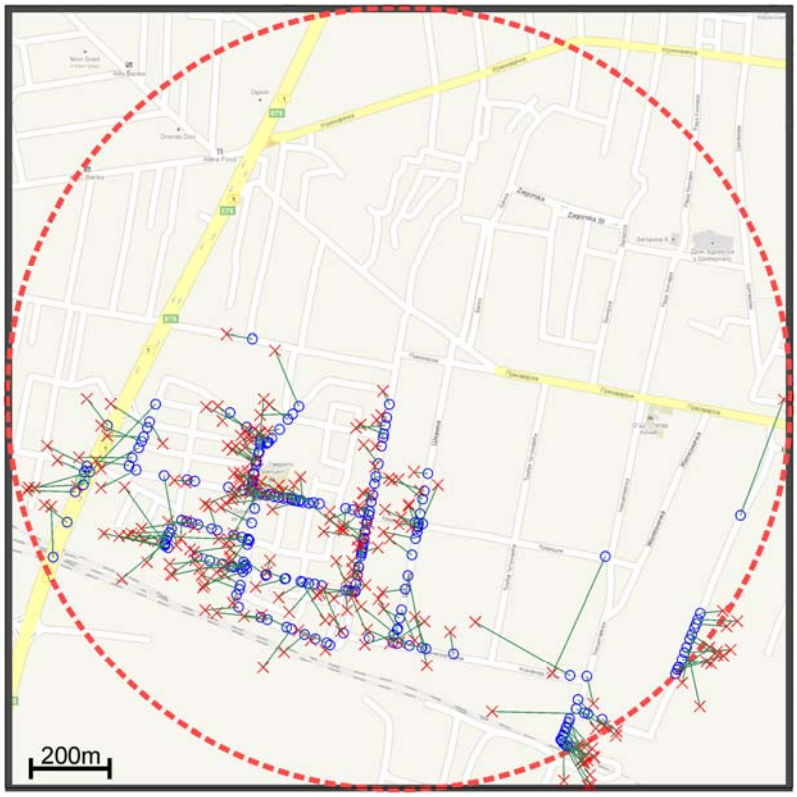

Fig. 5-20 Positioning with 1x1 partitioning

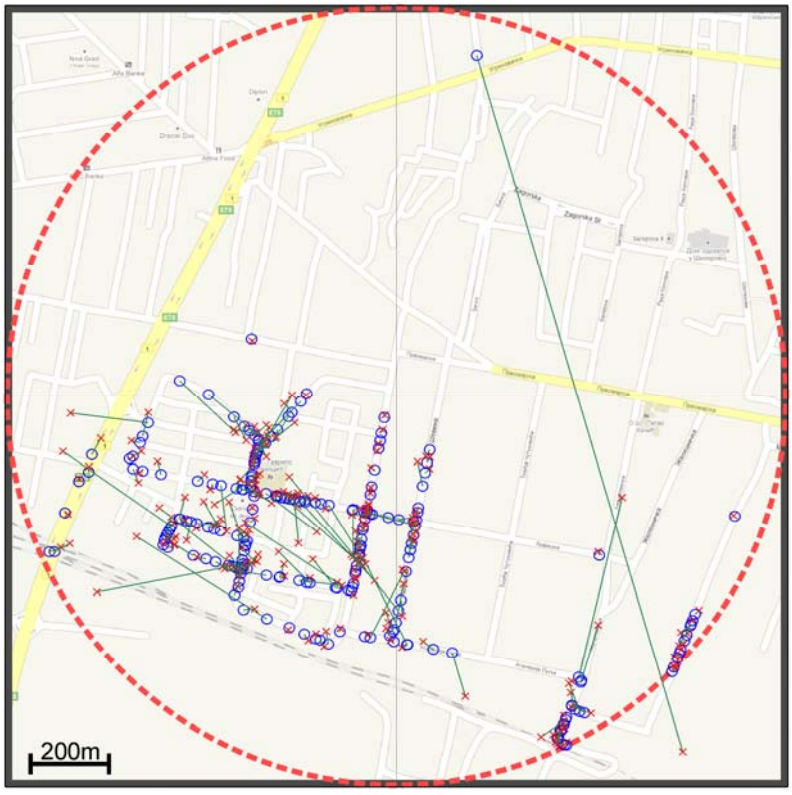

Fig. 5-21 Positioning with 2x2 partitioning

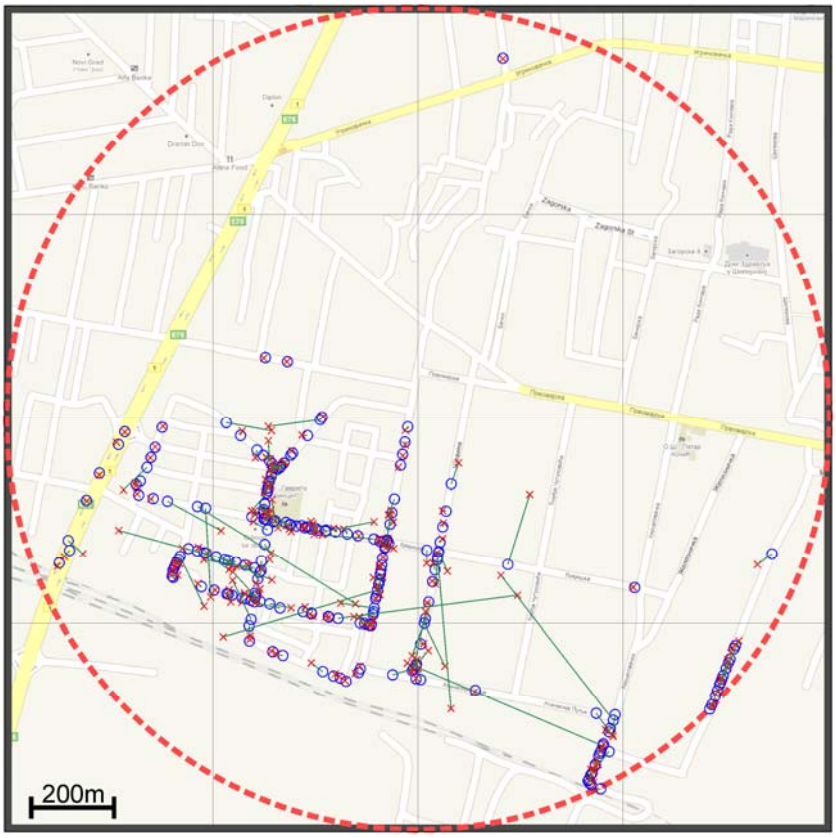

Fig. 5-22 Positioning with 4x4 partitioning

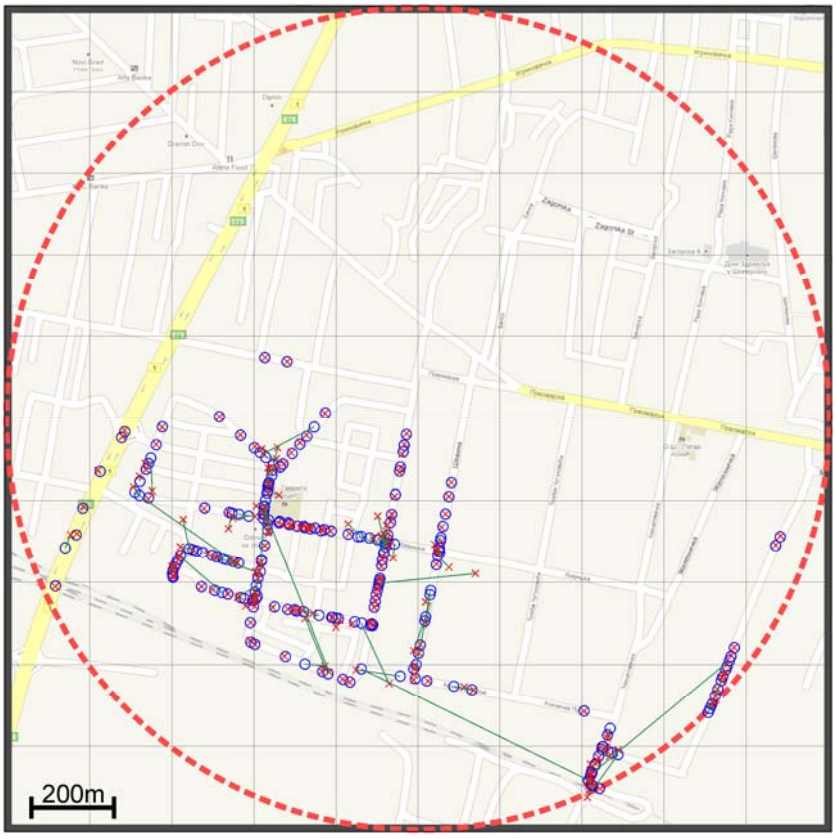

Fig. 5-23 Positioning with 10x10 partitioning

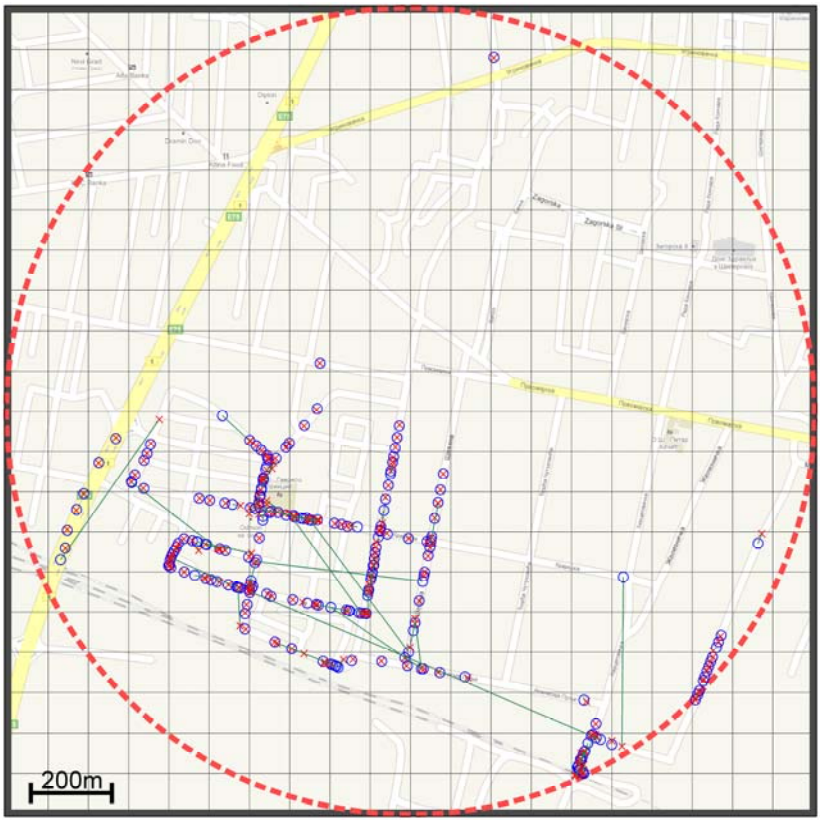

Fig. 5-24 Positioning with 20x20 partitioning

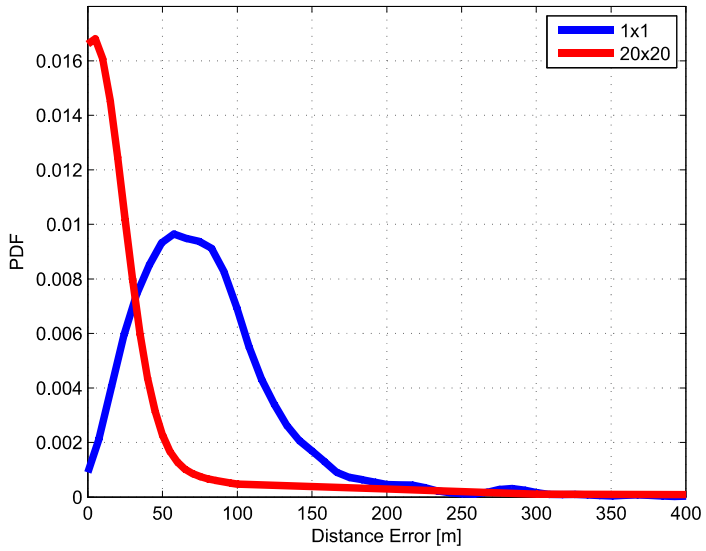

Fig. 5-25 Transformation of the DE's PDF with space-partitioning in outdoor environment

Figures 5-20 through 5-24 confirm that the location estimates are getting more precise with the additional segmentation of the model area. Starting with 1x1 partitioning, it can be seen that the DEs are spread over various values (green lines of various lengths). However, in this case, there are no extremely large DEs. Starting with 2x2 pattern shown in Fig. 5-21, the differentiation of distance errors can be noticed. Eventually, with 20x20 partitioning shown in

Fig. 5-24, there are only a few estimates with extremely large DEs and the vast majority with superb accuracy for this type of positioning technique. This behaviour is best observed through DE's PDF functions shown in Fig. 5-25 for bordering cases – 1x1 and 20x20 patterns.
Using the C-C ANN structures increases the overall complexity of the positioning models. The complexity parameters of the presented C-C models are given in Table 5-XVI.

Table 5-XVI Complexity of cascade-connected ANN models for PLMN positioning

Model	No. of perceptrons – Stage I	No. of perceptrons – Stage II	Total no. of perceptrons	Training time per epoch – Stage I [ms]	Training time per epoch – Stage II [ms]	Training time for optimally trained model [hours] [a]
1x1	-	128	128	-	111.0	6.2
2x2	55	512	567	18.1	124.0	7.1
3x3	84	1152	1236	104.7	136.9	10.5
4x4	124	2048	2172	120.4	158.1	10.5
5x5	176	3200	3376	160.2	213.0	20.7
10x10	607	12800	13407	500.7	665.7	64.8
20x20 [b]	464	9600	10064	462.9	616.0	59.9

[a] Models were trained on a single core of the Pentium Dual Core CPU E5200@2.5GHz (60W) with 2GB of RAM,
[b] Due to increasing complexity the ANNs were scaled to fit only the subspaces that contained measurement locations (75 for 20x20)

From Table 5-XVI, it can be seen that the number of perceptrons in both the first stage and the second stage of the model are rising with the increase in the number of subspaces. The first stage networks (type 2) are growing due to the increase in the number of subspaces whereas the second stage networks (type 1) remain of the same size, however, their number is increasing. Interestingly, although the number of perceptrons is growing much faster in the second stage, the (stage) training times per epoch remain comparable. This is due to the fact that each network in the second stage is trained with only a subset intended for its subspace. Consequently, the overall training time for the entire C-C ANN structure is increasing linearly with respect to the increase in the number of subspaces. The exception is made with 20x20 model, where the experiment to increase the efficiency was carried out. Being that, with the increase in the number of subspaces, the size of subspaces is getting smaller, there are more and more subspaces with no measured locations within (e.g. all the measurements from a subspace have been dispatched to the models for other sites). The 20x20 model, was sized according to the number of subspaces containing training data (measurements). As there are only 75 subspaces with measurements, this model appears even less complex than 10x10 model. The down side of this rationalization is the loss of generalisation – the model cannot estimate the position of a user to all of the subspaces (only the ones containing measurements). As this case (position estimation in a subspace with no training data) was not even tested, this rationalisation did not affect the accuracy performances, merely the complexity.

5.4 Comparison

If the positioning techniques are required to have the outdoor availability, usually satellite- and cellular-based positioning techniques are considered. The first group has superior accuracy but comes with a few drawbacks of their own. High impact on the handset (due to increased energy consumption and price) and questionable indoor availability are the two major ones (military owned infrastructure should not be neglected either). Although there are efforts in mitigating these issues there is still an apparent need for positioning system that would be able to provide both remarkable accuracy and indoor availability.

By using the available information in signals from PLMN, the user can be located two-folded: by timing measurements (e.g. TA, RTT, TDOA) and signal strength, phase and delay profile measurements (e.g. RSS and AOA). Overview of the several PLMN standardized positioning solutions was presented and their draft accuracy performance comparison is shown in Table 5-XVII.

Table 5-XVII Location error for standardized PLMN positioning techniques [5.13]

Positioning Technique	Location error interval [m]
Cell-ID	100-1000
Cell-ID+TA	-
AOA	>125
E-OTD	50-150
TOA	85-100
A-GPS	30-100

Each of the techniques presented in Table 5-XVII has its own downside. Although fairly simple to implement, Cell-ID technique has the unsatisfactory accuracy performance (as well as Cell-ID + TA in most cases). AOA and E-OTD techniques offer somewhat better accuracy but incur significant implementation costs. As for the A-GPS, several flaws inherent from GPS are still present. The research community has offered improvements to these positioning techniques[5] and they are, along with the positioning models presented in this work, mutually compared in Table 5-XVIII.

[5] The accuracy performances of techniques other than the ECIDTA, single ANN and C-C ANN models were copied from the respective publications.

Table 5-XVIII Comparative analysis of PLMN positioning models

Positioning Model	Average DE [m]	Median DE [m]	67th percentile DE [m]	95th percentile DE [m]	Environment[a]
Statistical Modelling Approach [5.14]	279	237	320	620	-
Genetic Algorithm [5.15]	324	-	450[b]	-	U
RSS DCM [5.16]	371	-	483	-	R
RTT+PDP RSS [5.17]	-	15	25	135	U
RTT SC [5.18]	-	15	20	115	U
E-CIDTA	130	105	135	245	U
Single ANN – M12	59	50	68	137	U
Single ANN – M12 indoor	105	101	107	158	I
C-C ANNs 1x1	82	72	90	177	U
C-C ANNs 20x20	26	2	4	168	U

[a] U – Urban, R – Residential, I – Indoor
[b] 450m with 72% confidence

The performances of statistical modelling and genetic algorithm approaches are unsatisfactory for most of the LBSs. Basically, they are somewhat better than basic Cell-ID positioning technique with the additional drawback, in case of genetic algorithm model, of high latency (7s computational time which further narrows the set of LBSs this technique might serve). The only worse performances are recorded with RSS DCM technique. With this technique the database was filled with simulated RSS values (obtained through propagation modelling) while the model was tested with the actual RSS measurements. The poor performances this technique exhibits might be an indicator for the lack of credibility of positioning techniques whose positioning performances are verified only by the computer simulations such as RTT SC and RTT+PDP RSS positioning techniques. Indeed, these two models display excellent accuracy with 15m median DE. Nonetheless, such accuracy was obtained only in simulations and has not been endorsed by the actual measurements. Moreover, the RTT SC deals with the selection of the three optimal RTT values whereas the actual UMTS signalling do not procure more than one RTT parameter for the most of the time (especially in residential and rural environments). Also, many UMTS networks do not even use the RTT parameter. Similar problem has to be resolved in order for the E-CIDTA positioning technique to be implemented. This technique, although offering fair positioning accuracy, uses as many TA parameters as there are radio visible BSs and, therefore, cannot be implemented without the changes in signalling. On the other hand, E-CIDTA shows improvement in performances with the increase in the redundant (more than three) TA values used. This raises the question whether the subset of three optimally selected RTT values (which is the main contribution of RTT SC technique) would

yield more location dependant information than the whole set. However, to follow upon this discussion would lead outside the scope of this work.

Regarding the RSS based PLMN techniques introduced in this work, the single ANN M12 (all available signals from both operators) shows the maximal achievement of a single ANN model which uses all available signals from multiple PLMN systems. The degradation of performances for indoor positioning is shown with the M12 indoor model. Both of these models display fair accuracy performances and the changes needed for their implementation can be regarded as software and signalling changes. On the other hand, the performances of C-C ANNs 1x1 model (which is still a single ANN model) can be regarded as the performances obtainable by a single ANN within the existing GSM system. Finally, using the same database as 1x1 model, the CC ANN models shows good positioning performances and clearly display the benefit of using the space-partitioning. The accuracy gain is the greatest at lower percentile DEs, and fades with high percentile DE (e.g. 95^{th} percentile DE of 1x1 – 177m vs. 168m with 20x20 model). Small latency is a good property of ANN based positioning models. However, rapidly increasing volume of the ANN structures with the increase in the number of subspaces and, consequently, high training times might present an down side for PLMN C-C ANN models. The complexity of these structures might be an especially degrading property with the large areas (with numerous sites) covered by the PLMN network. On the other side, these models can be successfully employed in cases where high precision is required on a subset of the environment (e.g. positioning of bus and cab vehicles). Bearing in mind the algorithm which assigns the appropriate positioning model (for each site), the slight mitigation of the complexity problem might be found in the fact that the models for each site can be trained and processed independently, enabling the positioning to be introduced gradually.

Also, it should be noted that, due to the potentially "boundless" coverage areas of PLMN (i.e. test-bed), the manner of implementation of the positioning algorithms is different to the one shown in WLAN. Hence, the environmental positioning error parameter is not easily applicable for PLMN models.

When comparing the results of space-partitioning in PLMN against the results obtained in WLAN environment, the partitioning gain is much more emphasized with outdoor positioning. This is most noticeable through the decrease in the average DE which was 10-15% within WLAN environment and goes up to four times in PLMN environment (partitioning gain is much greater than loss, i.e. almost no partitioning losses). The decrease in the median DE is also more noticeable in PLMN outdoor environment. The attained 1.8m median DE with 20x20 pattern is very good. However, some justifications for such performances can be offered. First of all, there are as much as 32 reference transmitters as MIs in PLMN C-C ANN

models, whereas there are only 8 with WLAN. Then, the radio visibility of these reference transmitters is much higher in PLMN than in WLAN environment which generates more location dependent fingerprints. These two facts cause the probability of correct subspace estimation to be better in the PLMN positioning case. In other words, there is a smaller number of estimates with wrongly determined subspace, i.e. extremely large DEs. Consequently, the partitioning loss areas are diminishing. Ergo, the average DE in outdoor positioning is decreasing significantly. Then, the scanner and equipment used for measurement were of notable capabilities. Basically, the whole GSM and DCS spectrums were scanned at a rate close to 1Hz[6]. In other words, new measurement for each channel was available every second. Due to the high spatial density of the measurements, the locations that lay on the paths covered by the measurements are accurately estimated. However, it might be the case that this way the generalisation capabilities of the C-C ANN structure have been impaired and that the localization requests made from outside the measuring paths would have notably worse accuracy. Further tests should prove or dispute the previous hypothesis. On the other hand, the benefit of using the C-C ANN structures against a single ANN was undoubtedly shown. Having the statistically same training and verification subsets, the C-C ANN have shown significantly better performances.

Finally, there is an aspect of outdoor positioning that has not been explored completely. The performances in WLAN indoor environment have been proven to first improve with the increase in the number of subspaces. With the final increase in the number of subspaces, those performances enter saturation (or even worsen slightly). In other words, the optimal number of subspaces in terms of accuracy was observed. The same behaviour, although anticipated, was not proven in outdoor PLMN positioning. Most likely, if the tests with even greater number of subspaces were conducted in PLMN this phenomenon would be recorded. However, due to the complexity of the C-C ANN models with higher number of subspaces and the time needed to train them, further tests were omitted. This matter may also be looked the other way around. Bearing in mind the greater RPs density within PLMN than WLAN environment, a valid assumption might be that the greater density of RPs increases the optimal number of subspaces. However, this premise shall be the object of further research.

[6] It can be expected that, in the proximate future, the mobile terminals of comparable hardware capabilities will be made available.

5.5 References

[5.1] J. Eberspacher, H. J. Vogel, C. Bettstetter, "GSM Switching,Services and Protocols", John Wiley & Sons Ltd, 2001, pp. 14-22.

[5.2] S. Y. Willassen, "Positioning a Mobile Station" Available: http://www.willassen.no/msl/node6.tml, 1998

[5.3] Radovan Jovanovic, BA thesis "Cell-ID + TA with triangulation“, Faculty of Electrical Engineering, 2005, unpublished.

[5.4] M. Simic, A. Neskovic, G. Paunovic, R. Jovanovic, M. Borenovic, „Positioning of users in cellular systems“, 12th Telecommunications Forum TELFOR 2004, Belgrade, Serbia and Montenegro.

[5.5] “R&S Cover Measurement System - Operating Manual version 3.6”, Vol. 1 and 2, Germany Rohde and Shwartz Test and Measurement Division.

[5.6] M. Matosevic, Z. Salcic, S. Berber, “A Comparison of Accuracy Using a GPS and a Low-Cost DGPS,” Instrumentation and Measurement, IEEE Transactions on Vol. 55, Issue: 5 (2006), pp. 1677 – 1683

[5.7] H. Laitinen, S. Ahonen, S. Kyriazakos, J. Lahteenmaki, R. Menolascino, S. Parkkila, "Cellular network optimization based on mobile location", Cellular Location Technology, 2001.

[5.8] 3GPP TS 45.008, release 7 (v7.15.0), Technical Specification Group GSM/EDGE Radio Access Network; Radio subsystem link control. http://www.3gpp.org/ftp/Specs/archive/45_series/45.008. Retrieved 2009-05.

[5.9] 3GPP TS 25.133 V5.18.0 (2007-09), 3rd Generation Partnership Project; Technical Specification Group Radio Access Network; Requirements for support of radio resource management. http://www.quintillion.co.jp/3GPP/Specs/25133-5i0.pdf Retrieved 2010-09-22.

[5.10] R&S®ROMES2GO, 3GPP Walk Test Solution, QoS assurance made, simple. http://www2.rohde-schwarz.com/file_12733/ROMES2GO_dat_en.pdf Retrieved 2010-09-22.

[5.11] TEMS™ Pocket 9.0 A complete measurement system in your hand. http://www.ascom.com/en/tems_pocket_9.0_eng.pdf Retrieved 2010-09-22.

[5.12] Lin T-N, Lin P-C, “Performance comparison of indoor positioning techniques based on location fingerprinting in wireless networks,”

International Conference on Wireless Networks, Communications and Mobile Computing, (2005) vol 2, pp 1569–1574

[5.13] Collomb Frédéric, Location Service Study Report (Loc_Serv_Study_Rep_PU.doc), Mobile and Vehicles Enhanced Services, 2002.

[5.14] T. Roos, P. Myllymäki, H. Tirri, "A statistical modeling approach to location estimation," IEEE Transactions on Mobile Computing, vol. 1, No 1, pp. 59-69 (January-March 2002).

[5.15] M.J. Magro, C.J. Debono, "A Genetic Algorithm Approach to User Location Estimation in UMTS Networks." Int. Conf. on Computer as a Tool, 2007, pp. 1136 – 1139

[5.16] C.J. Debono, C. Calleja, "The application of database correlation methods for location detection in GSM networks," 2008. 3rd International Symp. on Comm., Control and Signal Processing, pp. 1324–1329

[5.17] S. Ahonen, H. Laitinen, "Database correlation method for UMTS location," The 57th IEEE Semiannual Vehicular Technology Conference, Vol. 4, 2003 pp. 2696-2700

[5.18] S. Bartelmaos, K. Abed-Meraim, E. Grosicki, "General Selection Criteria for Mobile Location in NLoS Situations," IEEE Trans. on Wireless Comms, Vol. 7 (2008), pp. 4393 - 4403

6 Conclusion

6.1 Thesis Summary

This work tackles the problem of positioning in contemporary mobile communication systems. Development and verification of a positioning model in mobile communication systems often presents a complex task. Besides the satisfying accuracy, planning the positioning service ought to consider an extensive set of performance parameters such as:

- Required latency for the defined set of costumer services,
- Coverage,
- Scalability,
- Flexibility (the technique's openness for future enhancements),
- Availability, and
- The costs.

If the implementation costs of a positioning service are discussed, the implemented infrastructure support for other services except positioning (e.g. voice or data transport) ought to be taken into account. In other words, there are communication systems where positioning services present additional – value added services. Such is the case with both radio environments discussed in this work – WLAN and PLMN. Positioning techniques implemented in these mobile environments have substantial advantage in terms of implementation costs over most other positioning systems.

Within the WLAN environment, statistical and especially fingerprinting techniques have shown better accuracy performances than techniques using the propagation modelling approach. According to the previous studies, the average DE (Distance Error) with propagation modelling approach is above 3m whereas the fingerprinting techniques attain under 2m average DE. It should be pointed out that the other performance parameters (i.e. costs, scalability, flexibility, time needed to collect the fingerprinting database, etc.) were usually disregarded. Consequently, the shown accuracy performances ought to be regarded as the best case scenario or potentially achievable.

Considering the other available WLAN techniques, the ANNs as positioning algorithm, offer most preferable ratio between the accuracy and the time spent in model development (i.e. adopting the model to the propagation environment). Also the availability of ANN positioning is preferable, since these models do not insist upon three radio-visible APs.

This work compiles a number of new positioning models. All models (apart from one: E-CIDTA model) have been implemented with the use of ANNs. The analysis of existent ANN structures showed that the multilayer feedforward ANNs are preferable for positioning using the RSS information. The ANN model replaces the traditional electric field level estimation and subsequent estimation procedures (e.g. trilateration). The ANN as a positioning model successfully overcomes some of the flaws of the other techniques (e.g. detailed environment layout knowledge needed for propagation modelling approaches). The implementation does not require a large database of fingerprints (comparing to other models) and the detailed knowledge of the environment is not called for.

Two comprehensive measurement campaigns in a carefully selected WLAN environment were conducted. The first one comprised 433 RPs (Referent Points) where the measurements were carried in only one receiver orientation. The second campaign consisted of 403 RPs where in each RP the measurements were taken in four orthogonal receiver orientations.

The analysis of the ANN training process has been performed on WLAN positioning models in terms of maximizing the performances of presented models. The training lengths ranged from 100 to 500,000 epochs. The obtained WLAN models were compared to the other well-known indoor positioning models regarding the accuracy, availability, latency, feasibility in already deployed WLAN environments and implementation costs.

It has been shown that the single ANN approach presents a good choice for the positioning technique in already deployed WLAN networks that can readily respond to the requirements of a broad scope of LBSs. Its normalized accuracy as well as latency are amongst the best compared to other WLAN positioning techniques. The obtained average and median DEs with single ANN approach were 9.26m and 7.75m, respectively. Moreover, the model that uses cascade-connected (C-C) ANNs and space-partitioning has shown considerable advantages regarding, not only to the single ANN approaches, but also to the other known techniques which are well documented in the literature. Optimal space-partitioning increases the technique's accuracy in terms of the median and average absolute position errors – the median DE was reduced to 4.57m, whereas the average DE decreased to 8.14m. When comparing to the single ANN model with no space-partitioning, in a x24 space partitioned positioning with ANNs, the average absolute positioning error was reduced by 12%, while the median error was reduced by as much as 41%. The research had also shown that further increase in the number

of subspaces cease to benefit the positioning performances. Ergo, the optimal number of subspaces, 24, was recorded.

No rising issues with the C-C ANN models' scalability or latency were found. The latency with this approach is only slightly higher than for the single ANN approach. The single ANN approach is known to be very good in terms of latency – as pointed out before. As for the scalability, when the network infrastructure is expanded, the proposed technique does not require the complete fingerprinting database to be recollected, thus proving this technique to be reasonably scalable.

In addition, the extensive experimental analysis of RSSI, SNR and Noise level parameters usefulness for WLAN positioning purposes was conducted. Four ANN models with RSSI, SNR, Noise and RSSI & SNR parameters as inputs were tested. Analysis had shown that, contrary to the common knowledge, SNR parameter is equally suitable for WLAN positioning purposes as RSSI parameter – the models with RSSI, SNR and RSSI & SNR had almost identical positioning performances. In addition, as expected, the obtained results pointed out that the space distribution of the noise level parameter contains less location dependant information than RSSI or SNR.

The positioning in PLMN environment was also scrutinised. The behaviour of GSM's timing advance parameter was modelled and new E-CIDTA positioning technique that make use of TA models was presented. This mathematical model yielded 135m accuracy with 67% confidence.

The main efforts regarding the PLMN positioning were carried with the ANN models. Actual measurements obtained through an extensive measurement campaign, carried on more than 1,000,000 locations in Belgrade, were used to train and validate the presented models. The training lengths spanned 100 to 500,000 epochs.

Twenty-two models based on a single ANN architecture, using the RSS parameters for localization purposes were presented and scrutinised. The use of RSS parameters originating from one or more PLMN systems belonging to one or more network operators were considered. The single ANN models were employing RSS parameters from GSM, DCS, and UMTS systems, as well as their combinations. Single ANN models were verified on three different cell sites in light urban to urban environment.

The results undoubtedly demonstrated an initial increase in the accuracy of the models with an increase in the number of MIs (Model Inputs). This is best noticeable by observing the average DE of M1 model (seven GSM RSS values from one network operator) against the average DE of M8 (all available GSM signals from both network operators). The average DEs of the two models are 175m and 92m, respectively. A further increase in the number of MIs tends to

reduce dominantly the maximal positioning error (high-percentile DE) which can be seen from Table 5-VII. Another interesting effect was observed. Having the same number of MIs originating from a larger number of different physical BTS locations has a positive effect on positioning performances. This indicates that radio sources from an additional location can procure more location dependent information than the sources that collocate with previously used inputs. The aforementioned hypothesis can be deduced from M6 model (7 GSM inputs from MTS operator and 7 DCS inputs from VIP operator) outperforming the M4 model (7 GSM and 7 DCS inputs, all from MTS operator). Although both models have 14 RSS inputs, M4 model obtains its inputs from fewer BTS sites and achieves 90m median error whereas M6 model attains 86m median error.

The most inclusive models implemented in all three tested cell sites achieved less than 50m median DE and less then 70m DE in 67%. Bearing in mind that the models used solely RSS parameters, which are readily available in already deployed networks, this result becomes even more significant. Moreover, these models, with the use of an overloaded tracking algorithm and map matching feature, could be used for a broad range of LBS.

The obtained results were compared to other relevant PLMN positioning techniques. They overperformed all but the two models, RTT+PDP RSS [6.1] and RTT SC [6.2], that were based on timing measurements and, foremost, were not verified with actual RSS measurements but with computer simulation only.

The degradation of performances when the models are used in an indoor environment has also been investigated. The median error of 101m was attained. If one takes into account the fact that the models were trained with the measurements performed outdoors, this presents a fair result.

A slight drawback of the presented positioning models might be the additional signalling required to deliver all available RIs (Reference Inputs) to the network as well as the considerable setup time for a high-density network. On the other hand, the latency of the presented models ought to be negligible.

Finally, the additional 7 models employing the C-C ANN structures and different space-partitioning patterns were tried for PLMN positioning. The effect of using the space-partitioning was similar in both the WLAN and PLMN environments whereas the extent of benefits from using the space-partitioning was much greater in case of PLMN environment. The 1x1 model showed the fair performances that can be attained with a single ANN and the existing GSM infrastructure and signalling. Using the same signals (and the database of fingerprints) the new C-C ANN models improve in their accuracy with the increase in the number of subspaces. The model with most subspaces, 20x20 model, achieves better accuracy

performance comparing to all other cellular-based solutions. Namely, the median DE of only 2m was achieved. Moreover, the latency of these models is only slightly increased. With the ever increasing computer processing power, even the complexity of C-C models with a large number of subspaces, considered as a downside, should not present a significant drawback.

6.2 Contributions of the Thesis

The proposed multilayer feedforward ANNs have shown good positioning performances in both WLAN and PLMN environments, even with low RPs density. Single ANN models were thoroughly explored in terms of optimal training lengths, variable input number and type. The performances of all the models were validated through the use of extensive measurement campaigns.

- Several new performance evaluation parameters that ought to enable the indoor positioning techniques to be compared and classified in a more comprehensive and inclusive manner were proposed. These parameters take into account the accuracy, size of the environment, and the density of the infrastructure. Most importantly, the *environmental positioning error* parameter ought to enable positioning techniques to be compared inclusive of the size of their test bed, which was seldom the case before. The proposed performance parameters contribute to more broad scrutiny of the indoor positioning techniques.
- The extensive experimental analysis of RSSI, SNR and Noise level parameters usefulness for WLAN positioning purposes had shown that, contrary to the common knowledge, SNR parameter is equally suitable for WLAN positioning purposes as RSSI parameter.
- Regarding the PLMN positioning, the devised positioning algorithm, suitable to use with the ANNs, benefits from using the RSSI values from multiple systems, belonging to multiple operators. Moreover, the PLMN models were tested indoors and the degradation of accuracy performances, due to cross-environment model use, was reported.
- Foremost, this work brought the space-partitioning into positioning. The principle enables to dismantle the positioning process into two stages and solve each stage independently with the most suitable model. Moreover, the C-C ANN based models suitable for use with space-partitioning were proposed. This positioning solution enhances the accuracy performance parameters: the average and median error are reduced whereas the high percentile DEs are more or less unchanged. It ought to be

pointed out that the transformation of the DE distribution function is favourable for the use of overlaid tracking algorithms that would filter-out high distance errors and additionally improve the positioning performances. If the space-partitioning principle is implemented through the use of C-C ANNs, the latency of these models is very good, the scalability is fair, whereas the complexity when partitioning to a large number of subspaces might present a slight negative side.

6.3 Future Work

All valid research efforts end up pointing to more directions than there were at the beginning of the research. That is also the case with this work. There are many ideas for the further improvement.

The space-partitioning patterns might be adopted to make use of the user's behaviour. That is, the subspace boundaries could be made to cross over the areas where the user is less likely to be, thus increasing the probability of correct subspace detection and, consequently, improving the positioning performance. Furthermore, bearing in mind the transformation of DE's PDF induced by space-partitioning (the DEs are being divided into two groups – small and large, while the medium DEs are less likely to occur), decision making by majority voting (e.g. two-out-of-three decision making) could be applied to the first stage of the C-C structure in order to reduce the probability of extremely large DEs.

On a more formal side, it might be worth to mathematically express and justify the gain obtained by using space-partitioning starting from the theory of information. However, this does not present an easy and straightforward mission.

Further research would evaluate the performances of presented structures against the varying density of RPs. The greater density of RPs should invoke larger optimal number of subspaces and, probably, additional benefit from space-partitioning.

Regarding the PLMN ANN models, they could be enriched with system timing parameters such as TA and/or RTT (where available). Another direction might be to add the power delay profile to the fingerprint database. Both the timing and the power delay profile are location dependent information and should improve the overall positioning performances.

6.4 References

[6.1] S. Ahonen, H. Laitinen, "Database correlation method for UMTS location," The 57th IEEE Semiannual Vehicular Technology Conference, Vol. 4, 2003 pp. 2696-2700

[6.2] S. Bartelmaos, K. Abed-Meraim, E. Grosicki, “General Selection Criteria for Mobile Location in NLoS Situations,” IEEE Trans. on Wireless Comms, Vol. 7 (2008), pp. 4393 - 4403

Publications

- M. Borenović, A.Nešković, Dj. Budimir, “Multi-System-Multi-Operator Localization in PLMN Using Neural Networks”, ACCEPTED for the Wiley International Journal of Communication Systems
- M. Borenović, A.Nešković, Dj. Budimir, “Partitioning strategies when using cascade-connected ANN structures for indoor WLAN positioning”, ACCEPTED for the International Journal of Neural Systems (IJNS)
- M. Borenović, A.Nešković, Dj. Budimir, “Cross-System Localization in PLMN Using Neural Networks ”, 2010 IEEE Radio and Wireless Symposium (RWS2010)
- M. Borenovic, A. Neskovic, Dj. Budimir, “Cascade-connected ANN structures for indoor WLAN positioning”, 10th international Conference on Intelligent Data Engineering and Automated Learning (IDEAL'09), 23-26 September, 2009, Burgos, Spain
- M. Borenovic, L. Zezelj, A. Neskovic, Dj. Budimir, “Simulation and Comparison of WiMAX Propagation Models”, ETRAN Conference for Electronics, Telecommunications, Computers, Automatic Control and Nuclear Engineering, Vrnjacka Banja, Serbia, 2009
- M. Borenovic, A. Neškovic, “Positioning in Indoor Mobile Communications” book chapter, "Radio Communications", ISBN 978-953-7619-X-X, IN-TECH
- M. Borenović, A. Nešković, “Comparative Analysis of RSSI, SNR and Noise Level Parameters Applicability for WLAN Positioning Purposes”, IEEE EUROCON 2009
- M. Borenović, A. Nešković, “Positioning in WLAN Environment by use of Artificial Neural Networks and Space Partitioning”, Annals of Telecommunication journal
- O. Šarac, M. Borenović, A. Nešković, “Developement of the Empirical Propagation Model for Indoor WLAN Environment”, ETRAN Conference for Electronics, Telecommunications, Computers, Automatic Control and Nuclear Engineering, Palic, Serbia, 2008,
- M. Borenovic, A. Neskovic, Dj. Budimir, L. Zezelj, “Utilizing Artificial Neural Networks for WLAN Positioning”, IEEE International Symposium on Personal, Indoor and Mobile Radio Communications, 2008, Cannes, France
- M. Borenović, A. Nešković, N. Nešković, G. Paunović, “Positioning in WLAN Networks”, PosTel 2007, December 2007, Belgrade, Serbia
- M. Borenović, A. Nešković, M. Koprivica, “An Overview of Indoor Positioning Techniques”, 15th International Telecommunications Forum, TELFOR 2007, Belgrade, November 2007
- Miloš N. Borenović, Aleksandar M. Nešković, Mladen T. Koprivica, “Positioning in WLAN Networks with the Use of ANN”, 14th Telecommunications Forum TELFOR 2006, November 2006, Belgrade, Serbia
- Miloš N. Borenović, Mirjana I. Simić, Aleksandar M. Nešković, Miloš M. Petrović, “Enhanced Cell-ID + TA GSM Positioning Technique”, IEEE EUROCON 2005, November 2005, Belgrade, Serbia
- Mirjana Simić, Aleksandar Nešković, Đorđe Paunović, Radovan Jovanović, Miloš Borenović, *“Positioning Techniques in Cellular Networks”*, 12th Telecommunications Forum TELFOR 2004, November 2004, Belgrade, Serbia